DEPARTMENT OF TRANSPORTATION

Monitoring and Performance Analysis of the TH 610 Iron-Enhanced Filtration System

Omid Mohseni, Principal Investigator
Barr Engineering Co.

AUGUST 2020

Research Project
Final Report 2020-23

To request this document in an alternative format, such as braille or large print, call 651-366-4718 or 1-800-657-3774 (Greater Minnesota) or email your request to ADArequest.dot@state.mn.us. Please request at least one week in advance.

Technical Report Documentation Page

1. Report No. MN 2020-23	2.	3. Recipients Accession No.
4. Title and Subtitle Monitoring and Performance Analysis of the TH 610 Iron-Enhanced Filtration System		5. Report Date August 2020 6.
7. Author(s) Omid Mohseni		8. Performing Organization Report No.
9. Performing Organization Name and Address Barr Engineering Co. 4300 MarketPoint Dr. Minneapolis, MN 55435		10. Project/Task/Work Unit No. 11. Contract (C) or Grant (G) No. (C) 1000622
12. Sponsoring Organization Name and Address Minnesota Department of Transportation Office of Research & Innovation 395 John Ireland Boulevard, MS 330 St. Paul, Minnesota 55155-1899		13. Type of Report and Period Covered Final Report 14. Sponsoring Agency Code
15. Supplementary Notes http://mndot.gov/research/reports/2020/202023.pdf		

16. Abstract (Limit: 250 words)

In 2011, the Minnesota Department of Transportation (MnDOT) installed an iron-enhanced sand filter (IESF) at Trunk Highway (TH) 610 and County Road 81 in Maple Grove, Minnesota. This feature is a two-cell filtration system into which part of Trunk Highway 610 and County Road 81 drain. From 2012 through 2018, MnDOT monitored the influents and effluents into the IESF to determine its effectiveness in removing particulate and dissolved phosphorus from stormwater runoff from the nearby highways. MnDOT also retained Barr Engineering Co. (Barr) to analyze the data collected during this period. As part of the data analysis, Barr developed a hydrologic model to account for all inflows and outflows from the system. The model was calibrated to the data collected in 2018 and applied to the prior years. The results of data analysis and watershed modeling showed that all influents and effluents have not been accounted for and the collected data were inconclusive in assessing the effectiveness of this IESF. This report summarized the analyses performed on the data collected, determined the potential effectiveness of the IESF, and provided some guidelines for design and future monitoring of other IESFs.

17. Document Analysis/Descriptors Hydrology, Phosphorus, Sampling, Seepage, Weirs		18. Availability Statement No restrictions. Document available from: National Technical Information Services, Alexandria, Virginia 22312	
19. Security Class (this report) Unclassified	20. Security Class (this page) Unclassified	21. No. of Pages 91	22. Price

MONITORING AND PERFORMANCE ANALYSIS OF THE TH 610 IRON-ENHANCED FILTRATION SYSTEM

FINAL REPORT

Prepared by:

Omid Mohseni
Barr Engineering Co.

August 2020

Published by:

Minnesota Department of Transportation
Office of Research & Innovation
395 John Ireland Boulevard, MS 330
St. Paul, Minnesota 55155-1899

This report represents the results of research conducted by the authors and does not necessarily represent the views or policies of the Minnesota Department of Transportation or Barr Engineering Co. This report does not contain a standard or specified technique.

The authors, the Minnesota Department of Transportation, and Barr Engineering Co. do not endorse products or manufacturers. Trade or manufacturers' names appear herein solely because they are considered essential to this report.

ACKNOWLEDGMENTS

The author would like to thank Katie Turpin-Nagel and Eric Novotny for their contribution in the analysis of data collected from 2012 through 2016. The author would like to thank Harold Bottolfson (transportation program specialist with MnDOT) for collecting all the monitoring data, Barbara Loida (technical liaison with MnDOT), Beth Neuendorf (Technical Advisory Panel member and technical liaison with MnDOT), Nick Olson (Technical Advisory Panel member) and Katie Fleming (project coordinator) for their feedback and guidance throughout the project.

TABLE OF CONTENTS

CHAPTER 1: Introduction **1**

CHAPTER 2: Monitoring **3**

CHAPTER 3: Data Analysis **6**

3.1 Hydrologic Data 6

3.1.1 Measured Hydrologic Data 6

3.1.2 Hydrologic Data Assessment and Analysis 13

3.2 water quality data 14

3.2.1 Measured Water Quality Data 14

3.2.2 Phosphorus Data Analysis by Concentration 15

3.3 Final notes on hydrology and water quality data analysis 17

CHAPTER 4: Hydrologic model of the Filtration System **18**

4.1 Site Details 18

4.2 Hydrologic modeling approach 20

4.3 model parameters 21

4.4 Model Calibration Results 22

4.5 Model Application to Other Periods 25

CHAPTER 5: Modeling Results **29**

CHAPTER 6: Conclusions and Recommendations **37**

APPENDIX A 2012 through 2015 Pollutographs

APPENDIX B 2016 through 2018 Pollutographs

LIST OF FIGURES

Figure 1.1 Aerial photo of the TH 610 IESF with a schematic of the two-cell filtration system, the filter drainage area and the inflow and outflow monitoring locations 2

Figure 2.1 Schematic of a longitudinal cross-section of the two-cell filtration system and the monitoring locations 3

Figure 2.2 *Left*: Schematic of the inflow monitoring setup with the locations of pressure transducers and the Thel-mar weir, and *right*: a photo of the Thel-mar weir installed inside the manhole of the inflow monitoring location 4

Figure 2.3 Aerial photo off the TH 610 filtration system with the approximate locations of piezometers 7003 and 7004 in the filter and piezometer 7002 in the berm 5

Figure 3.1 Measured filter outflow and rainfall in 2012 6

Figure 3.2 Measured filter outflow and rainfall in 2013 7

Figure 3.3 Measured filter outflow and rainfall in 2014 7

Figure 3.4 Measured filter outflow and rainfall in 2015 8

Figure 3.5 Measured filter outflow and rainfall in 2016 8

Figure 3.6 Measured filter outflow and rainfall in 2017 9

Figure 3.7 Measured filter outflow and rainfall in 2018 9

Figure 3.8 The 2016 measured water surface elevations upstream and downstream of the inflow weir, and lines showing elevations of the berm crest and the v-notch of the inflow weir 10

Figure 3.9 The 2017 measured rainfall, water surface elevations upstream and downstream of the inflow weir, and lines showing elevations of the berm crest and the v-notch of the inflow weir 11

Figure 3.10 The 2018 measured rainfall, water surface elevations upstream and downstream of the inflow weir, and lines showing elevations of the berm crest and the v-notch of the inflow weir 11

Figure 3.11 The 2017 measured piezometer (7003) levels, and lines showing elevations of the berm crest, the v-notch of the inflow weir, and top and bottom of the filter 12

Figure 3.12 Measured piezometer (7004, 7003 and 7002) levels in 2018, and lines showing elevations of the berm crest, the v-notch of the inflow weir, and top and bottom of the IESF 13

Figure 3.13 A box and whisker plot of annual influent and effluent total phosphorus (TP) from 2012 through 2018 16

Figure 3.14 A box and whisker plot of annual influent and effluent dissolved phosphorus (DP) from 2012 through 2018 16

Figure 4.1 The 2018 measured rainfall, observed and simulated water levels in the wet pond, the simulated water surface elevation in the IESF, and lines showing elevations of the berm crest, the v-notch of the inflow weir, and top and bottom of the IESF 24

Figure 4.2 The 2018 simulated water level in the IESF, the 2018 measured piezometer levels (7002, 7003 and 7004) in the IESF and berm, and lines showing elevations of the berm crest, the v-notch of the inflow weir, and top and bottom of the IESF 24

Figure 4.3 The 2017 measured rainfall, observed and simulated water levels in the wet pond, the simulated water surface elevation in the IESF, and lines showing elevations of the berm crest, the v-notch of the inflow weir, and top and bottom of the IESF 25

Figure 4.4 The 2017 simulated water level in the IESF, the measured piezometer (7003) level in the IESF, and lines showing elevations of the berm crest, the v-notch of the inflow weir, and top and bottom of the IESF 26

Figure 4.5 The 2016 measured rainfall, observed and simulated water levels in the wet pond, the simulated water surface elevations in the IESF, and lines showing elevations of the berm crest, the v-notch of the inflow weir, and top and bottom of the IESF 28

Figure 4.6 The 2015 measured rainfall, observed and simulated water levels in the wet pond, the simulated water surface elevations in the IESF, and lines showing elevations of the berm crest, the v-notch of the inflow weir, and top and bottom of the IESF 28

LIST OF TABLES

Table 4.1 Drainage areas and depths..... 18

Table 4.2 Elevations and dimensions of structures 19

Table 4.3 Seepage parameters 19

Table 5.1 Influent and effluent flow averaged concentrations of total phosphorus (TP) and dissolved phosphorus (DP) in 2018..... 31

Table 5.2 Influent and effluent flow averaged concentrations of total phosphorus (TP) and dissolved phosphorus (DP) in 2017..... 32

Table 5.3 Influent and effluent flow averaged concentrations of total phosphorus (TP) and dissolved phosphorus (DP) in 2016..... 33

Table 5.4 Influent and effluent loads of total phosphorus (TP) and dissolved phosphorus (DP) in 2018 .. 34

Table 5.5 Influent and effluent loads of total phosphorus (TP) and dissolved phosphorus (DP) in 2017 .. 35

Table 5.6 Influent and effluent loads of total phosphorus (TP) and dissolved phosphorus (DP) in 2016 .. 36

LIST OF ABBREVIATIONS

Barr	Barr Engineering Co.
cfs	cubic feet per second
DO	dissolved oxygen
DP	dissolved phosphorus
fps	feet per second
ft	feet
IESF	iron-enhanced sand filter
in	inches
lbs	pounds
MnDOT	Minnesota Department of Transportation
NWL	normal water level
TH	Trunk Highway
TP	total phosphorus
WSE	water surface elevation

EXECUTIVE SUMMARY

The Minnesota Department of Transportation (MnDOT) installed an iron-enhanced filtration basin at Trunk Highway 610 and County Road 81 in Maple Grove, Minnesota. The basin is a two-cell filtration system into which part of TH 610 and County Road 81 drain. The east cell is a pretreatment pond and the west cell is an iron-enhanced sand filter (IESF). The IESF was monitored from 2012 through 2018 to determine its effectiveness in removing total phosphorus (TP) and dissolved phosphorus (DP) from stormwater runoff from the nearby highways. MnDOT constructed an outflow monitoring location where flows were measured by a Thel-mar weir. MnDOT also constructed an inflow monitoring location in a manhole inside the berm separating the cells. The connecting pipe between the two cells would route the flow between the two cells through the manhole. There was no device or probe inside the inflow monitoring location to measure flow until 2016. There was only a pressure transducer recording water levels inside the manhole, which could also represent the water levels in the wet pretreatment pond. MnDOT installed a second Thel-mar weir in June 2016 inside the manhole to measure inflows. MnDOT also installed piezometers in the IESF and the berm separating the two cells in 2017 and 2018. From 2012 through 2018, MnDOT collected water samples at the inflow and outflow monitoring locations. A selected number of samples were sent to a laboratory to measure influent and effluent concentrations of TP and DP.

A comparison between influent and effluent concentrations of TP and DP showed that the IESF was removing TP but not DP. In six years out of the seven-year period of monitoring, the mean annual effluent concentrations of DP was higher than the mean annual influent concentrations.

The results of monitoring also showed that the annual volume of measured outflow was higher than the annual volume of measured inflow in 2016, 2017 and 2018. To account for all inflows and outflows, a hydrologic model was developed to estimate the seepage through the berm and to account for runoff from the pervious areas of the IESF drainage basin. The hydrologic model was used to estimate the influent and effluent loads of the IESF.

The hydrologic model was calibrated against the measured water levels of the pretreatment pond, i.e. the water level in the manhole. In addition, the model approximated the piezometer readings in the IESF. The results of the hydrologic model showed that the measured volume of outflow was significantly higher than potential runoff from the IESF drainage area in 2016 and somewhat higher in 2017 and 2018. Because of significant periods of malfunctioning of the probes, the hydrologic model did not provide an accurate result of the IESF water balance. Nevertheless, the model was used to calculate the flow-weighted average concentrations of influent and effluent TP and DP, and influent and effluent loadings. Because of the adverse slope of the connecting pipe, i.e., the complexity of simulating flow from the wet pretreatment pond into the IESF, and also significant discrepancy in the 2013 and 2014 data, the model was not used to simulate the influent and effluent loads from 2012 through 2015.

The results of the load calculations showed that the IESF removed a significant amount of DP in 2016, nearly no DP in 2017, and more effluent than influent DP in 2018. The results of the model showed that the IESF exhibited long periods of saturated conditions in 2017 and 2018. Long periods of saturated

conditions in the IESF would result in anoxia in the water column, which could result in internal loading in the IESF. In addition, vegetation growth on the surface of the IESF was observed since 2015. By 2018, there was significant vegetation cover over the IESF surface area. It is very likely that over time, the vegetation cover resulted in a significant phosphorus loading, which could not be monitored or quantified. The combination of longer periods of saturated conditions in the IESF and vegetation growth were the likely causes of a significant drop in efficiency of the IESF in removing DP.

CHAPTER 1: INTRODUCTION

In 2011, the Minnesota Department of Transportation (MnDOT) installed an iron-enhanced filtration basin at Trunk Highway (TH) 610 and County Road 81 in Maple Grove, Minnesota. This feature is a two-cell filtration system into which part of TH 610 and County Road 81 drain (**Error! Reference source not found.**). The east cell is a wet pretreatment pond, known as Bruce Pond, and the west cell is a filtration basin equipped with an iron-enhanced sand filter (IESF) to remove dissolved phosphorus from runoff. The total watershed area of the sand filtration basin is 5.42 acres with 4.58 acres (approximately 85%) of the watershed routed through the wet pretreatment pond (hereafter wet pond). The total impervious area in the watershed is 2.8 acres. Water flows to the site through three highway drainpipes entering in north, south, and east areas of the wet pretreatment pond. Water then flows from the wet pond to the IESF through an 18-inch reinforced-concrete pipe connecting the two cells. A berm is present between the wet pond and the IESF. An overflow section of the berm allows larger storm events to enter the IESF. The crest of the overflow berm is approximately 20 feet long at an elevation of 889.14 feet.

Once water travels through the filtration media, it is collected into three drain tiles that bring water directly to a single outflow structure. The outflow structure collects and baffles the water before it leaves through an underground pipe that connects to the main storm sewer line.

MnDOT collected water samples at two inflow and outflow monitoring locations from 2012 through 2018. The inflow and outflow monitoring locations are upstream and downstream of the IESF, respectively, and refer to inflows into and outflows of the IESF. Flow was measured at the outflow monitoring location by measuring stages upstream of a compound weir. From 2012 through 2015, only water stages were measured at the inflow monitoring location; therefore, no inflow data was available for that period, and consequently the laboratory analysis of water samples at the inflow monitoring location did not provide any information on the phosphorus loading—only on concentrations of dissolved phosphorus (DP) and total phosphorus (TP). In June 2016, a compound weir was installed in the manhole at the inflow monitoring location to provide an estimate of influent loading. In early 2017, a report was developed summarizing the data collected in 2016 by analyzing flows into and out of the filter basin and influent and effluent concentrations of DP and TP. In 2017, MnDOT installed two piezometers in the berm and the filter basin to determine seepage through the berm and to assess the water levels in the filter. In 2018, another piezometer was installed in the filter to further define the water levels in the filter. MnDOT also authorized Barr to develop a hydrologic model to estimate other inflows into the filter basin.

This report summarizes the monitoring, hydrologic analysis, and performance of the TH 610 IESF in removing TP and DP from stormwater runoff. Chapter 2 describes the monitoring conducted at the two monitoring locations, Chapter 3 provides an overview of the data collected from 2012 through 2018, Chapter 4 describes the hydrologic model to further enhance the assessment of the IESF, Chapter 5 summarizes the findings, and Chapter 6 provides conclusions and recommendations for the design of a monitoring system for similar best management practices.

Figure 1.1 Aerial photo of the TH 610 IESF with a schematic of the two-cell filtration system, the filter drainage area and the inflow and outflow monitoring locations

CHAPTER 2: MONITORING

Water samples and water levels were collected at two locations from February 2012 through October of 2018 to monitor phosphorus removal provided by the IESF. The two monitoring stations were (1) inside a manhole on the connecting pipe between the two cells (inflows) and (2) inside the outflow structure of the west cell on the northwest part of the pond (outflows) (Figure 1.1 and Figure 2.1). A Thel-mar weir (compound weir) was installed at the outflow monitoring location to measure the outflow from the IESF. No weir was installed at the inflow monitoring location.

Each sampling location included an ISCO 6212 water sampler programmed to collect 24 water samples into individual 1-liter bottles throughout a storm event. Water depths were recorded using ISCO 4250 and 4230 flow meters. Precipitation depths were recorded using a rain gauge at the inflow monitoring location.

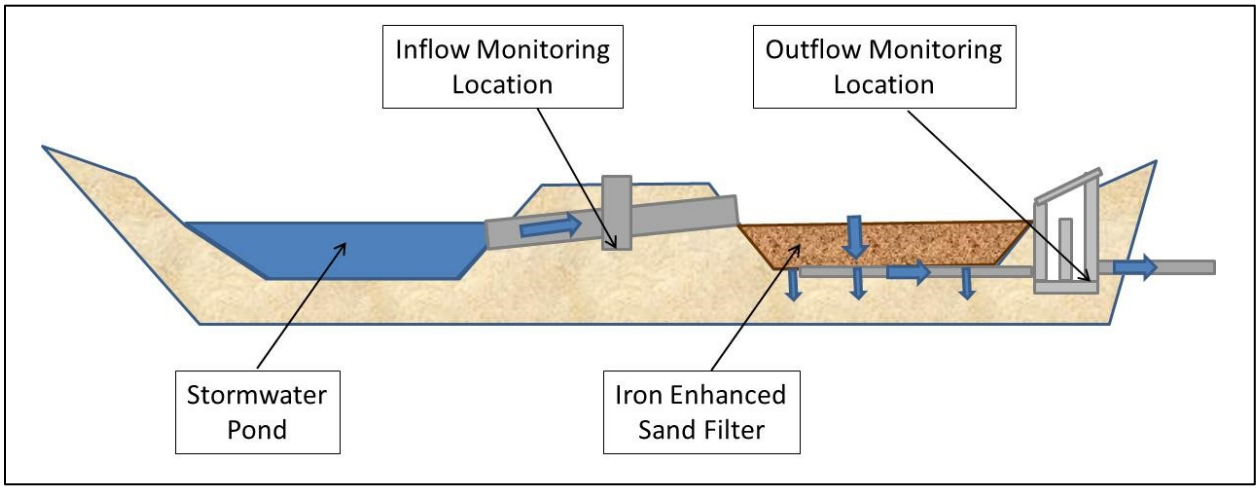

Figure 2.1 Schematic of a longitudinal cross-section of the two-cell filtration system and the monitoring locations

The inflow monitoring equipment, originally only a pressure transducer, was located in a manhole in the berm between the wet pond and the IESF (**Error! Reference source not found.**). The inflow monitoring setup was modified in June of 2016 to measure the inflows into the IESF. A 15-inch Thel-mar weir was installed in the inflow manhole with the apex of the v-notch 3.23 feet above the bottom of the manhole. A level monitor was installed upstream of the weir and flow rates were determined based on the water level and a rating curve supplied by the manufacturer. Because of the adverse slope of the connecting pipe between the wet pond and the IESF, the compound weir could be easily submerged; therefore, on July 14, 2016, a second pressure transducer was installed directly downstream of the weir to help determine when tailwater from the IESF impacted the rating curve of the weir. A schematic of the installation and a picture of the Thel-mar weir are shown in Figure 2.2.

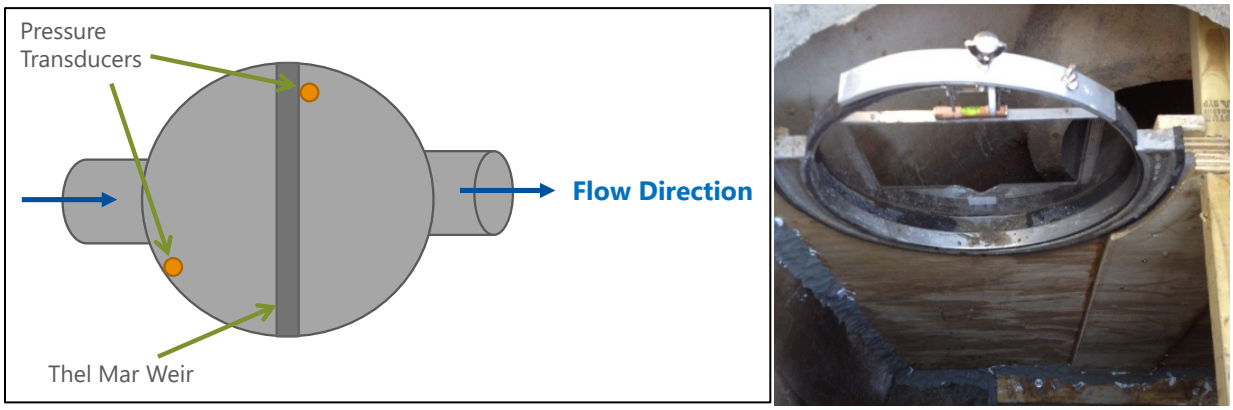

Figure 2.2 *Left*: Schematic of the inflow monitoring setup with the locations of pressure transducers and the Thel-mar weir, and *right*: a photo of the Thel-mar weir installed inside the manhole of the inflow monitoring location

The water samples were collected during each event. Up to seven sample bottles were chosen for analysis from the 24 collected at both the inflow and outflow monitoring locations based on position of the sample in the corresponding inflow and outflow hydrographs. The outflow samples included a sample when the triggered depth was met, a sample closest to the peak flow rate of the event, and up to five additional samples to accurately represent the entire runoff event. The sample bottles were sent to a lab for analysis where influent and effluent TP and DP of the samples were measured.

Two piezometers were installed on April 19, 2017: one in the berm between the two cells (labeled as 7002) and another inside the filter close to the berm (labeled as 7003). A third piezometer was installed inside the filter close to the IESF outlet (labeled as 7004) on August 28, 2018. The locations of the piezometers are shown in Figure 2.3. The purpose of installing the three piezometers was to better understand the water level inside the IESF, how quickly the IESF would drain and, if possible, to estimate the seepage from the wet pond into IESF. The length of the Piezometer 7002 pipe was 8.05 feet with approximately 6 feet of the piezometer positioned in the ground. The top of the riser was surveyed in 2018 at 892.82 feet. The length of the Piezometer 7003 pipe was 4.62 feet with approximately 2.6 feet positioned inside the filter. The top of the riser was 889.85 feet. The length of Piezometer 7004 pipe was 5.32 feet where the top of the riser was surveyed at 884.66 feet. The observed water level data for piezometers 7002 and 7003 were provided starting on December 21, 2017. Observed water level data for piezometer 7004 were provided starting on August 28, 2018.

Figure 2.3 Aerial photo of the TH 610 filtration system with the approximate locations of piezometers 7003 and 7004 in the filter and piezometer 7002 in the berm

CHAPTER 3: DATA ANALYSIS

Two types of data were collected in 2012–2018: (1) hydrologic data that included water levels, flow data, and piezometer levels and (2) water quality data that included TP and DP.

3.1 HYDROLOGIC DATA

3.1.1 Measured Hydrologic Data

Hydrologic data from 2012 through 2015 include flow data at the outflow monitoring location. The flow data were measured via a 15-inch Thel-mar weir and then transported via telemetry to the MnDOT office in Fort Snelling. Figure 3.1 through Figure 3.7 show the IESF measured outflow data and rain for each year.

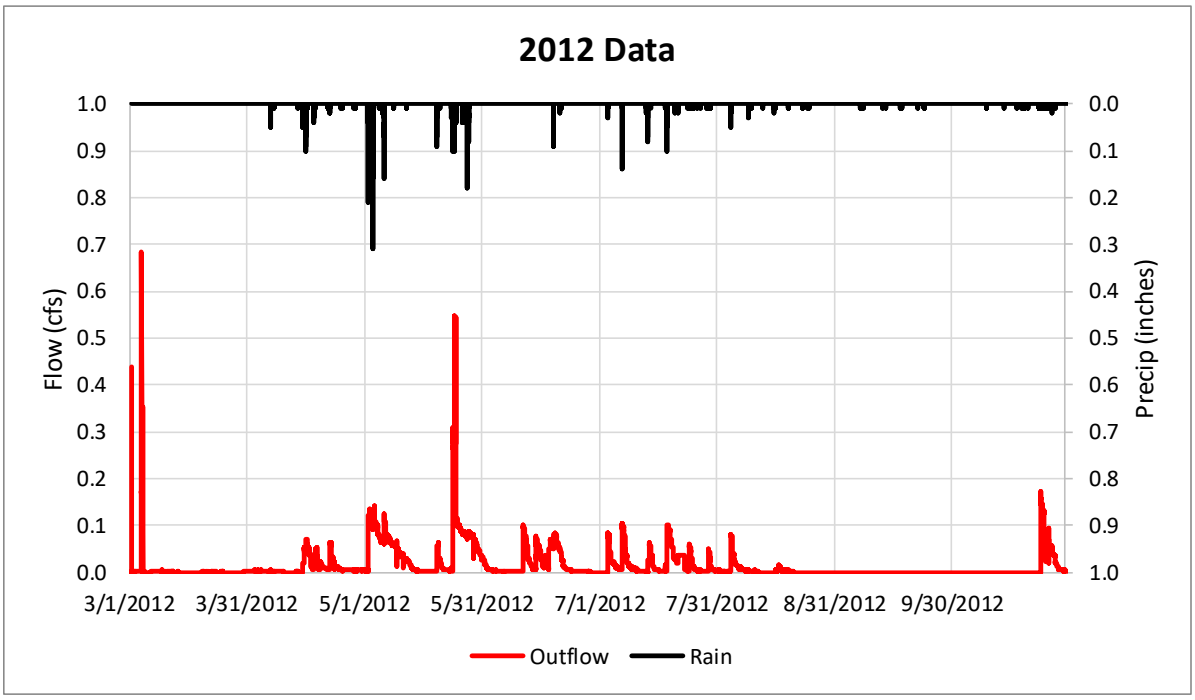

Figure 3.1 Measured filter outflow and rainfall in 2012

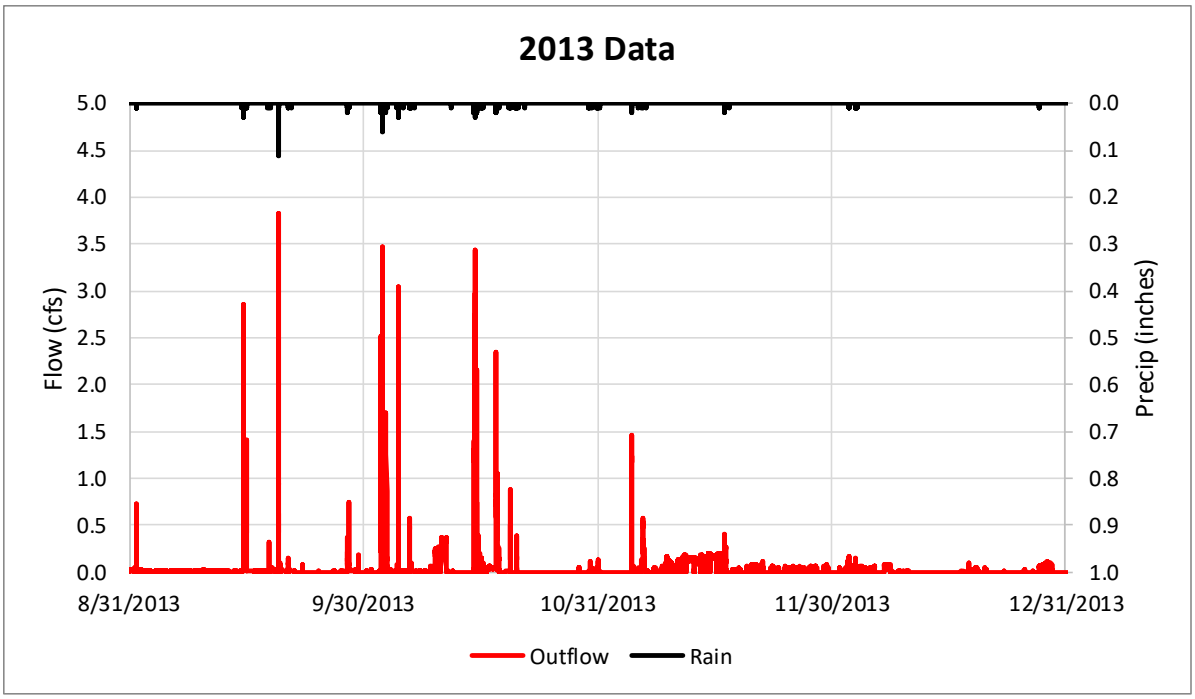

Figure 3.2 Measured filter outflow and rainfall in 2013

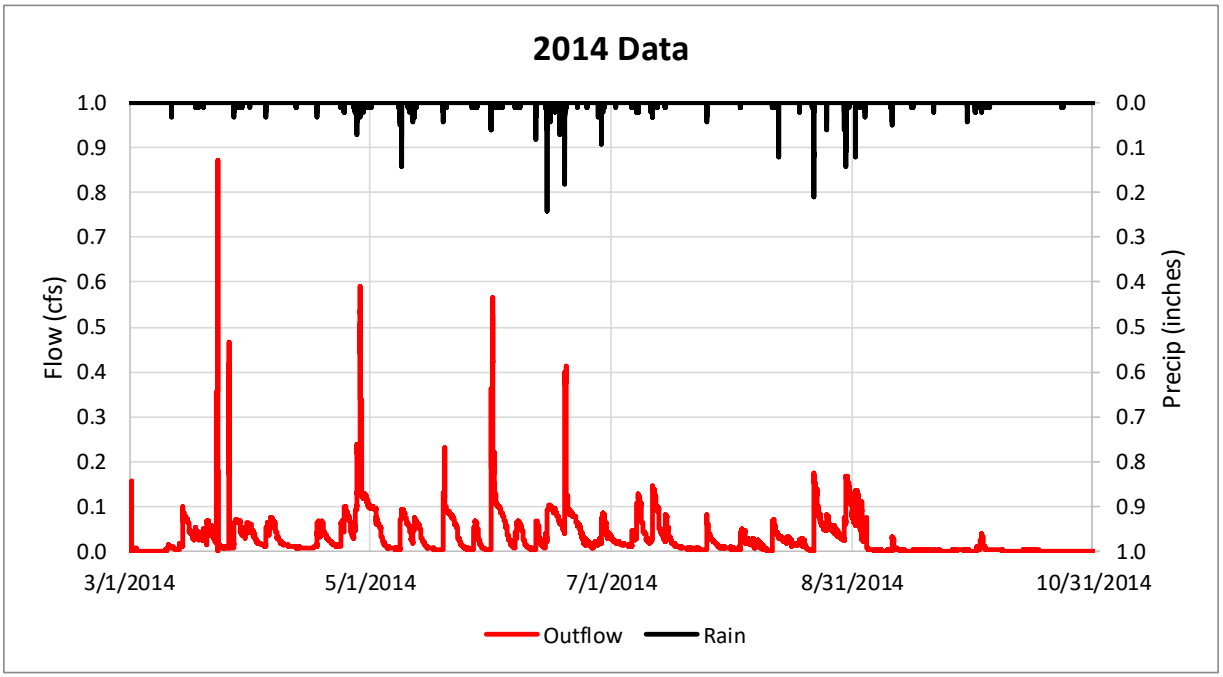

Figure 3.3 Measured filter outflow and rainfall in 2014

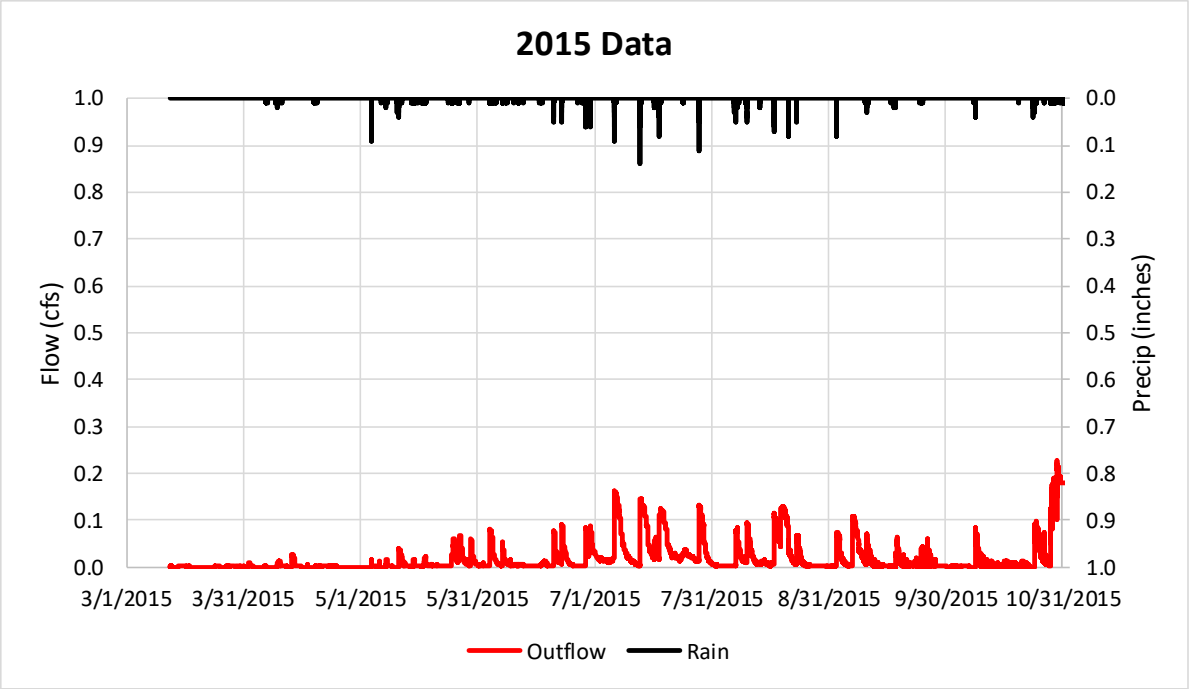

Figure 3.4 Measured filter outflow and rainfall in 2015

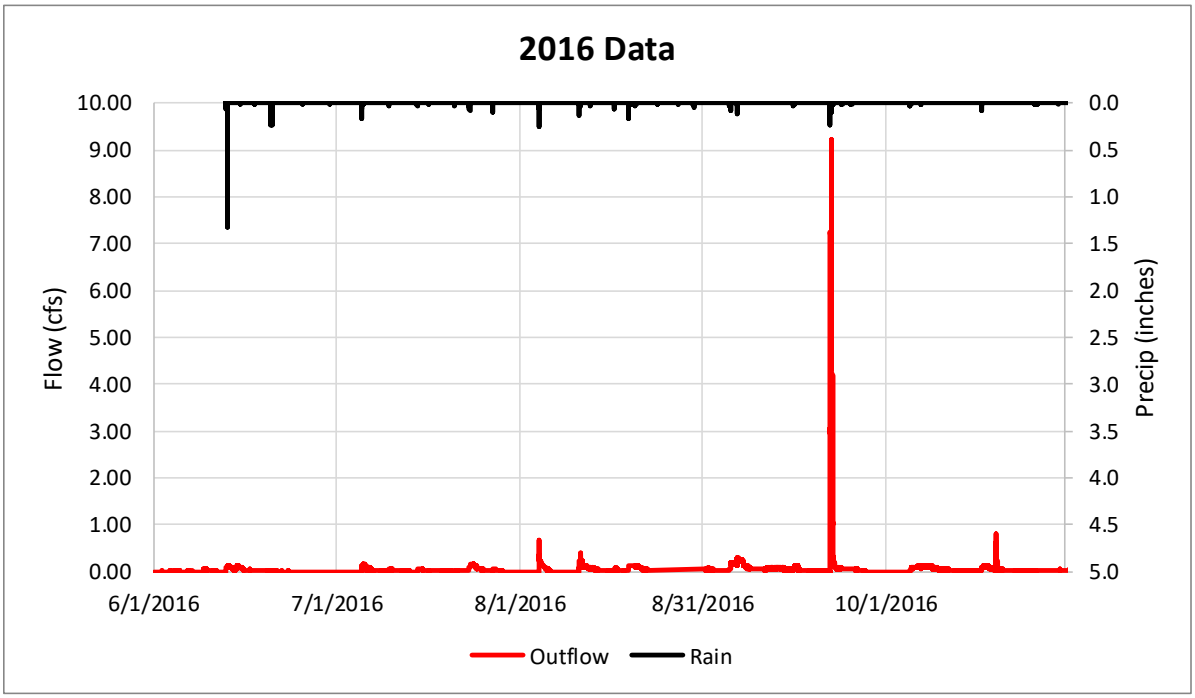

Figure 3.5 Measured filter outflow and rainfall in 2016

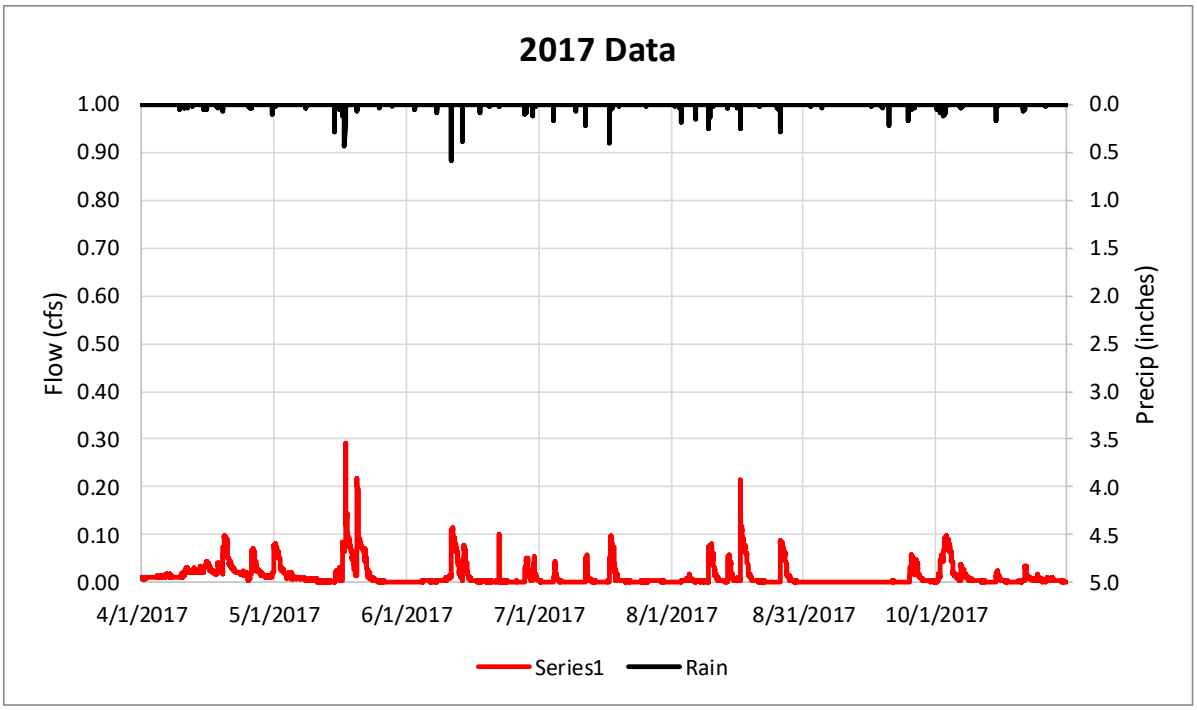

Figure 3.6 Measured filter outflow and rainfall in 2017

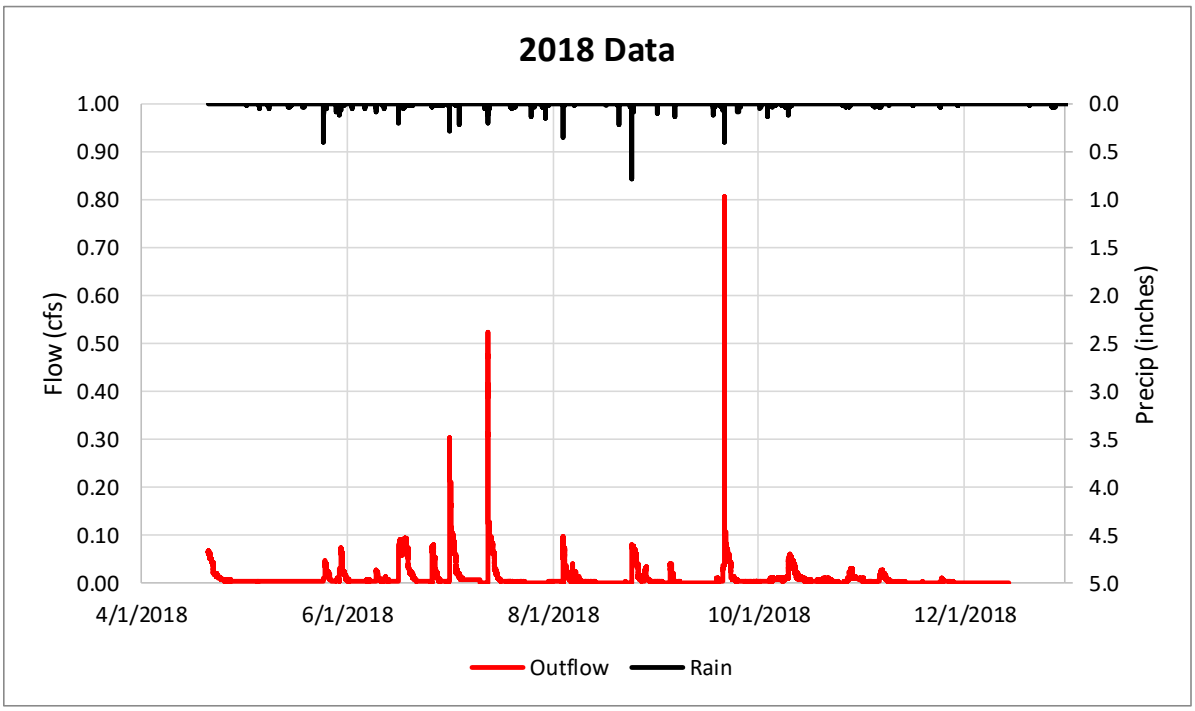

Figure 3.7 Measured filter outflow and rainfall in 2018

Water levels were measured at the inflow monitoring location from 2012 through 2018. No reference was provided for the water level data measured from 2012 through 2015. For the data measured from 2016 through 2018, the reference was set at the bottom of the manhole between the two cells of the filtration system. Since the bottom of the manhole was surveyed, those data sets have been converted into water surface elevations. Because the flow rate through the connecting pipe is very small, the head loss through the pipe is negligible and the water surface elevations upstream of the weir at the inflow monitoring location can closely represent water levels in the wet pond. Figure 3.8 through Figure 3.10 show the measured water levels at the inflow monitoring locations.

Water levels were also measured downstream of the weir at the inflow monitoring location in 2016, 2017, and 2018. Figure 3.8 through Figure 3.10 also show the measured water levels downstream of the weir which represent tailwater levels for the inflow weir.

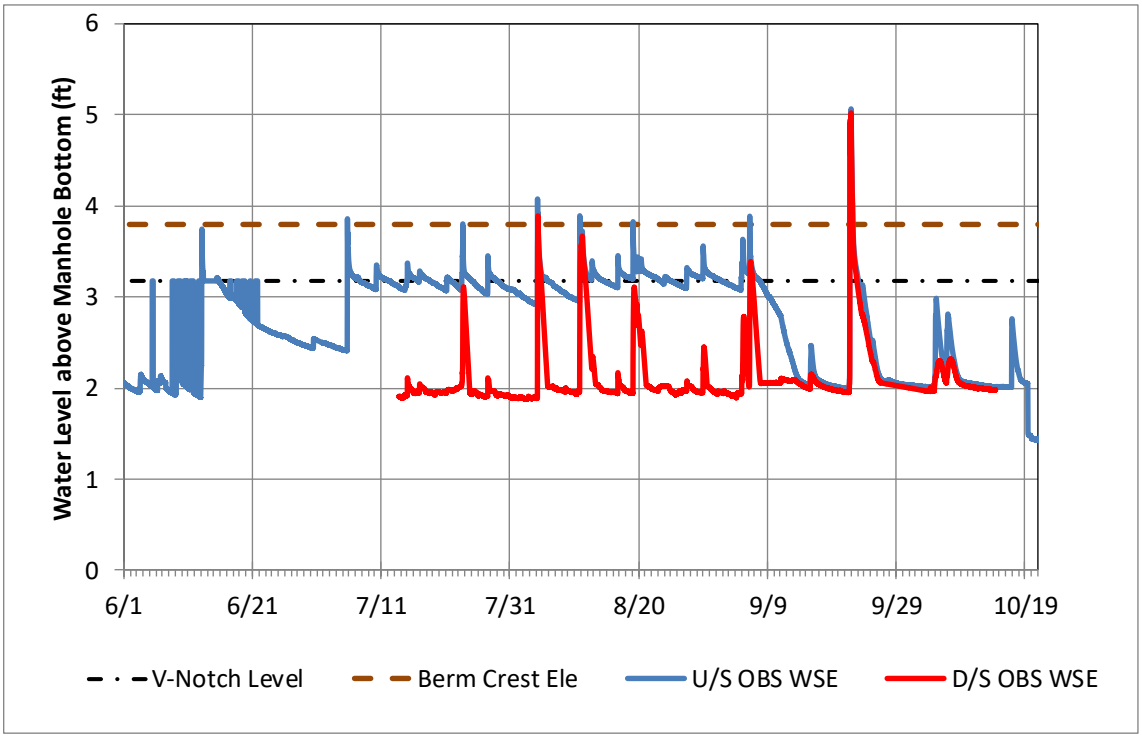

Figure 3.8 The 2016 measured water surface elevations upstream and downstream of the inflow weir, and lines showing elevations of the berm crest and the v-notch of the inflow weir

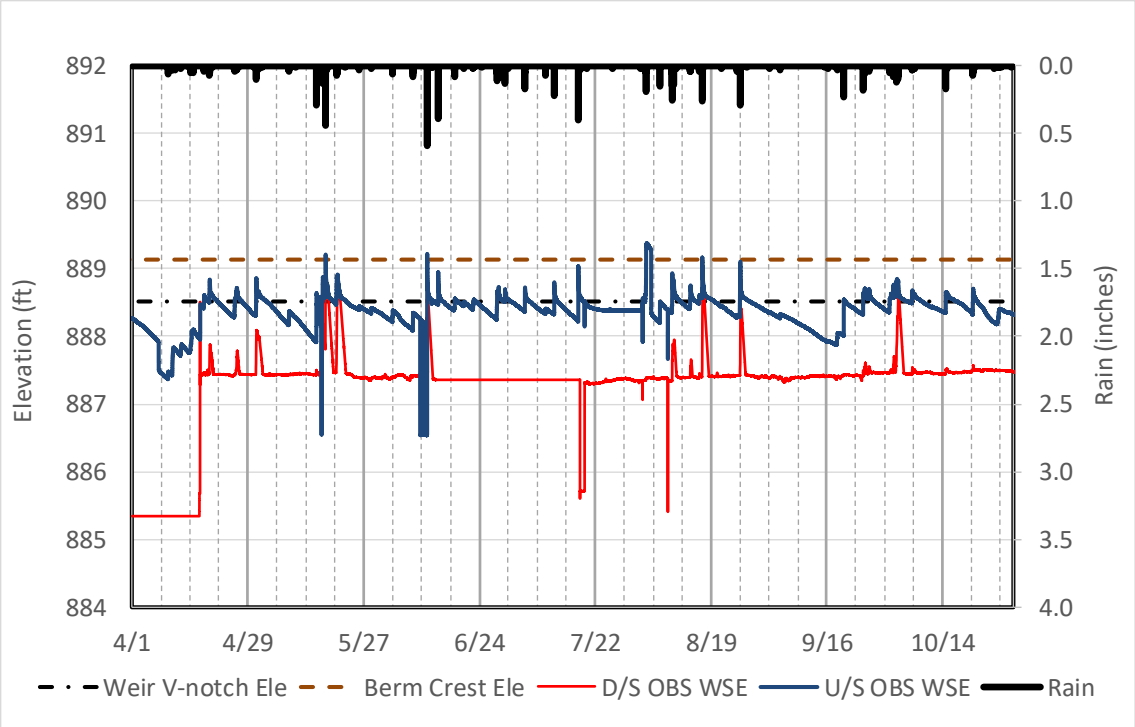

Figure 3.9 The 2017 measured rainfall, water surface elevations upstream and downstream of the inflow weir, and lines showing elevations of the berm crest and the v-notch of the inflow weir

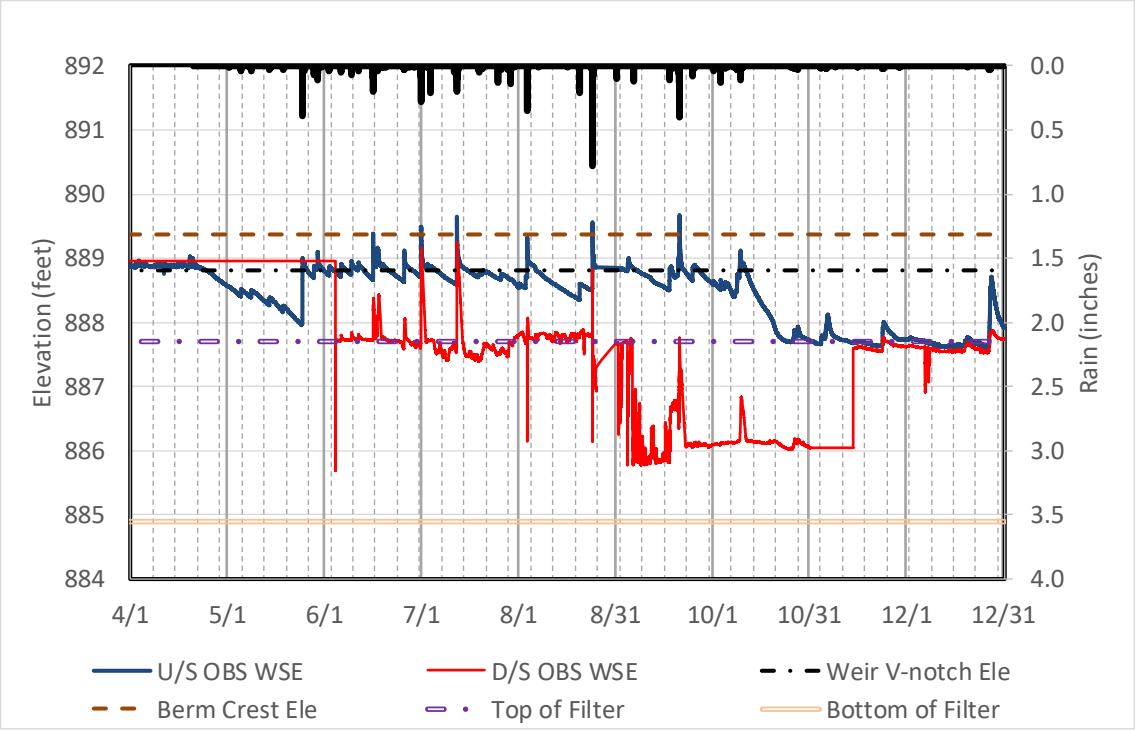

Figure 3.10 The 2018 measured rainfall, water surface elevations upstream and downstream of the inflow weir, and lines showing elevations of the berm crest and the v-notch of the inflow weir

Figure 3.11 and Figure 3.12 show the piezometer levels in the IESF and the berm between the two cells of the filtration system. The locations of piezometers were presented in Section 2.0.

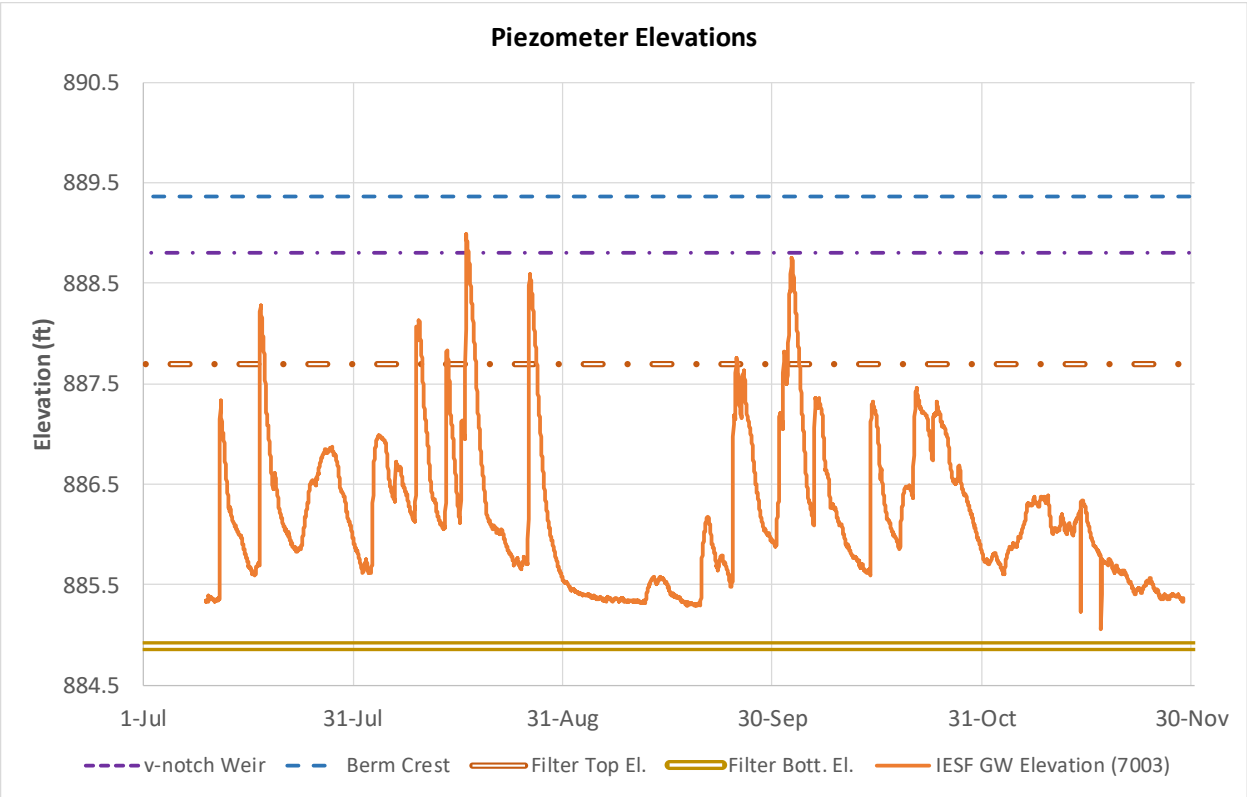

Figure 3.11 The 2017 measured piezometer (7003) levels, and lines showing elevations of the berm crest, the v-notch of the inflow weir, and top and bottom of the filter

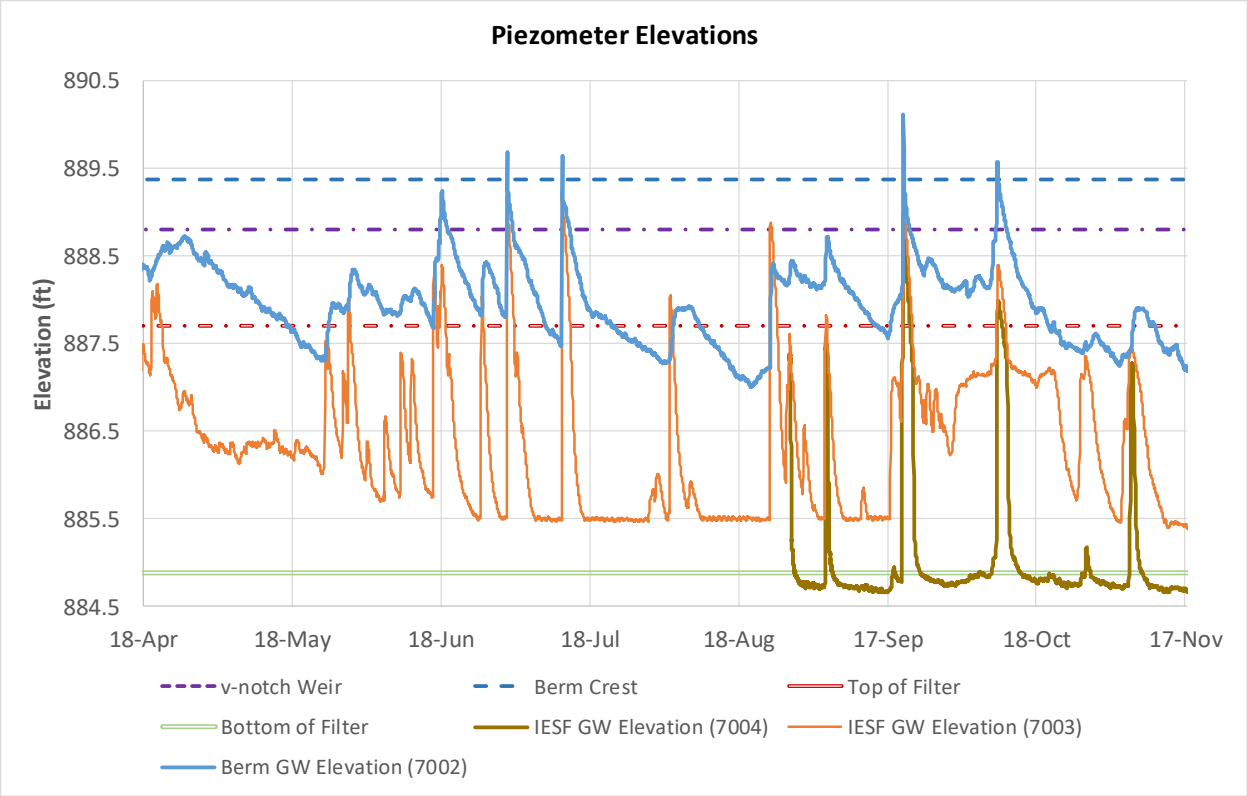

Figure 3.12 Measured piezometer (7004, 7003 and 7002) levels in 2018, and lines showing elevations of the berm crest, the v-notch of the inflow weir, and top and bottom of the IESF

3.1.2 Hydrologic Data Assessment and Analysis

The measured outflows from the IESF show that the flow rate out of the IESF was often less than 1.0 cubic feet per second (cfs) with most of the data showing flow rates less than 0.1 cfs. However, the 2013 data (Figure 3.2) show numerous events with flows more than 1.0 cfs. It is important to note that the rainfall pattern in 2013 is either the same or even smaller than in other years; however, in 2013 peak outflows are significantly larger than in other years and appear to be erroneous. In addition, the 2013 outflow data were only available after September 1, 2013.

The other anomaly in outflows is the event in September 2016 when the peak outflow reaches 9 cfs. The rainfall event resulting in such a high peak outflow is relatively small and this discrepancy cannot be explained by the amount of rainfall that occurred prior to that event. Figure 3.8 shows a significant drop in the measured water surface elevation (WSE) in the wet pond in September 2016 which was due to failure and collapse of the weir in the inflow monitoring location. It is likely that the high outflow recorded in 2016 was the result of inundation of the IESF during that incident. However, late in September of 2018, the IESF was inundated as a result of significant leakage through the inflow weir and a rainfall event (Figure 3.10), but the peak outflow only reached 0.8 cfs. It is likely that the actual rainfall was significantly higher than what was measured by the onsite rain gauge and the pond water level increased significantly and resulted in the failure of the inflow weir. (It was reported by MnDOT that the

onsite rain gauge was occasionally covered by debris as a result of birds nesting on top of the gauge and the MnDOT staff had to continuously clean the gauge).

Some of the peak outflows in March and April, i.e., in 2012 and 2014, appear to be the result of snowmelt and not the amount of precipitation prior to those events.

By reviewing the outflow data and potential inflow from the impervious areas, it became evident that the outflow volume was significantly higher than the inflow volume. For example, the measured volume of outflow and estimated volume of inflow from impervious areas, including the surface of the wet pond and IESF, were 6.9 and 4.1 acre-feet (ft), respectively, in 2012; 7.9 and 4.0 acre-ft in 2015; 5.8 and 5.2 acre-ft in 2017; and 4.3 and 4.0 acre-ft in 2018. By including pond evaporation, the outflow volume was at least 10% larger than the inflow volume. The difference became even larger when the measured inflow was compared to measured outflow in 2016, 2017, and 2018, when the inflow weir was installed. The gap between outflow and inflow volumes is even larger in the other years of monitoring, e.g. in 2013 outflow was 28 acre-ft and inflow 2.6 acre-ft. The discrepancy between outflow and inflow volumes can be partially explained by measurement errors; however, since outflow volume was always larger than the inflow volume, it is evident that the IESF was receiving more flow than what was measured at the inflow monitoring location.

Figure 3.8 through Figure 3.10 show the WSE in the wet pond and downstream of the inflow weir. The data show that both pressure transducers have exhibited periods of malfunctioning, e.g. the WSE in the wet pond does not seem to be correct during the month of June of 2016 (Figure 3.8) or in mid-May, mid-June, and a period of three weeks in late July and early August of 2017 (Figure 3.9). The pressure transducer downstream of the weir exhibited extended periods of malfunctioning in 2017 and 2018. The poor data collected from the downstream pressure transducer would not allow a correct estimate of the flow over the inflow weir during large storm events, when the water level in the IESF would submerge the inflow weir.

The piezometer readings in 2017 and 2018 show that the IESF was partially saturated for long periods in the fall of 2017 and 2018. The 2018 piezometer readings in the area near the outflow location do not show that the IESF was saturated for long periods. Those data may be the result of drainage around the drain tiles under the IESF. If both dataset are correct, then at least some areas of the IESF were saturated for extended periods in 2017 and 2018.

3.2 WATER QUALITY DATA

3.2.1 Measured Water Quality Data

Water samples were collected during each event. From 2012 through 2015, between three to five samples per each event were analyzed for TP and DP. The samples were analyzed using the EPA 365.1 method. The total number of sampled events were 11, 10, 9, and 10 for 2012, 2013, 2014, and 2015, respectively. During a number of sampled events, there was no water level recorded or flow measured

at the two monitoring locations. Appendix A provides the pollutographs of TP and DP concentrations collected during each event along with rainfall, water level at the inflow monitoring location, and flow rate through the outflow monitoring location.

In 2016, the total of sampled events was seven and five samples per event were analyzed to measure the TP and DP concentrations. The pollutographs of these samples are also shown in Appendix A.

In 2017 and 2018, the number of sampled events increased to 13 and 16, respectively, with seven samples per event for measuring TP and DP concentration. The pollutographs of the 2017 and 2018 sampling events are shown in Appendix B.

3.2.2 Phosphorus Data Analysis by Concentration

Individual collection samples for TP were grouped by year and sample location for comparison. All seven years analyzed are displayed for comparison in Figure 3.13. Figure 3.13 shows a significant decrease in TP concentration from the inflow to the outflow monitoring locations for years 2012–2014. Year 2015 also displays a reduction in TP concentration due to the IESF, but the difference was not calculated to be significant at the 95% confidence level. Years 2016–2018 again show a significant decrease in total TP concentrations. In 2018, the median influent and effluent concentrations were 0.134 and 0.098 mg/l, respectively.

Significant differences between the influent and effluent concentrations are also present when looking at DP (Figure 3.14). However, concentrations are increasing as water travels through the IESF. Significant increases in DP were observed in years 2014 through 2017 and continued in 2018. Concentrations also increased from the inflow to the outflow monitoring location in years 2012 and 2013, but the datasets were not determined to be statistically different at the 95% confidence level. The year 2014 had the lowest median influent DP concentration of 0.012 mg/l. In 2018, the median influent and effluent DP concentrations were at 0.066 and 0.085 mg/l, respectively.

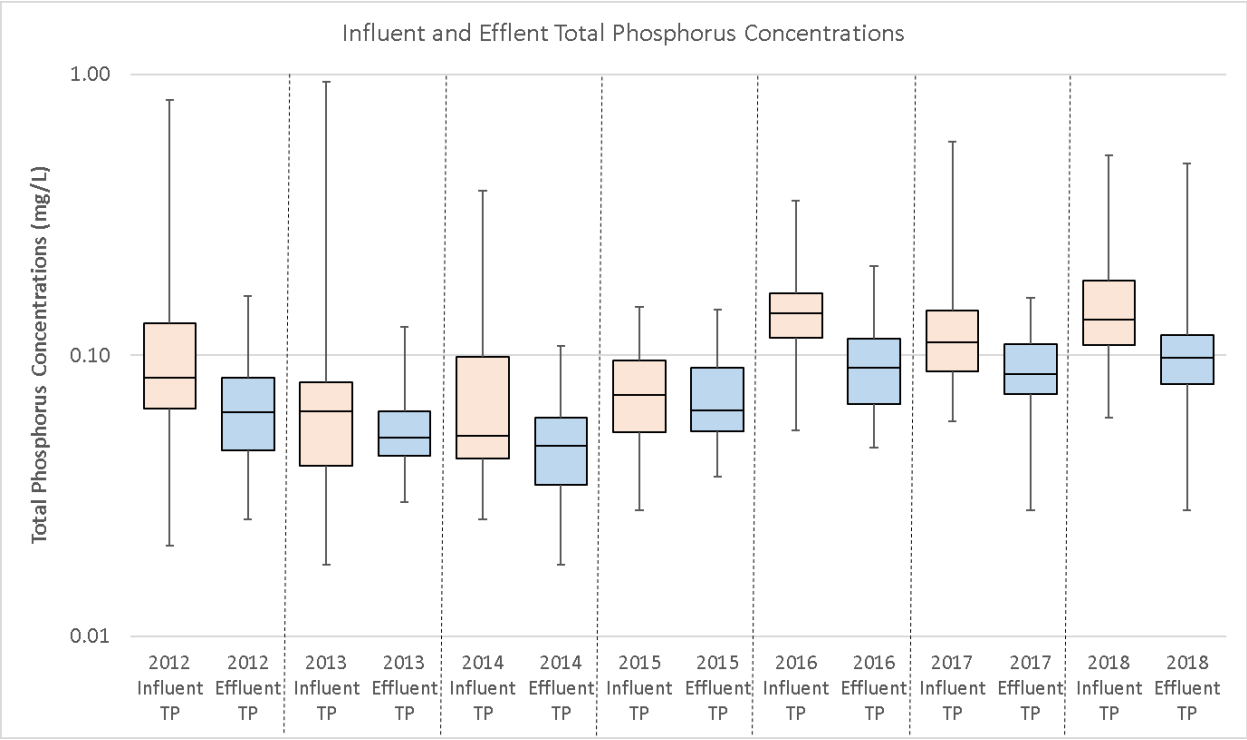

Figure 3.13 A box and whisker plot of annual influent and effluent total phosphorus (TP) from 2012 through 2018

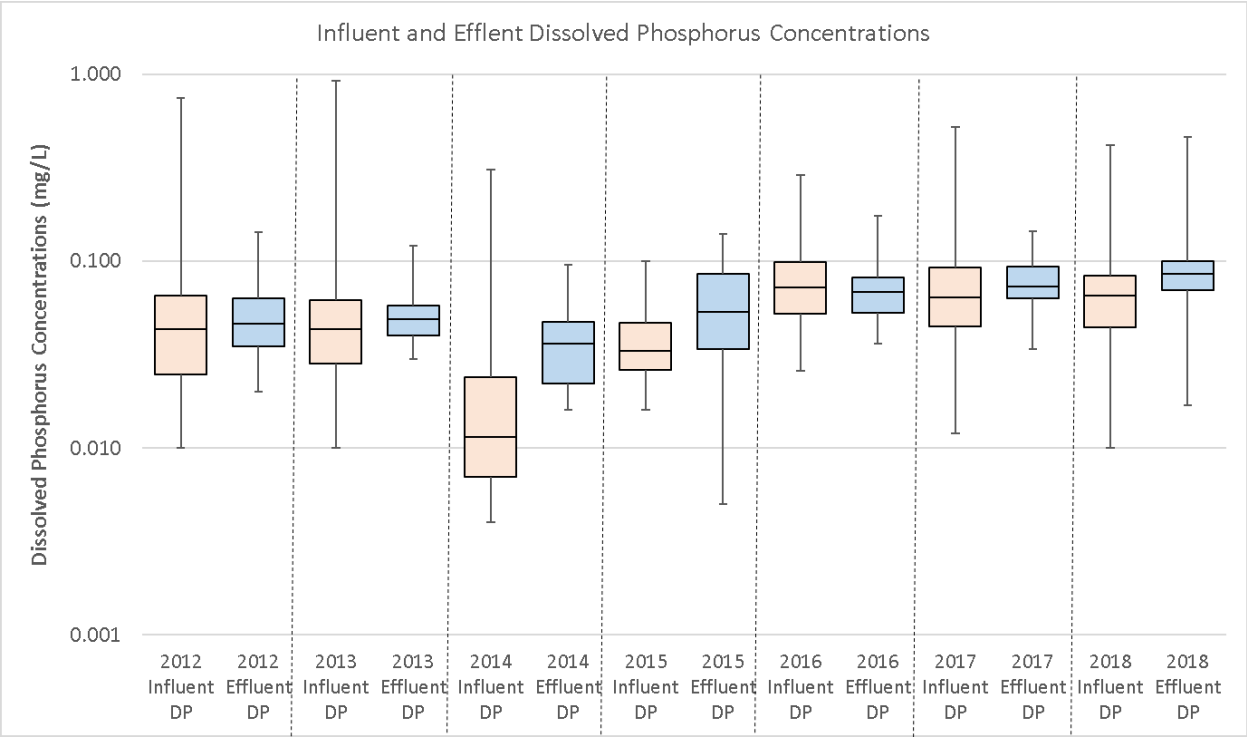

Figure 3.14 A box and whisker plot of annual influent and effluent dissolved phosphorus (DP) from 2012 through 2018

3.3 FINAL NOTES ON HYDROLOGY AND WATER QUALITY DATA ANALYSIS

The water quality data collected from 2012 through 2016 showed that the TH 610 filtration system did not seem to be removing DP from the highway stormwater runoff. This conclusion was based on comparing the effluent and influent DP concentration. Based on other studies done on IESFs, some removal of DP from stormwater runoff was expected. To determine whether the TH 610 IESF was actually removing DP from surface runoff, it was decided to estimate the DP loads into and out of the filter. However, for estimating the DP loads accurate measurement of inflows and outflows is necessary. The hydrology data assessment showed that the annual volume of outflow was larger than the annual volume of inflow, which would exacerbate the ineffectiveness of the TH 610 IESF. As a result, MnDOT retained Barr to develop a hydrologic model to estimate other components of inflow to the IESF for a more realistic performance assessment of the filtration basin. The piezometer readings in the IESF in 2017 and 2018 were also the results of further investigation if the IESF was exhibiting extended saturation conditions and therefore not removing DP. Note that the extended duration of water sitting in the IESF, i.e. partial saturation of IESF, the oxygen is consumed by organic matters (detritus) which will result in anoxic conditions. During anoxia, demand for oxygen results in redox reactions in saturated portion of the filter, i.e., release of oxygen by converting Fe^{+3} to Fe^{+2}, which would result in releasing phosphorus from the iron-bound phosphorus (Sondergaard et al., 2003). The following sections discuss the water balance model of the filtration basin and the performance assessment of the IESF.

CHAPTER 4: HYDROLOGIC MODEL OF THE FILTRATION SYSTEM

The initial data analysis of the volumes of inflow and outflow of the IESF in 2017 and 2018 showed that the outflow volume was greater than inflow volume. In addition, changes in water level of the wet pond indicated that there was a seepage from the wet pond into the IESF during periods of high water level. To account for all sources of inflow to and outflow from the IESF, a hydrologic model was developed for the wet pond and IESF. The model was calibrated to the measured water levels of the wet pond in 2018 and then used for the other monitoring periods of the filtration system. This section provides a description of model parametrization, model parameters, and model calibration and application.

4.1 SITE DETAILS

The drainage areas of the wet pond and IESF were delineated using LiDAR data. Table 4.1 lists the general information of drainage area and the other information provided by MnDOT. Table 4.2 lists all relevant elevations and dimensions of structures used for the model development. Table 4.3 lists information on the berm dimensions that informed seepage calculations between the wet pond and the IESF.

Table 4.1 Drainage areas and depths

Description	Values	Comments
Drainage Area of Wet Pond (acres)	4.58	
Impervious Areas (acres)	2.79	
Pervious Area (acres)	1.79	
Surface Area of Wet Pond (acres)	0.15	
Drainage Area of IESF (acres)	0.70	This is the immediate drainage area
Surface Area of IESF (acres)	0.14	

Table 4.2 Elevations and dimensions of structures

Description	Values	Comments
Berm Overflow Elevation (ft.)	889.37	Between two cells
Berm Overflow Crest Length (ft.)	20	Between two cells
Berm Overflow Height (ft.)	3.8	Between two cells
Inflow Weir V-Notch Elevation (ft.)	888.81	Inflow monitoring location
Height of the Inflow Weir (ft.)	3.23	Inflow monitoring location
Pipe upstream Invert Elevation (ft.)	887.11	Between the manhole and IESF
Pipe downstream Invert Elevation (ft.)	887.39*	Between the manhole and IESF
IESF Surface Elevation (ft.)	887.7	Assuming a horizontal surface
IESF porosity	0.2–0.4	Assumed range of porosity
IESF Water Holding Volume (acre-ft.)	0.118	Assuming a porosity of 0.3

*The surveyed downstream invert elevation of the connecting pipe to the IESF was 887.39; however, measured water level data indicates that the control elevation of the connecting pipe was closer to 887.65.

Table 4.3 Seepage parameters

Description	Values	Comments
Seepage Width (ft.)	90	The width along the berm between the two cells
Seepage Average Length (ft.)	30	Water travel distance between the two cells

4.2 HYDROLOGIC MODELING APPROACH

Initially, a hydrologic model was developed in Excel with a 15-minute time step. However, the size of the data and macros made the model run very slowly, making it impractical for this IES. As a result, the same model was coded using the C-programming language. Some minor modifications were made to some of the processes.

The model was developed such that it could be used for a variable time step because the data from 2012 through 2015 were collected and reported at different time intervals (e.g., 1 minute time steps for rainfall and 15 minute time steps for water levels).

Two watersheds were included in the model, one for the wet pond and one for the IESF. In the hydrologic model it was assumed that the surface runoff was only from the impervious areas and all rain over pervious areas was infiltrated. By reviewing the inflow and outflow data collected in 2017, it was determined that water volumes due to base flow from the drainage areas of the wet pond and the immediate drainage area of the filter basin were needed to balance the water volumes of the entire system. This same conclusion was realized for the 2018 water balance. Therefore, factors impacting water levels in the filter basin include:

- Wet Pond Inflows
    - Precipitation over the wet pond
    - Watershed direct runoff from impervious areas
    - Subsurface flow from pervious areas into the wet pond
- Wet Pond Outflows
    - Evaporation from the wet pond
    - Seepage through the berm from the wet pond into the IESF
    - Discharge through the pipe connecting the wet pond and the IESF
    - Discharge over the riprapped section of the berm during high flows
- IESF Inflows
    - Precipitation over the filter basin
    - Seepage through the berm from the wet pond into the IESF
    - Discharge through the pipe connecting the wet pond and the IESF
    - Subsurface flow from pervious areas into the filter basin
    - Discharge over the riprapped section of the berm during high flows
- IESF Outflows
    - Infiltration from bottom of the filter basin
    - Discharge from the filter basin through drain tile

Inflow and outflow parameters were calibrated to match the observed water levels measured for the wet pond and to approximate the piezometer readings in the IESF.

4.3 MODEL PARAMETERS

Direct precipitation was input into the model based on precipitation measured by the gauge located directly onsite, except for July and November of 2018. For these months, the rain gauge appeared plugged for numerous precipitation events. Precipitation data from Crystal Airport, which is approximately 5 miles southeast of the site, were used to supplement the missing precipitation information collected onsite. The 2018 water balance modeling period started on April 20, 2018, and ended on December 31, 2018. While precipitation data, as well as water level data, was available prior to April 20, 2018, there was not enough data to accurately model snowmelt. Therefore, the hydrologic model started after the snowmelt period. Prior to this, the soil of the drainage area was most likely frozen.

Direct watershed runoff for the site was modeled by dividing the runoff for each watershed into two categories: impervious surface runoff and pervious surface runoff. It was assumed that all precipitation that fell on impervious surfaces became runoff and added to the volume of the wet pond. Precipitation that fell on pervious surfaces was entered into the system as subsurface flow rather than surface flow. Rainfall that infiltrated the pervious areas contributed to the water volumes of the wet pond and filter basin through subsurface movement. Approximately 10% of the water that infiltrated the pervious areas of the wet pond was found to contribute to the water volume of the wet pond. For the IESF, approximately 40% of the water that infiltrated the pervious areas was found to contribute to the water volume of the IESF. The base flow resulting from subsurface storage in the pervious areas surrounding the wet pond or the IESF was modeled using the concept of linear reservoirs as presented in Equation 4-1:

$$V_j = KS_j \qquad \text{4-1}$$

In Equation 4-1, V_j is the volume of base flow during time step j, S_j is subsurface storage during time step j, and K is the linear reservoir constant, a calibration parameter, which was determined to be 0.3 for the pervious area tributary to both the wet pond and the IESF. Note that the subsurface storage was updated at each time step of the model by accounting for inflows (e.g., rain over the pervious area) and outflows (e.g., the base flow computed by equation 4-1).

The seepage from the wet pond into the IESF through the berm separating the two cells was modeled using Darcy's equation. Seepage was estimated based on the head difference between water levels in the wet pond and IESF. It was also assumed that seepage ceased when the water level in the wet pond dropped below the surface of the IESF. This assumption was based on the measured water levels of the wet pond and its rate of change when the wet pond water level was approximately at the surface of IESF. The horizontal saturated hydraulic conductivity in Darcy's equation was a calibration parameter, which was determined to be 1.0×10^{-4} feet per second (fps) or 4.3 inches per hour. A saturated hydraulic conductivity of 4.3 inches per hour is typical of well-drained sandy soils. It is very likely that the saturated hydraulic conductivity of the berm is smaller than this value, however, additional seepage may have been occurring around and under the connecting pipe because the soil under the pipe cannot be

compacted and often the area under such connecting pipes inside embankments become preferential path of seepage with seepage rates typically higher than the rest of embankment.

For the period of record where noticeable leakage through the manhole weir was occurring (October 5, 2018, through December 31, 2018), the seepage rate in the model was increased to 2.0×10^{-3} fps (86 inches per hour) to match the water levels in the wet pond. The leakage of water through the weir created a new normal water level (NWL) of approximately 887.7 in the wet pond. When water levels of the wet pond dropped to this elevation, seepage rates in the model dropped to zero because the water surface elevation of the wet pond matched the top elevation of the IESF.

Discharge from the wet pond to the IESF through the pipe network was modeled using the survey information of the structures (e.g., weir elevations, pipe invert elevations) and the modeled water surface elevations of the wet pond and IESF. The 15-minute time intervals were divided and one minute time steps were used to accurately estimate the flow from the wet pond to the IESF. At the end of each time step, the volume and water level in the wet pond were corrected for the amount of water which passed over the weir. For the computation of flow over the weir, the model accounted for the water level in the IESF when it was inundated to determine if tailwater impacted the flow over the weir. Note that the standard rating curve of the v-notch weir or Thel-mar weir must be corrected when the weir is submerged.

Evaporation was used in the hydrologic model to estimate outflows from the wet pond. Evaporation from the wet pond was estimated using the 2018 monthly lake evaporation for Minneapolis, Minnesota. Evaporation was used for the IESF water balance when the IESF was inundated. The IESF exhibited standing water on top for an extended period during very few events.

Infiltration from the bed of the wet treatment pond was determined to be near zero; however, infiltration from the bed of the IESF was determined to be significant. In fact, the water level in the IESF could not approximate the piezometer levels if infiltration from the bed of the IESF was not computed. Infiltration was estimated using water levels in the IESF and vertical saturated hydraulic conductivity of the bed. The saturated hydraulic conductivity of the bed was a calibration parameter, determined to be 4.5×10^{-6} fps (0.2 inches per hour).

The porosity of filter was also tweaked to simulate measured water levels in the filter, and it was determined that 0.35 would give the best results for model calibration.

Discharge from the IESF was directly input into the model based on outflow measured at the outlet manhole. No effort was made to calibrate this data. According to the MnDOT staff, no obvious errors were observed in the measured data during the modeling period (4/20/2018 to 12/31/2018) (i.e., erroneous discharges).

4.4 MODEL CALIBRATION RESULTS

The hydrologic model was calibrated against the measured water levels of the wet pond in 2018. The model calibration was performed to minimize the root mean square error between the simulated and

measured wet pond water levels. In addition, care was given to approximate the measured piezometer levels in the IESF. It is important to note that measured water levels in April and part of May were the result of snowmelt and the hydrologic model did not simulate frozen soil, snowpack, and snowmelt. As a result, the model could not simulate the piezometer levels in April and May of 2018. However, the water-retaining capacity of the IESF was relatively small; as a result, the model could approximate the observed piezometer levels in the IESF for the rest of the year. Referring to Figure 3.12, during the last months of the year, the two piezometer readings were significantly different and more similar at their peak levels. Therefore, the goal was to approximate the general response of the IESF to rainfall events and then to simulate a water level between the two piezometer readings when the IESF was being drained.

Total rainfall for the 2018 modeling period was 17.1 inches. The root mean square error between the measured and simulated water levels upstream of the weir in the inflow monitoring location was less than 0.1 feet (slightly better than those reported in the 2018 report). The model continuity error (water balance error) was calculated to be 0.01 acre-ft for the wet pond. The model continuity error for the IESF was about 0.2 acre-ft, or roughly 4% of the total outflow from the IESF.

The model results are shown in Figure 4.1. The results of calibration showed that 4.25 acre-ft of water entered the wet pond during the 2018 analysis period (4/20/2018 to 12/31/2018), and 4.43 acre-ft flowed out of the pond. The outflow included 3.1 acre-ft through the manhole weir and overflow section of the berm, 0.28 acre-ft of evaporation, and 1.05 acre-ft of seepage through the berm and leakage of the manhole weir. The outflow from the wet pond is greater than the inflow largely due to the leakage of the manhole weir during the last few months of the year. In early October 2018, noticeable leakage was occurring through the manhole weir, which adjusted the NWL of the wet pond.

For the IESF, 4.77 acre-ft of water flowed into the filter during the 2018 modeling period, of which 0.2 acre-ft was rainfall over the filter surface area, 0.42 acre-ft was the contribution of its immediate drainage area, 1.05 acre-ft was seepage through the berm, and 3.1 acre-ft was inflow from the wet pond. The total outflow was 5.19 acre-ft and included the flow over the outflow weir, infiltration and a small amount of evaporation. Based on monitoring data, inflow was 73% of outflow; however, based on model results, less than 65% of inflow to the IESF was sampled at the inflow monitoring location. Note that the calibration could have been performed by increasing the contribution of the immediate drainage basin of the IESF and thus increasing the rate of infiltration through the bottom of the IESF, and decreasing the mass balance error of the IESF. Such an approach was investigated; however, based on the contribution of the porous area of the wet pond and simulated water levels in the IESF, it was determined that the current calibrated model was more realistic.

Figure 4.2 shows the simulated and measured water levels in the IESF. Overall, the model closely simulates the piezometer readings. The discrepancies are primarily during the periods when the rainfall gauge was not working and the rainfall data from the Crystal Airport were used. The model also shows that from September through October there was at least 2 feet of water sitting in the IESF. Part of that water came from the leakage of the inflow weir and part started before the leakage.

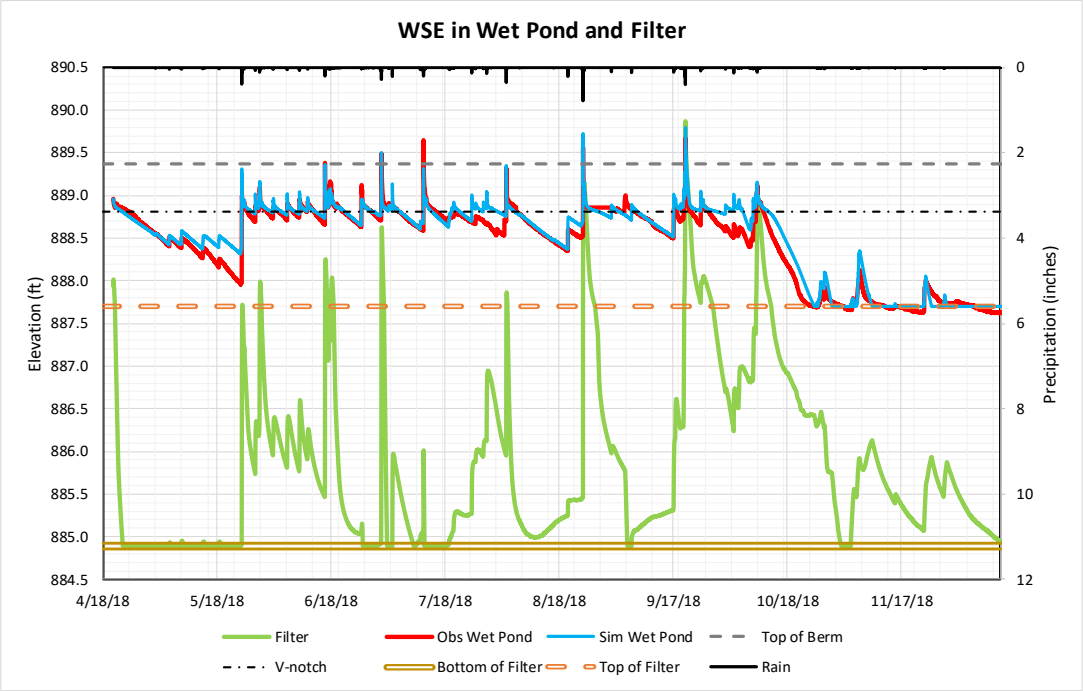

Figure 4.1 The 2018 measured rainfall, observed and simulated water levels in the wet pond, the simulated water surface elevation in the IESF, and lines showing elevations of the berm crest, the v-notch of the inflow weir, and top and bottom of the IESF

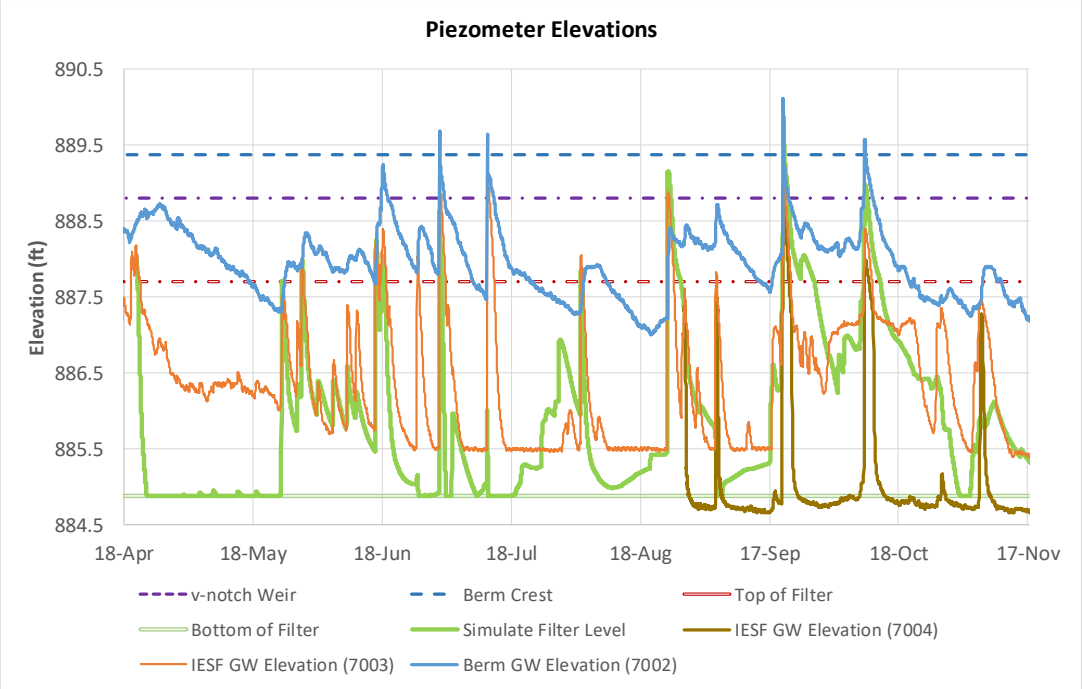

Figure 4.2 The 2018 simulated water level in the IESF, the 2018 measured piezometer levels (7002, 7003 and 7004) in the IESF and berm, and lines showing elevations of the berm crest, the v-notch of the inflow weir, and top and bottom of the IESF

4.5 MODEL APPLICATION TO OTHER PERIODS

The calibrated model was then used to simulate the water levels in the wet pond and IESF and to estimate the total inflow in 2016 and 2017. All calibration parameters were maintained the same as in 2018 except the hydraulic conductivity of the berm, which was used to calculate the seepage through the berm. Based on the report from the MnDOT staff who were collecting the samples and monitoring the filtration system, the inflow weir was leaking slightly in 2016 and 2017 and the leakage was repaired at the beginning of 2018. To account for the small leakage through the inflow weir, the hydraulic conductivity of the berm was increased from $1x10^{-4}$ fps in 2018 to $2x10^{-4}$ fps in 2016 and 2017. The results of the hydrologic model for the 2017 monitoring period are presented in Figure 4.3 and Figure 4.4. Figure 4.3 shows the wet pond and the IESF water levels and the measured rainfall. Total rainfall for the 2017 modeling period was 21.4 inches. In spite of several periods of malfunctioning of the inflow weir pressure transducer, e.g., in mid-May, mid-June, the last two weeks of July and the first week of August, the model appears to be correctly capturing the response of the wet pond to storm events and the seepage through the berm between the two cells of the filtration system. Figure 4.4 shows the comparison of the measured and simulated water levels in the IESF from July through November of 2017. The model appears to be closely simulating the main trends in water levels in IESF, except for the last period. Note that in the 2018 recorded piezometer readings, water level varied across the IESF.

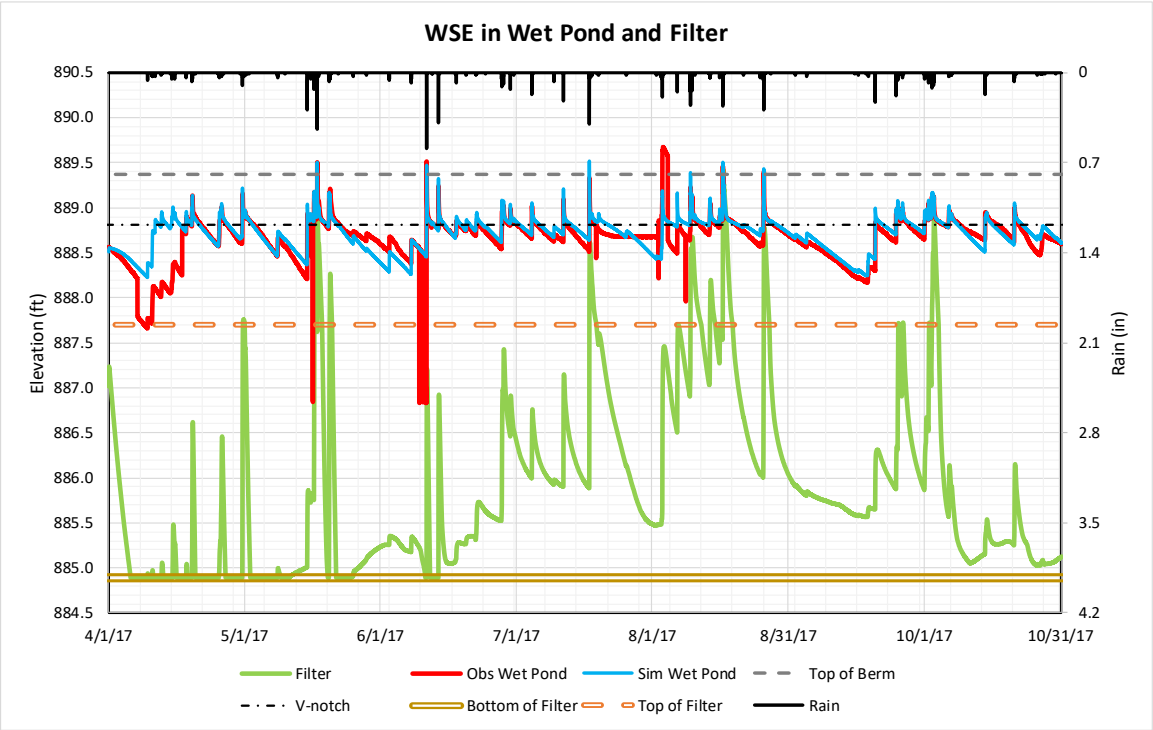

Figure 4.3 The 2017 measured rainfall, observed and simulated water levels in the wet pond, the simulated water surface elevation in the IESF, and lines showing elevations of the berm crest, the v-notch of the inflow weir, and top and bottom of the IESF

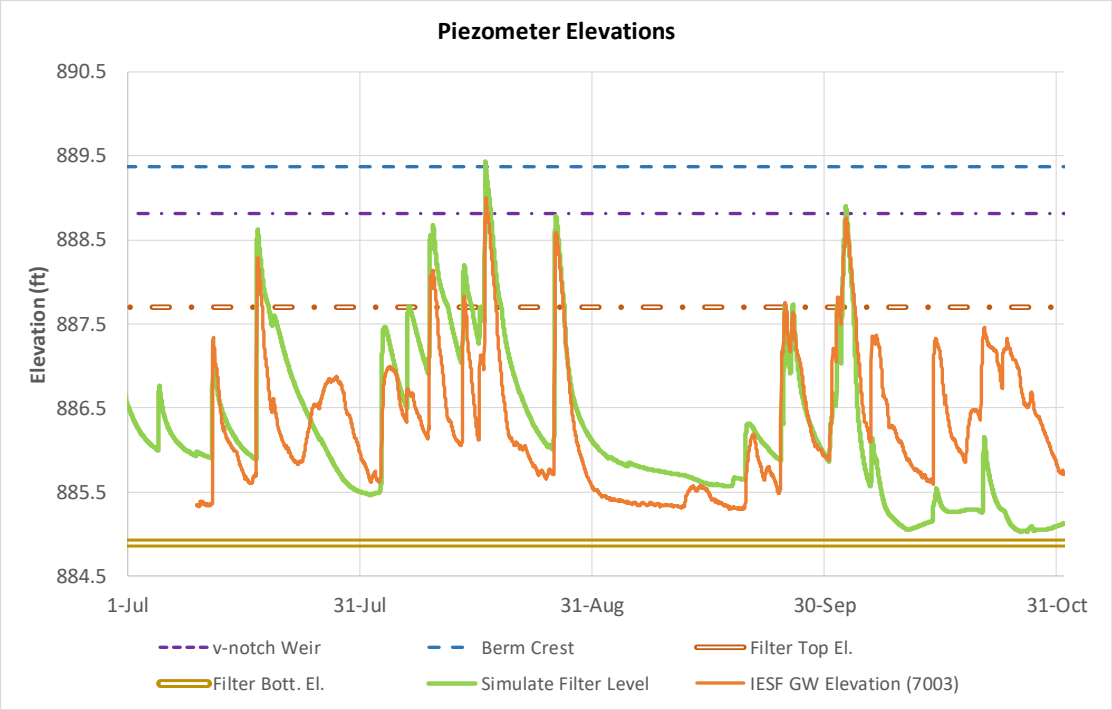

Figure 4.4 The 2017 simulated water level in the IESF, the measured piezometer (7003) level in the IESF, and lines showing elevations of the berm crest, the v-notch of the inflow weir, and top and bottom of the IESF

Both the model results and piezometer readings show that the IESF exhibited over 0.5 feet of water sitting in the filter for over three months that could impact the removal of DP from flows entering the IESF and even releasing some of the previously removed phosphorus from the IESF.

The model results in simulating water levels in the wet pond and IESF during the 2016 monitoring period are shown in Figure 4.5 (note that there was no piezometer installed in the IESF prior to 2017). The monitoring period of 2016 started in June right before a big storm on June 13, 2016. As a result the pressure transducer of the inflow weir exhibited some problems at the beginning of the 2016 monitoring period. In addition, the inflow weir failed in early November which was then repaired by late October. For the period that the inflow weir failed, the model was adjusted to approximate the flow from the wet pond into IESF through the connecting pipe without a weir. Since the pipe had an adverse slope and would run partially full during the low water levels in the wet pond, the model approximated the outflow assuming free fall at the outlet or full pipe flow. In this approximation, the approach did not incorporate the complex flow patterns of a partially full pipe/full pipe condition in the connecting pipe and did not account for the tailwater effect.

Figure 4.5 shows that the model accurately simulates the measured water levels of the wet pond from early July until mid-September before the inflow weir failed. Figure 4.5 also shows that for most of 2016, the IESF was being drained effectively and the IESF was not saturated for an extended period. It is important to note that 2016 has been one of the wettest years in the record and the amount of rainfall

in the modeling period was recorded to be 26.5 inches, which was significantly higher than the rainfall that occurred during the 2017 and 2018 monitoring periods, which were 21.4 and 17.1 inches, respectively. The root mean square error from July 1, 2016, after the piezometer started working properly, until September 9, 2016, right before the failure of the weir was about 0.05 feet. Note that for this period, the measured outflow and rainfall were 5.2 acre-ft and 12.35 inches, respectively. To balance the IESF inflow, outflow and storage, runoff should have been generated from the entire drainage area and not just the impervious area. Therefore, it is very likely that there were significant errors in the measured outflows.

The model was not used to simulate the water levels for the period prior to 2016 with the exception of 2015 because of two reasons: (1) accurately estimating the outflow through the connecting pipe between the cells was a significant undertaking because the flow through the connecting pipe was outlet control due to the adverse slope, and it was often running as a full pipe only for a certain length of the pipe and partially full for the remaining length of the pipe, and (2) the measured outflow during the 2013 and 2014 monitoring period showed a very large difference between outflow and potential inflow into the filtration system and the model could not properly produce such conditions in the system. The outflow and inflow volumes in 2013 were 28 and 2.6 acre-ft, respectively; and in 2014 were 15 and 6.9 acre-ft. In order, to show the model capability in simulating the wet pond water level prior to 2016, the model was used to simulate water levels for the 2015 monitoring period. Figure 4.6 shows the model results for the 2015 monitoring period. In general, the model shows that the water level in the wet pond was at near the top of the IESF and seepage through the berm was very small, i.e. most of the inflow to the IESF was through the connecting pipe. The water balance error for the wet pond was 0.01 acre-ft, but the water balance error for the IESF was 3.9 acre-ft and the model could not resolve the gap between outflow and inflow. The model results also show that the IESF drained very quickly throughout the year, with the exception of a period in May. This is partly due to the fact that the measured outflow was significantly larger than the simulated inflow and therefore IESF was drained very effectively.

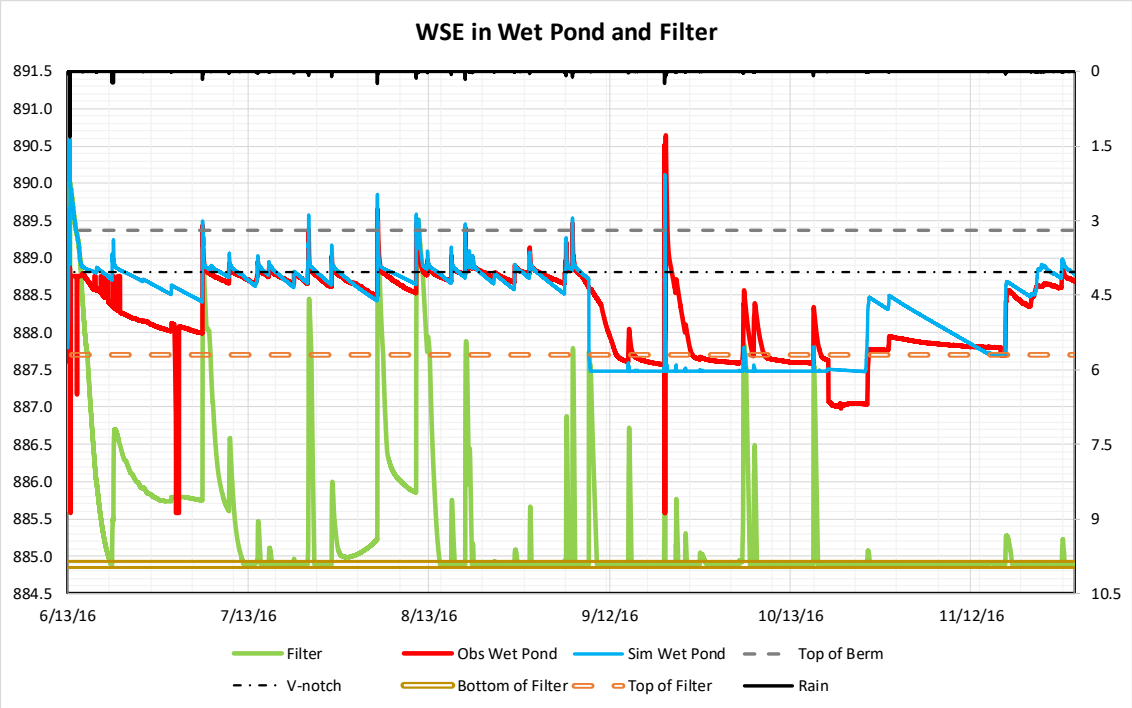

Figure 4.5 The 2016 measured rainfall, observed and simulated water levels in the wet pond, the simulated water surface elevations in the IESF, and lines showing elevations of the berm crest, the v-notch of the inflow weir, and top and bottom of the IESF

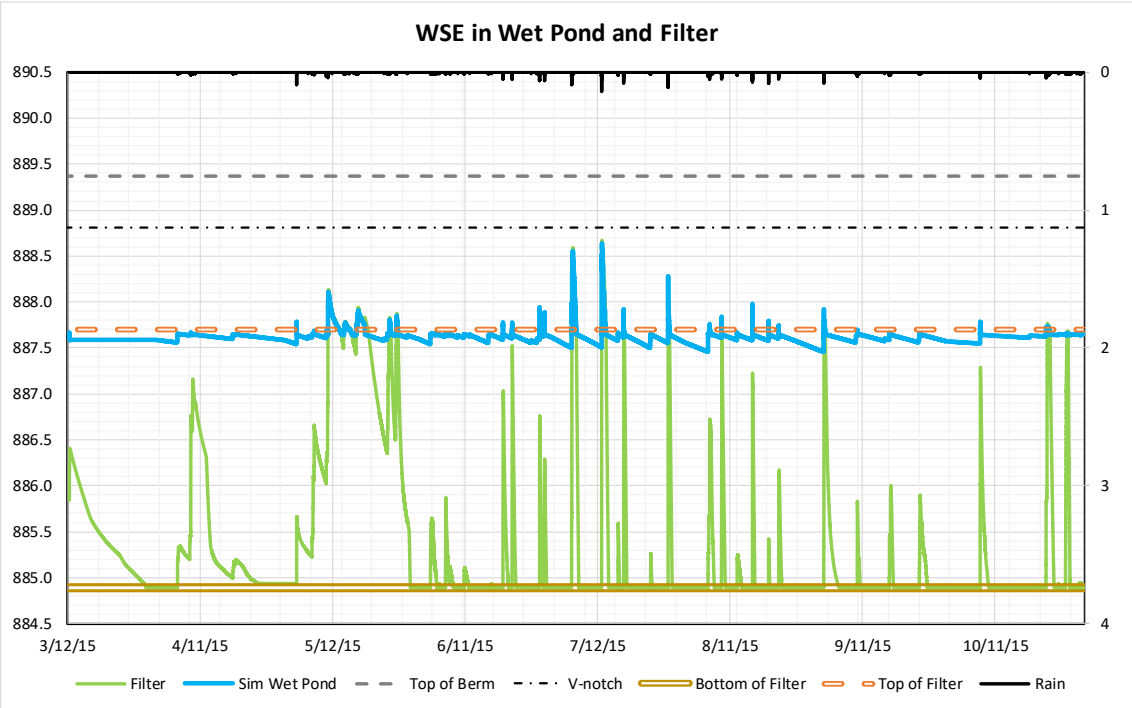

Figure 4.6 The 2015 measured rainfall, observed and simulated water levels in the wet pond, the simulated water surface elevations in the IESF, and lines showing elevations of the berm crest, the v-notch of the inflow weir, and top and bottom of the IESF

CHAPTER 5: MODELING RESULTS

The model was used to estimate the influent and effluent loads of the IESF during three monitoring years: 2016, 2017 and 2018. As discussed in Section 4.5 , other periods were not simulated due to an increased uncertainty in the model inflows to the IESF.

The results of the hydrology model was used to determine the volume of inflow to the IESF during each sampling event. The volume of inflow was the sum of flow over the v-notch weir, the berm, the seepage through the berm and contribution of the pervious areas draining into IESF. The measured outflow at the outflow monitoring location and the estimated infiltration from the IESF were used to determine the volume of outflow from the IESF. These volumes were used to estimate flow-averaged concentration during each every sampling event and to estimate influent and effluent loads.

Table 5.1, Table 5.2 and Table 5.3 list the influent and effluent flow-weighted mean concentrations of the events during the 2018, 2017 and 2016, respectively. The influent flow-weighted mean concentrations have been calculated by incorporating all inflows into the IESF, except the rain over the surface of IESF. The flow-weighted mean concentrations have been calculated by using the estimated flows at a time closest to the sampling time. While this approach provides a measure of how the IESF has been effective in removing TP and DP from the system, it is not thoroughly conclusive because the sampling time and measured flow times are often different and the bias in the selected samples can impact the results. Nevertheless, the results show that the IESF was effective in removing TP but not DP. The results also show that the IESF was not capable of removing TP in every event; three events in 2018, two events in 2017 and one event in 2016 exhibited negative removal efficiencies in removing TP. The number of events with negative removal efficiency in removing DP are significantly higher; ten events in 2018, seven events in 2017 and 4 events in 2016.

Note that the volumes of inflows and outflows are not equal. There are events that the inflow and outflow volumes are an order of magnitude different, e.g., the 9/4/2018 event. The shaded cells show the events for which the outflow volume was higher than the inflow volume. Modeled inflow included flow over the weir, the berm (if any), seepage and the IESF immediate drainage area, and event outflow included measured outflow and infiltration through the bottom of IESF. The infiltration volume is relatively very small, i.e. the measured outflow was the main reason of discrepancy during those events.

There are also two events in Table 5.2 and Table 5.3 that show the IESF was less efficient in removing particulate phosphorus (PP) than removing DP; the 8/16/2017 event in Table 5.2 and the 8/30/2016 event in Table 5.3. It appears that there were some measurement errors during these two events because these are the only events during which the measured influent TP and DP concentrations were very similar (see page B-3 and B-9 in Appendix B).

The loads are presented in Table 5.4, Table 5.5 and Table 5.6. The results show that the TH 610 IESF had a TP removal efficiency of 38%, 34% and 77% in 2018, 2017 and 2016, respectively. By removing the events during which the total volume of outflow was greater than total volume of inflow, the results appear to be slightly better. The results also show that the IESF had a DP removal efficiency of -35%, 2%

and 75% in 2018, 2017 and 2016, respectively. While there are many sources of uncertainty in estimating the removal efficiency of the IESF, in general, it appears that the IESF did not have the potential in removing DP in 2017 and 2016, as it expected and in 2018, the IESF appears to become a DP source instead of a best management practice in removing DP.

However, there seems to be a trend in removing DP since 2016, i.e., the IESF became less efficient. This could be due to two factors. Since 2016, vegetation had been growing over the IESF and by 2018 it covered a large portion of the surface area of the IESF. Vegetation could have been a source of phosphorus loading which was not accounted for in the assessment of the TH 610 IESF. In addition, the model results and the piezometer readings indicate that in 2018 and 2017, the IESF exhibited longer periods of saturation, which could result in anoxia and release of phosphorus (see Figure 4.2, Figure 4.4, and Figure 4.5).

Table 5.1 Influent and effluent flow averaged concentrations of total phosphorus (TP) and dissolved phosphorus (DP) in 2018

Event	Measured precipitation (in)	Modeled Event Inflow (ft^3)[1]	Event Outflow (ft^3)[2]	Total Phosphorus (mg/l)			Dissolved Phosphorus (mg/l)			Particulate Phosphorus (mg/l)		
				Influent Average Conc.	Effluent Average Conc.	Removal Efficiency	Influent Average Conc.	Effluent Average Conc.	Removal Efficiency	Influent Average Conc.	Effluent Average Conc.	Removal Efficiency
4/13/2018	0.02	-	-									
4/19/2018	0.00	-	-									
5/25/2018	0.91	7,780	5,077	0.167	0.065	61%	0.042	0.059	-43%	0.125	0.006	95%
5/29/2018	0.62	7,677	6,502	0.113	0.063	44%	0.012	0.056	-360%	0.101	0.007	93%
6/6/2018	0.19	1,790	1,218	0.077	0.089	-15%	0.040	0.075	-90%	0.038	0.014	64%
6/9/2018	0.25	2,601	2,107	0.095	0.097	-2%	0.050	0.088	-76%	0.045	0.009	81%
6/11/2018	0.13	1,289	1,451	0.090	0.083	8%	0.057	0.080	-41%	0.034	0.003	90%
6/16/2018	1.76	17,555	13,289	0.130	0.096	26%	0.028	0.083	-202%	0.103	0.013	87%
6/19/2018	0.23	488	2,765	0.242	0.139	43%	0.137	0.096	30%	0.104	0.043	59%
6/26/2018	0.32	2,805	5,061	0.134	0.119	11%	0.063	0.106	-70%	0.071	0.013	82%
7/12/2018	0.80	7,184	16,903	0.181	0.137	24%	0.082	0.100	-22%	0.099	0.037	62%
8/24/2018	1.55	14,534	11,180	0.166	0.050	70%	0.090	0.045	51%	0.076	0.005	93%
9/4/2018	0.00	270	3,001	0.196	0.105	47%	0.099	0.089	10%	0.097	0.015	84%
9/18/2018	0.10	1,469	972	0.418	0.095	77%	0.318	0.084	74%	0.100	0.011	89%
9/20/2018	2.20	21,842	11,557	0.096	0.366	-282%	0.063	0.329	-427%	0.033	0.037	-10%
10/9/2018	1.03	11,866	5,389	0.108	0.097	10%	0.081	0.087	-8%	0.027	0.009	65%

[1] Event inflow to the IESF includes modeled inflows over the upstream weir and overflow weir, modeled seepage through the berm, and modeled watershed runoff.

[2] Event outflow from the IESF includes measured outflows over the downstream weir and infiltration through the IESF bed.

Table 5.2 Influent and effluent flow averaged concentrations of total phosphorus (TP) and dissolved phosphorus (DP) in 2017

Event	Measured precipitation (in)	Modeled Event Inflow (ft^3)[1]	Event Outflow (ft^3)[2]	Total Phosphorus (mg/l)			Dissolved Phosphorus (mg/l)			Particulate Phosphorus (mg/l)		
				Influent Average Conc.	Effluent Conc.	Removal Efficiency	Influent Average Conc.	Effluent Conc.	Removal Efficiency	Influent Average Conc.	Effluent Conc.	Removal Efficiency
4/18/2017	0.67	7138	10566	0.124	0.092	26%	0.029	0.079	-176%	0.095	0.013	86%
4/25/2017	0.64	5882	6149	0.105	0.118	-12%	0.030	0.091	-200%	0.074	0.026	64%
5/1/2017	0.86	9657	7385	0.230	0.102	56%	0.156	0.085	45%	0.074	0.016	78%
5/17/2017	1.73	13540	17790	0.269	0.135	50%	0.105	0.099	6%	0.164	0.036	78%
5/20/2017	1.15	13916	15152	0.097	0.085	13%	0.062	0.066	-7%	0.036	0.019	47%
6/11/2017	0.79	5887	12473	0.243	0.085	65%	0.051	0.075	-45%	0.192	0.010	95%
6/28/2017	0.63	6308	4224	0.113	0.086	23%	0.061	0.078	-26%	0.051	0.009	83%
7/17/2017	1.10	12682	7642	0.140	0.084	40%	0.075	0.074	2%	0.065	0.010	84%
8/9/2017	0.98	11732	6275	0.077	0.087	-14%	0.039	0.081	-107%	0.037	0.006	83%
8/16/2017	1.29	16934	12907	0.127	0.088	31%	0.110	0.068	38%	0.017	0.020	-14%
8/26/2017	1.12	14558	10986	0.137	0.085	38%	0.108	0.080	26%	0.030	0.005	82%
10/2/2017	1.16	14161	12249	0.081	0.080	1%	0.046	0.073	-60%	0.035	0.007	81%
10/14/2017	0.34	1915	1734	0.092	0.044	52%	0.068	0.043	36%	0.025	0.001	97%

[1] Event inflow to the IESF includes modeled inflows over the upstream weir and overflow weir, modeled seepage through the berm, and modeled watershed runoff.

[2] Event outflow from the IESF includes measured outflows over the downstream weir and infiltration through the IESF bed.

Table 5.3 Influent and effluent flow averaged concentrations of total phosphorus (TP) and dissolved phosphorus (DP) in 2016

Event	Measured precipitation (in)	Modeled Event Inflow (ft^3)[1]	Event Outflow (ft^3)[2]	Total Phosphorus (mg/l)			Dissolved Phosphorus (mg/l)			Particulate Phosphorus (mg/l)		
				Influent Average Conc.	Effluent Average Conc.	Removal Efficiency	Influent Average Conc.	Effluent Average Conc.	Removal Efficiency	Influent Average Conc.	Effluent Average Conc.	Removal Efficiency
6/12/2016	2.92											
7/10/2016	0.33	2,001	1,645	0.163	0.056	66%	0.074	0.049	34%	0.089	0.007	92%
7/27/2016	0.40	1,104	549	0.129	0.067	48%	0.040	0.054	-35%	0.089	0.013	85%
8/4/2016	1.82	19,914	11,510	0.311	0.143	54%	0.255	0.102	60%	0.056	0.041	27%
8/10/2016	2.29	21,498	2,843	0.136	0.114	17%	0.061	0.078	-28%	0.075	0.036	53%
8/30/2016	0.25	3,066	3,691	0.072	0.159	-121%	0.066	0.071	-7%	0.006	0.088	-1440%
11/27/2016	0.31	2,144	2,758	0.149	0.070	53%	0.045	0.065	-45%	0.104	0.005	95%

Table 5.4 Influent and effluent loads of total phosphorus (TP) and dissolved phosphorus (DP) in 2018

	Total Phosphorus (lbs)			Dissolved Phosphorus (lbs)		
Loads	Influent Load	Effluent Load	Removal Efficiency	Influent Load	Effluent Load	Removal Efficiency
4/13/2018	-	-	-	-	-	-
4/19/2018	-	-	-	-	-	-
5/25/2018	0.065	0.020	70%	0.020	0.017	12%
5/29/2018	0.055	0.024	55%	0.007	0.022	-207%
6/6/2018	0.010	0.006	45%	0.006	0.005	19%
6/9/2018	0.015	0.012	20%	0.008	0.011	-39%
6/11/2018	0.008	0.006	22%	0.005	0.006	-17%
6/16/2018	0.174	0.063	64%	0.033	0.055	-64%
6/19/2018	0.007	0.021	-197%	0.004	0.015	-286%
6/26/2018	0.023	0.032	-41%	0.011	0.028	-158%
7/12/2018	0.093	0.098	-6%	0.041	0.083	-101%
8/24/2018	0.151	0.030	80%	0.090	0.027	70%
9/4/2018	0.003	0.016	-384%	0.002	0.013	-729%
9/18/2018	0.043	0.006	87%	0.033	0.005	85%
9/20/2018	0.147	0.204	-39%	0.090	0.183	-104%
10/9/2018	0.081	0.006	92%	0.002	0.006	-194%
All events	**0.87**	**0.54**	**38%**	**0.35**	**0.48**	**-35%**
Modified[1]	**0.76**	**0.40**	**47%**	**0.30**	**0.35**	**-18%**

[1] Modified by excluding the events in the shaded cells of the first column, when outflow was greater than inflow

Table 5.5 Influent and effluent loads of total phosphorus (TP) and dissolved phosphorus (DP) in 2017

	Total Phosphorus			Dissolved Phosphorus		
Loads	Influent Load	Effluent Load	Removal Efficiency	Influent Load	Effluent Load	Removal Efficiency
4/18/2017	0.052	0.060	-16%	0.009	0.050	-453%
4/25/2017	0.039	0.044	-12%	0.014	0.035	-143%
5/1/2017	0.113	0.046	60%	0.074	0.038	49%
5/17/2017	0.221	0.146	34%	0.089	0.118	-32%
5/20/2017	0.085	0.079	7%	0.053	0.062	-17%
6/11/2017	0.072	0.069	4%	0.033	0.063	-92%
6/28/2017	0.044	0.022	50%	0.025	0.021	17%
7/17/2017	0.101	0.044	57%	0.057	0.038	33%
8/9/2017	0.064	0.035	46%	0.035	0.032	8%
8/16/2017	0.122	0.072	41%	0.107	0.056	48%
8/26/2017	0.137	0.059	57%	0.102	0.054	47%
10/2/2017	0.069	0.064	7%	0.039	0.060	-54%
10/14/2017	0.010	0.005	48%	0.008	0.005	39%
All events	**1.13**	**0.75**	**34%**	**0.65**	**0.63**	**2%**
Modified[1]	**0.66**	**0.35**	**47%**	**0.45**	**0.30**	**32%**

[1] Modified by excluding the events in the shaded cells of the first column, when outflow was greater than inflow

Table 5.6 Influent and effluent loads of total phosphorus (TP) and dissolved phosphorus (DP) in 2016

	Total Phosphorus (lbs)			Dissolved Phosphorus (lbs)		
Loads	Influent Load	Effluent Load	Removal Efficiency	Influent Load	Effluent Load	Removal Efficiency
6/12/2016	-					
7/10/2016	0.019	0.006	68%	0.010	0.005	44%
7/27/2016	0.009	0.002	76%	0.003	0.002	44%
8/4/2016	0.370	0.061	83%	0.306	0.053	83%
8/10/2016	0.164	0.020	88%	0.084	0.013	84%
8/30/2016	0.015	0.036	-133%	0.014	0.020	-37%
11/27/2016	0.022	0.012	44%	0.008	0.011	-46%
All events	**0.60**	**0.14**	**77%**	**0.42**	**0.10**	**75%**
Modified[1]	**0.40**	**0.07**	**83%**	**0.32**	**0.06**	**81%**

[1] Modified by excluding the events in the shaded cells of the first column, when outflow was greater than inflow

CHAPTER 6: CONCLUSIONS AND RECOMMENDATIONS

Based on the results of monitoring the TH 610 IESF, a number of recommendations are provided for monitoring of future installations of iron-enhanced sand filters. Note that the Minnesota Pollution Control Agency (MPCA) has developed the design criteria for IESFs, which are being continuously updated based on the experience gained by practitioners on numerous installations. Herein, the focus will be on monitoring of IESF.

In general, field data collection is an expensive, challenging task with numerous uncontrolled factors affecting data collection and therefore the assessment of any installations. As a result, when an IESF is designed with the idea of being monitored, the focus of design should be on minimizing the uncontrolled factors. The TH 610 IESF showed that when all inflows and outflows cannot be monitored, then it would be difficult to determine how well the system removes DP and TP from stormwater runoff. The proposed recommendations are primarily for new installations with a monitoring plan.

- If a berm is to be built between the pretreatment pond and IESF, a liner should be used in the design of the berm to prevent or significantly reduce any seepage between the wet pond and IESF.
- An IESF will function as a sink for the surrounding area during storm events. As a result, the immediate drainage area of the IESF should be small to reduce the contribution of the non-monitored drainage area. As recommended by MPCA, the designed IESF should be capable of draining within 48 hours after the completion of a storm. The design guidelines do not specify the storm, but it is assumed that the guidelines are referring to the outlet control structure and the drain tiles being capable of draining the volume of water contained in the filter within 48 hours. Immediate drainage area of the filter can prolong the time to drain the filter. Therefore, a smaller drainage area will allow the system to be drained more effectively and not exhibit anoxia in the filter basin.
- Install several piezometers in the filter to monitor water levels in the filter.
- Take a measurement of dissolved oxygen (DO) in the filter at the site.
- The surface of the filter should be continuously monitored and cleaned from any vegetation in the IESF.
- The inflow monitoring system should be designed to avoid the tailwater effects.
    - Crest of inflow weir (or the v-notch) should be set high enough so the inundated filter basin will not impact the flow measurement during large storm events.
    - It is preferred to build the overflow structure between the wet pond and IESF such that the volume of overflow can be accurately estimated during large storm events.
    - The overflow structure should be located far enough from the inflow points into the wet pond to prevent short circuiting and allowing the wet pond to function as a pretreatment pond.
- It is important to have a functioning onsite rain gauge to accurately estimate the amount of rainfall over the basin and the drainage area of the filtration system. A functioning rain gauge will inform the monitoring team if the spikes in flow monitoring devices are due to rainfall

events or malfunctioning of devices. In addition, the rain gauge will provide the order of magnitude of inflow to the IESF during each storm event.

- Biweekly or monthly visits of the installation are necessary to check all instruments are functioning accurately (e.g., rain gauge, pressure transducer, automatic samplers, etc.)
- It is important to complete some preliminary data analysis after each storm event. Any anomaly in the results of the preliminary data analysis can inform the monitoring team to apply necessary corrections to the monitoring plan. As part of a routine data analysis complete the following tasks:
    - Check for any erratic flow in the recorded hydrograph.
    - Estimate and compare volumes of outflow and inflow for each event.
        - Determine the length of period after the end of storm that the volume outflow becomes equal to the volume of inflow.
    - Select the samples for laboratory analysis such that the volumes of inflow and outflow become equal.
    - Plot the recorded rainfall versus volume of monitored outflow and inflow during the event.
        - Over time, the data should fall closely around a linear relationship between volume of runoff and rainfall.
    - Check for anomaly in the recorded concentrations.
    - Compare the time series of piezometer readings with time series of DO measurements.
    - From the DO measurement time series, identify the periods that DO becomes zero, i.e., anoxic conditions. Determine the periods that the filter would exhibit anoxia. This can vary from one site to another based on the source and type of pollutants.

APPENDIX A
2012 THROUGH 2015 POLLUTOGRAPHS

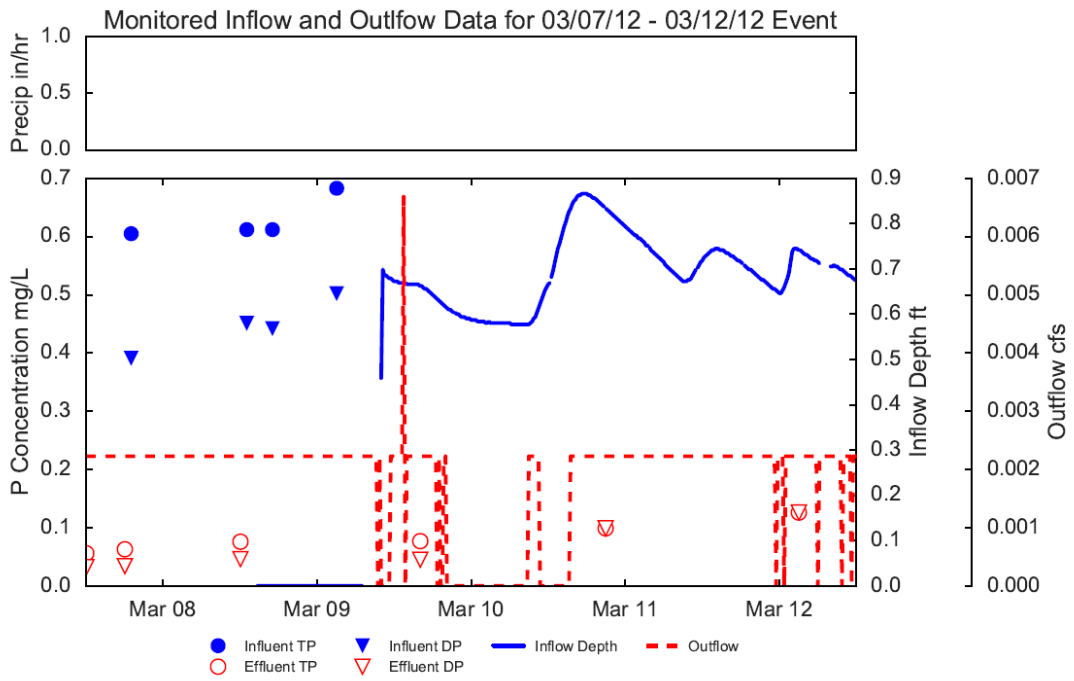

Figure A. 1 Measured influent and effluent TP and DP concentrations, inflow depth, and outflow for the March 7 through March 12, 2012 monitoring event.

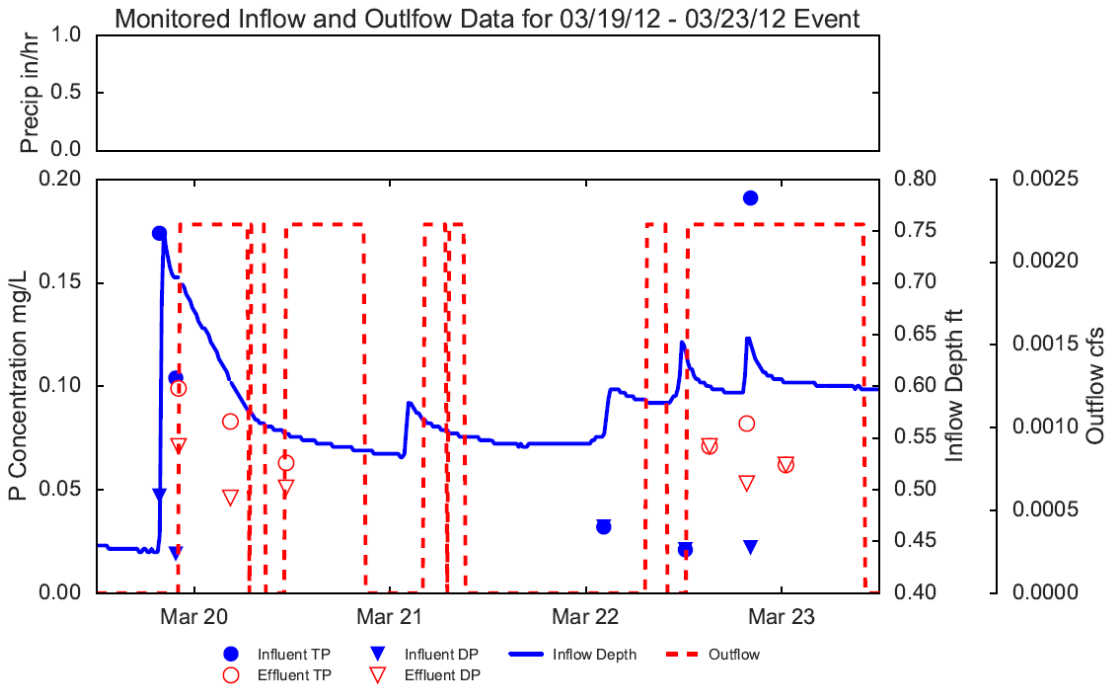

Figure A. 2 Measured influent and effluent TP and DP concentrations, inflow depth, and outflow for the March 19 through March 23, 2012 monitoring event.

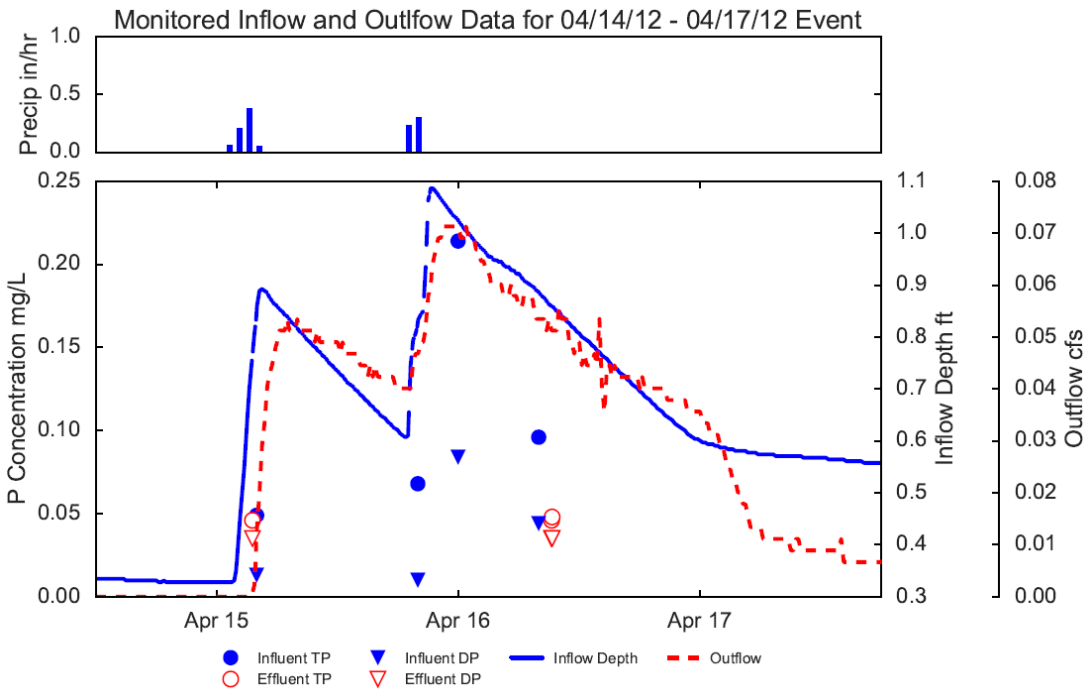

Figure A. 3 Measured influent and effluent TP and DP concentrations, inflow depth, outflow, and precipitation for the April 14 through April 17, 2012 monitoring event.

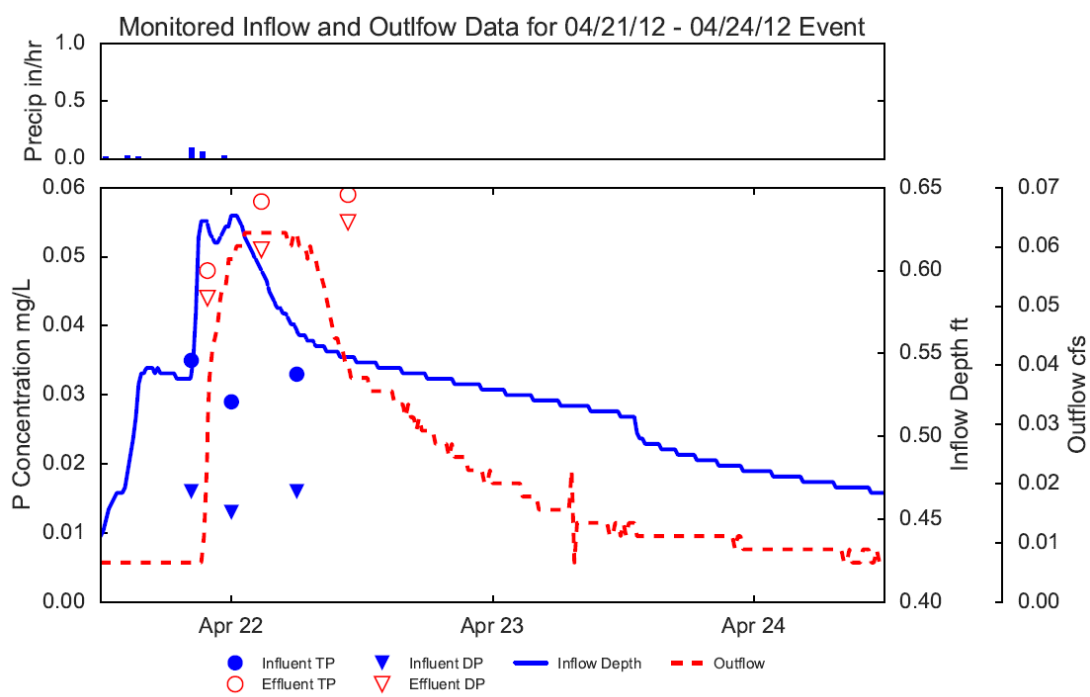

Figure A. 4 Measured influent and effluent TP and DP concentrations, inflow depth, outflow, and precipitation for the April 21 through April 24, 2012 monitoring event.

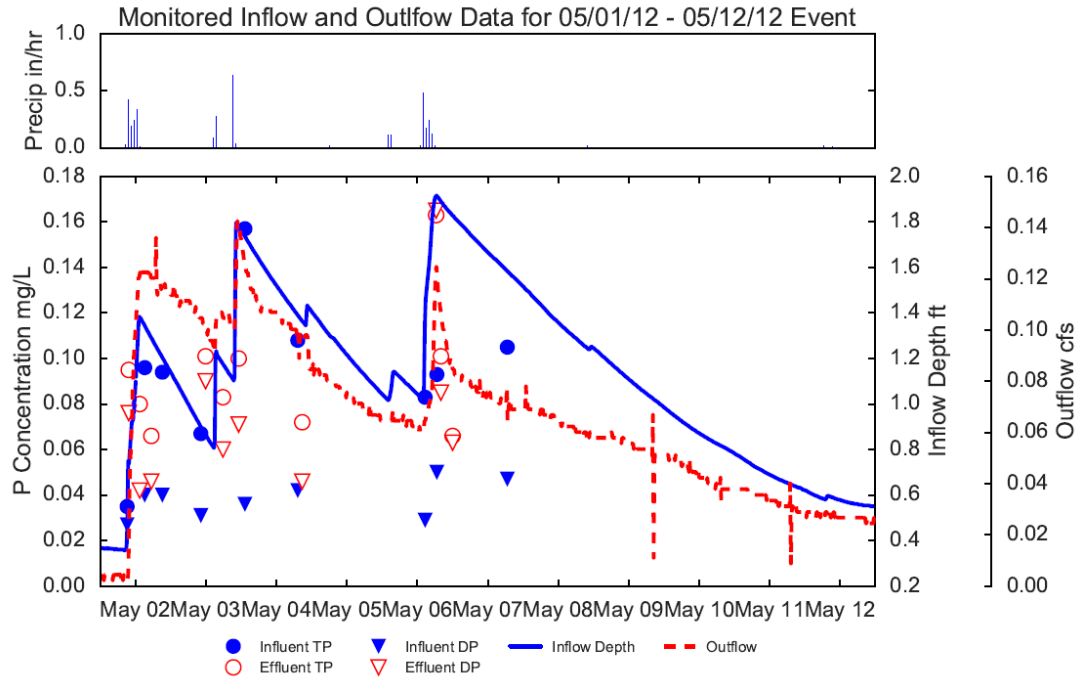

Figure A. 5 Measured influent and effluent TP and DP concentrations, inflow depth, outflow, and precipitation for the May 1 through May 12, 2012 monitoring event.

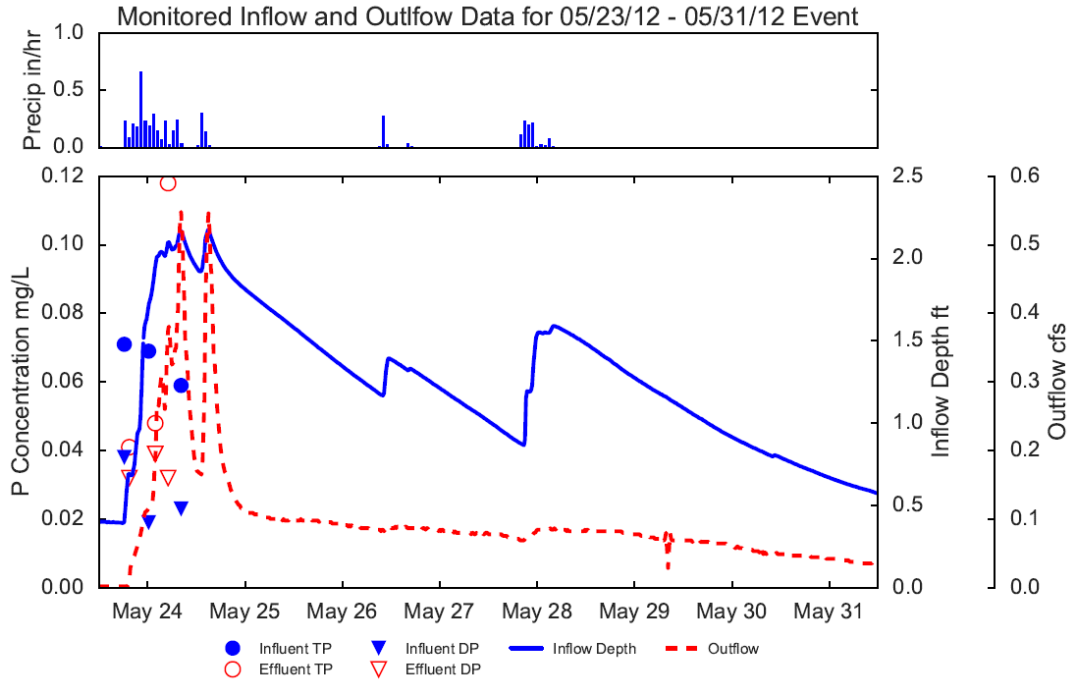

Figure A. 6 Measured influent and effluent TP and DP concentrations, inflow depth, outflow, and precipitation for the May 23 through May 31, 2012 monitoring event.

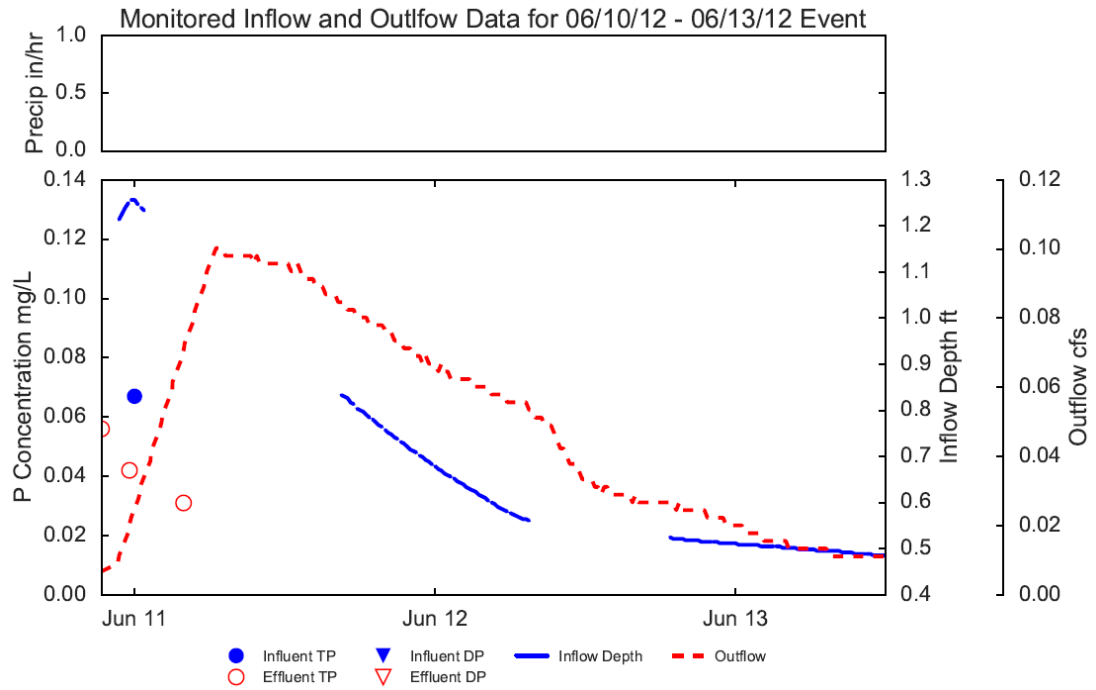

Figure A. 7 Measured influent and effluent TP and DP concentrations, inflow depth, and outflow for the June 10 through June 13, 2012 monitoring event.

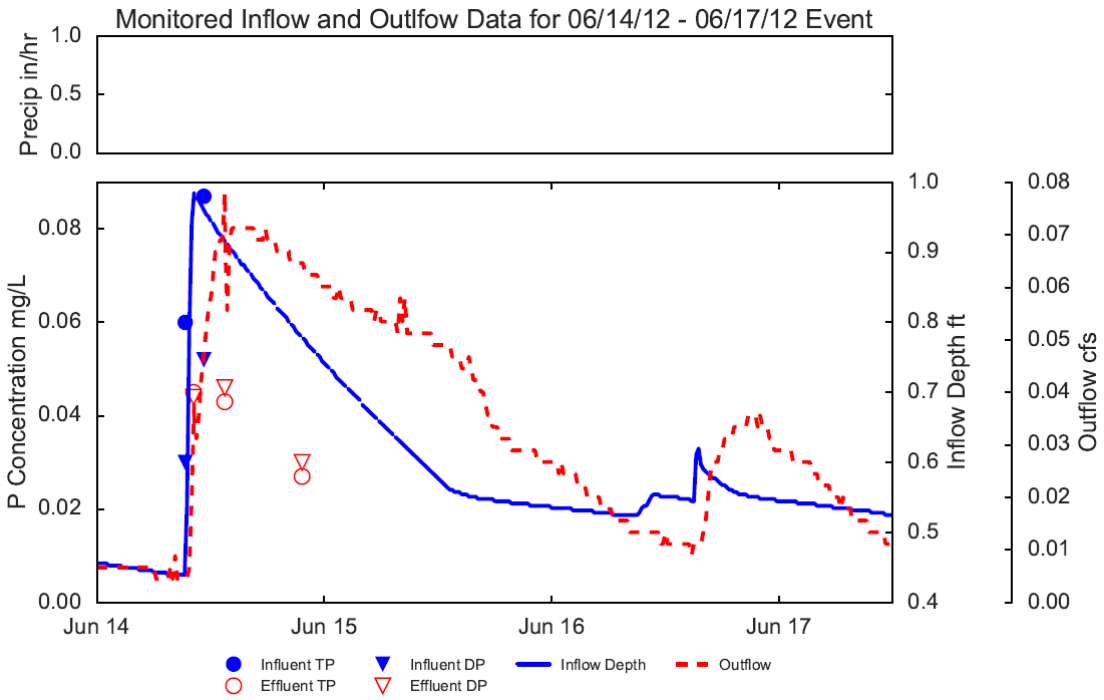

Figure A. 8 Measured influent and effluent TP and DP concentrations, inflow depth, and outflow for the June 14 through June 17, 2012 monitoring event.

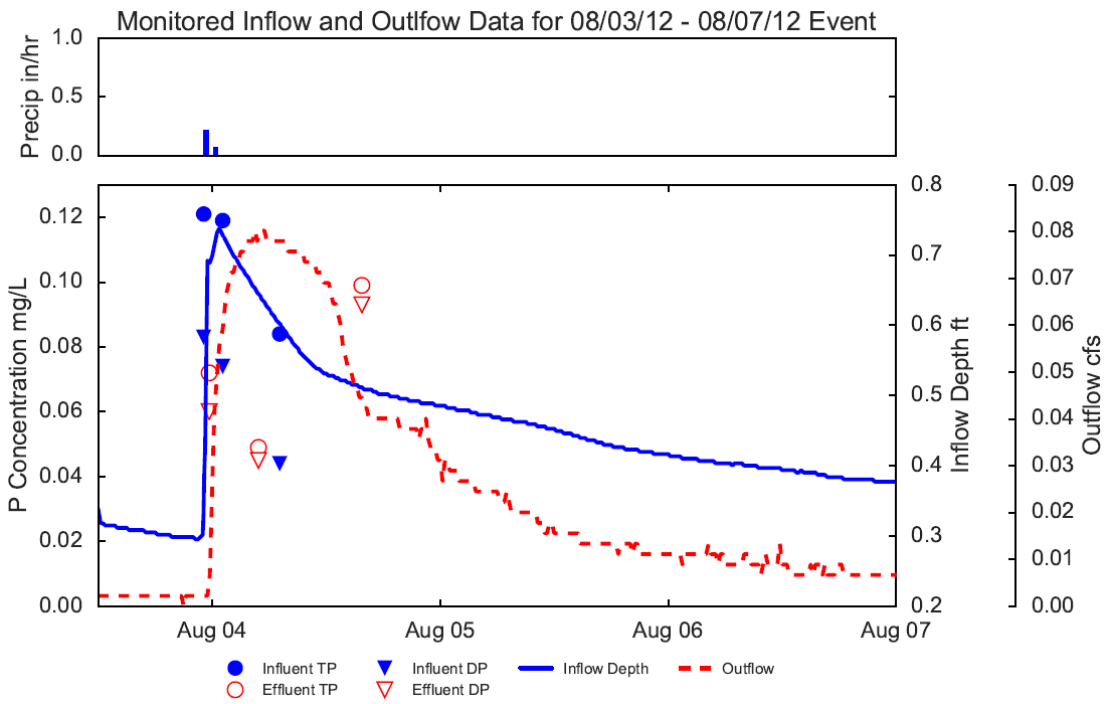

Figure A. 9 Measured influent and effluent TP and DP concentrations, inflow depth, outflow, and precipitation for the August 3 through August 7, 2012 monitoring event.

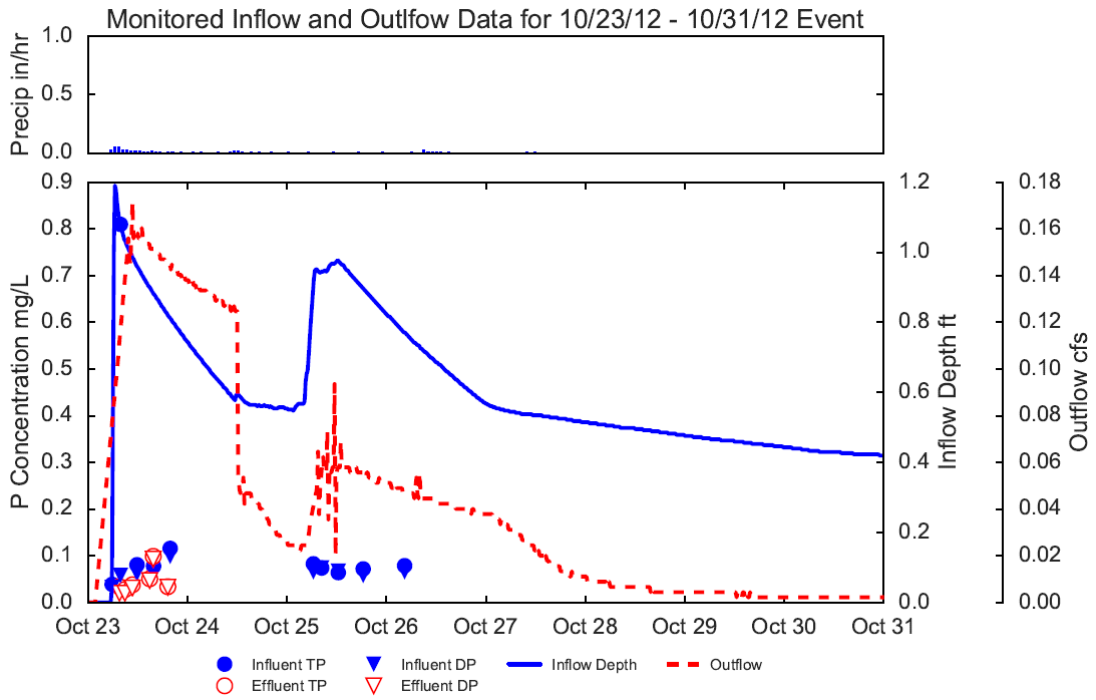

Figure A. 10 Measured influent and effluent TP and DP concentrations, inflow depth, outflow, and precipitation for the October 23 through October 31, 2012 monitoring event.

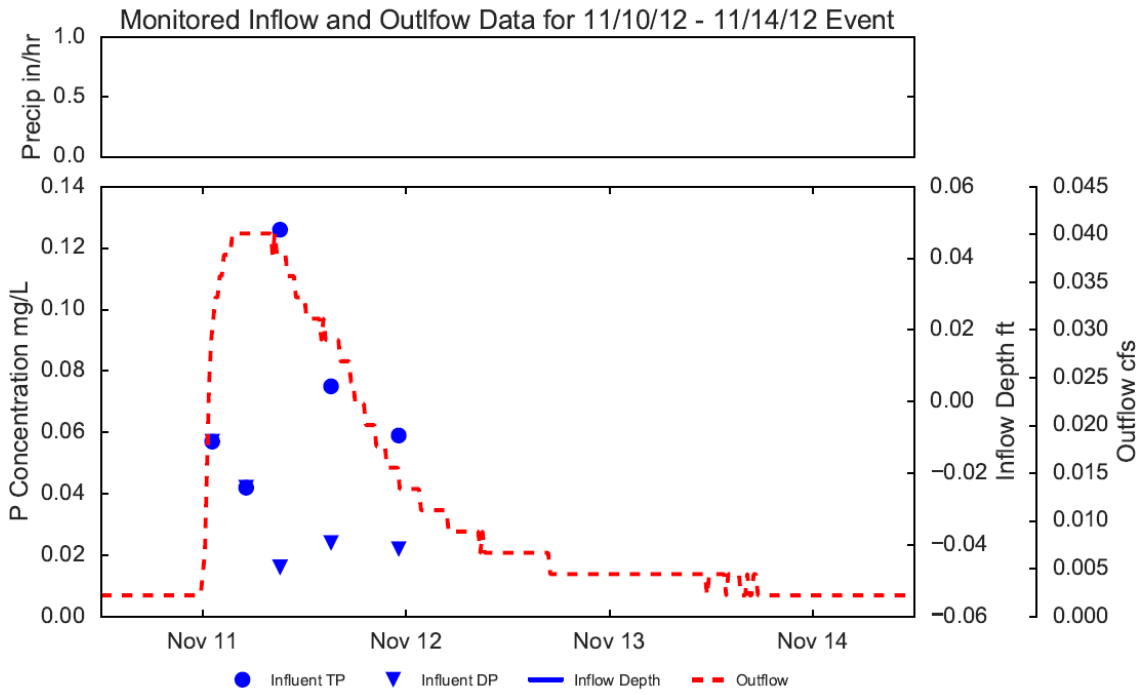

Figure A. 11 Measured influent TP and DP concentrations, and outflow for the November 10 through November 14, 2012 monitoring event.

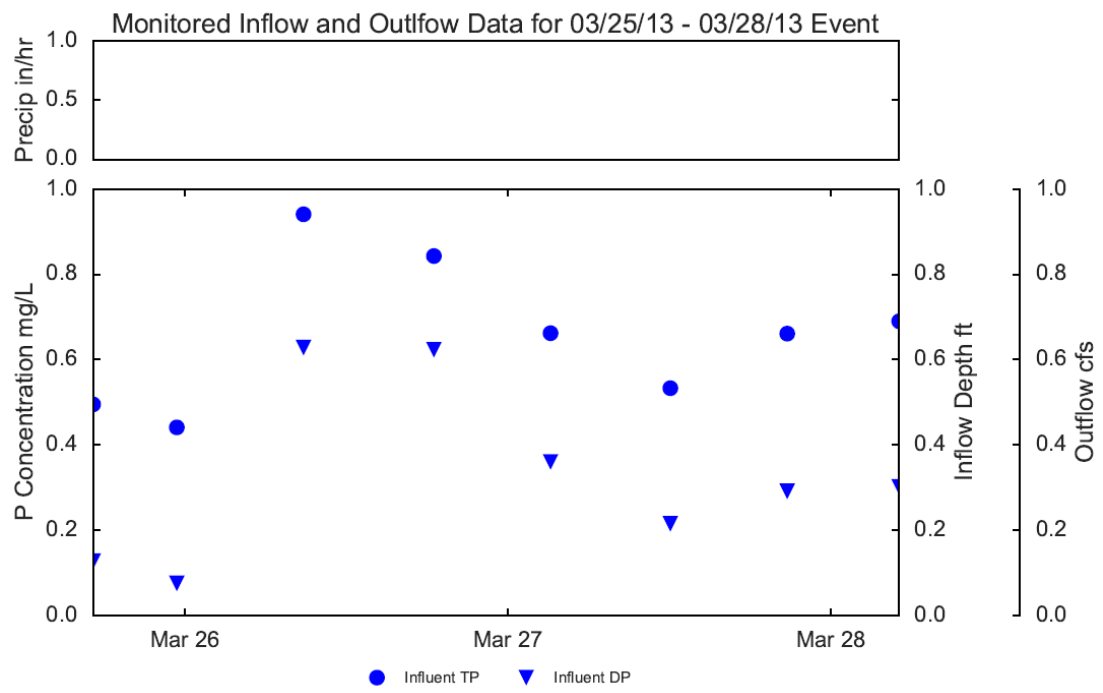

Figure A. 12 Measured influent TP and DP concentrations for the March 25 through March 28, 2013 monitoring event.

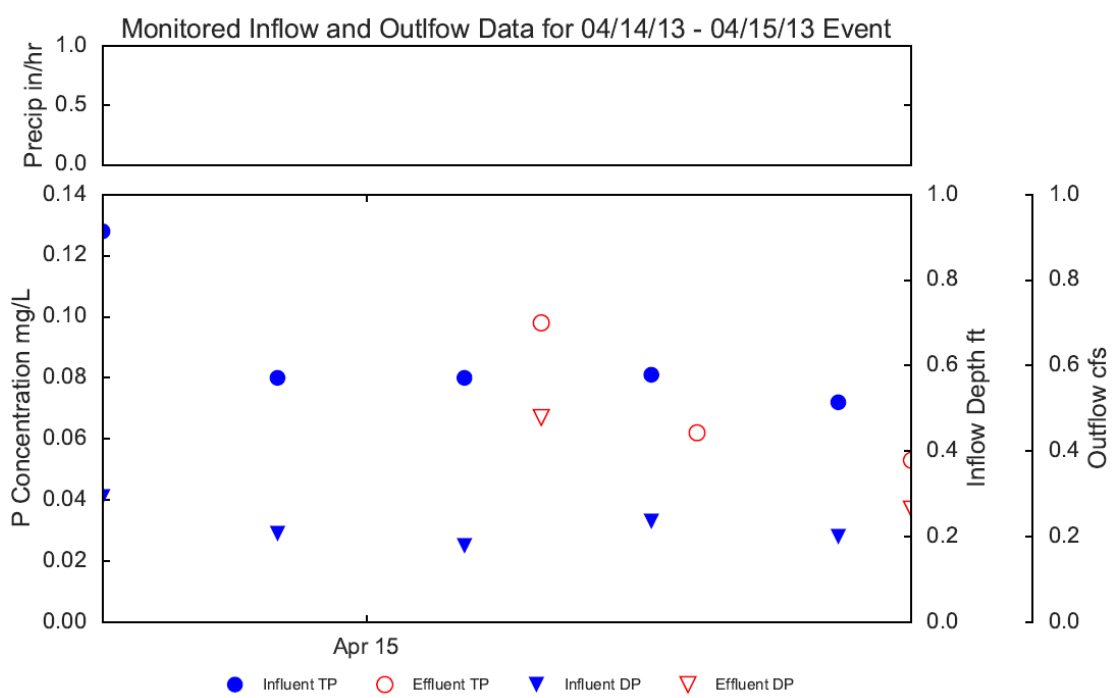

Figure A. 13 Measured influent and effluent TP and DP concentrations for the April 13 through April 15, 2013 monitoring event.

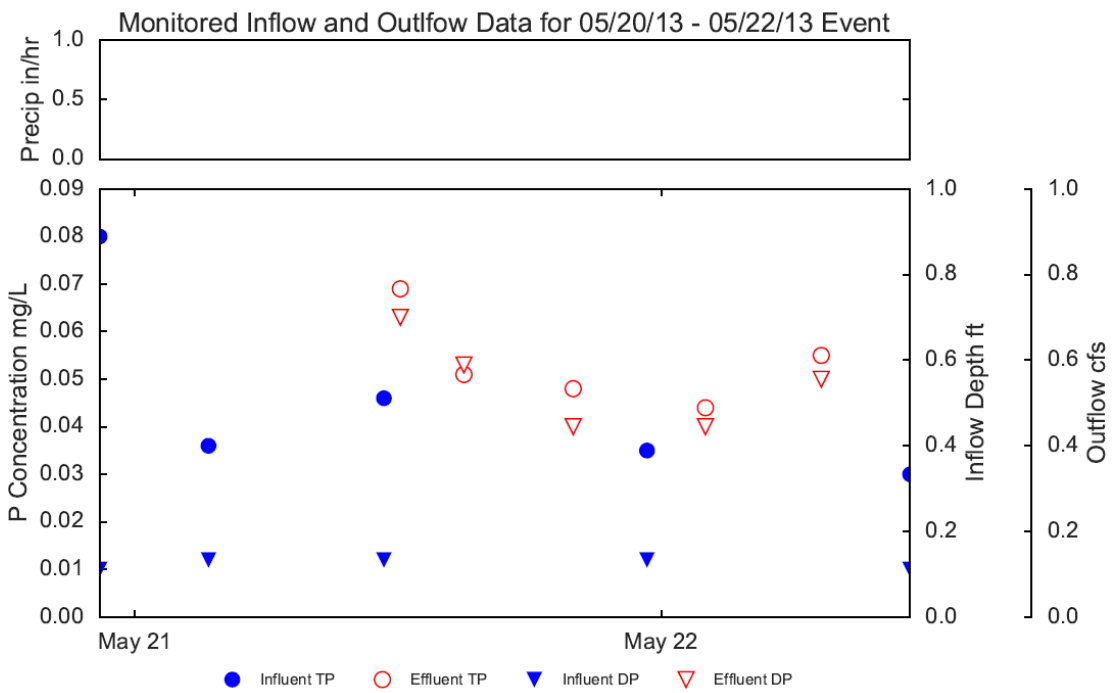

Figure A. 14 Measured influent and effluent TP and DP concentrations for the May 20 through May 22, 2013 monitoring event.

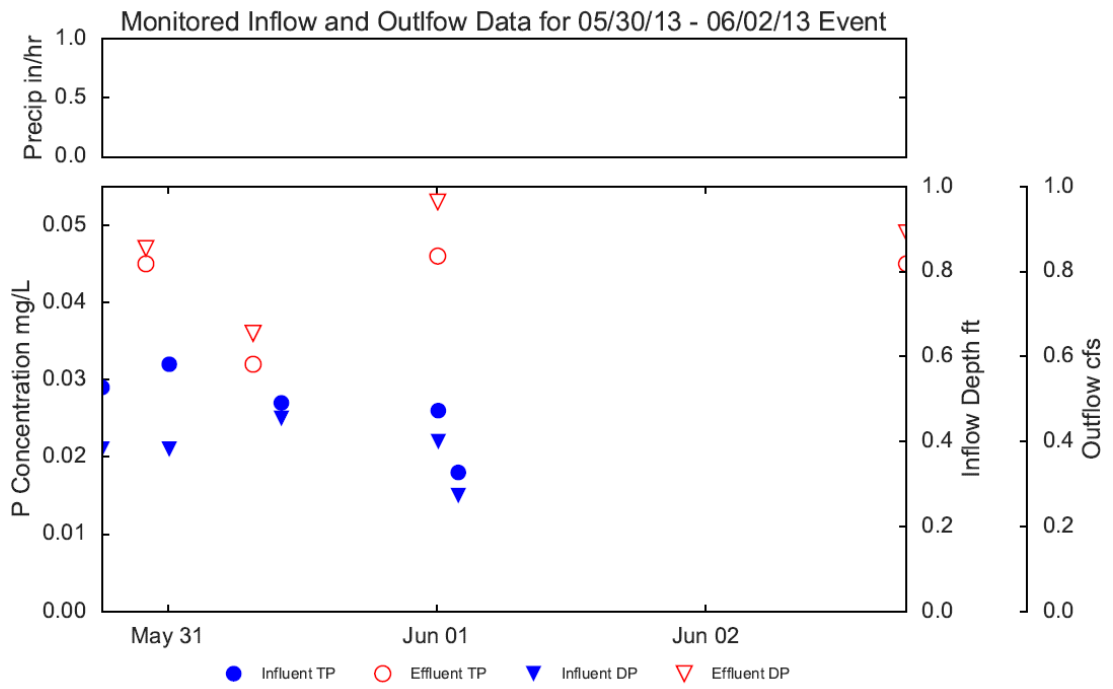

Figure A. 15 Measured influent and effluent TP and DP concentrations for the May 30 through June 2, 2013 monitoring event.

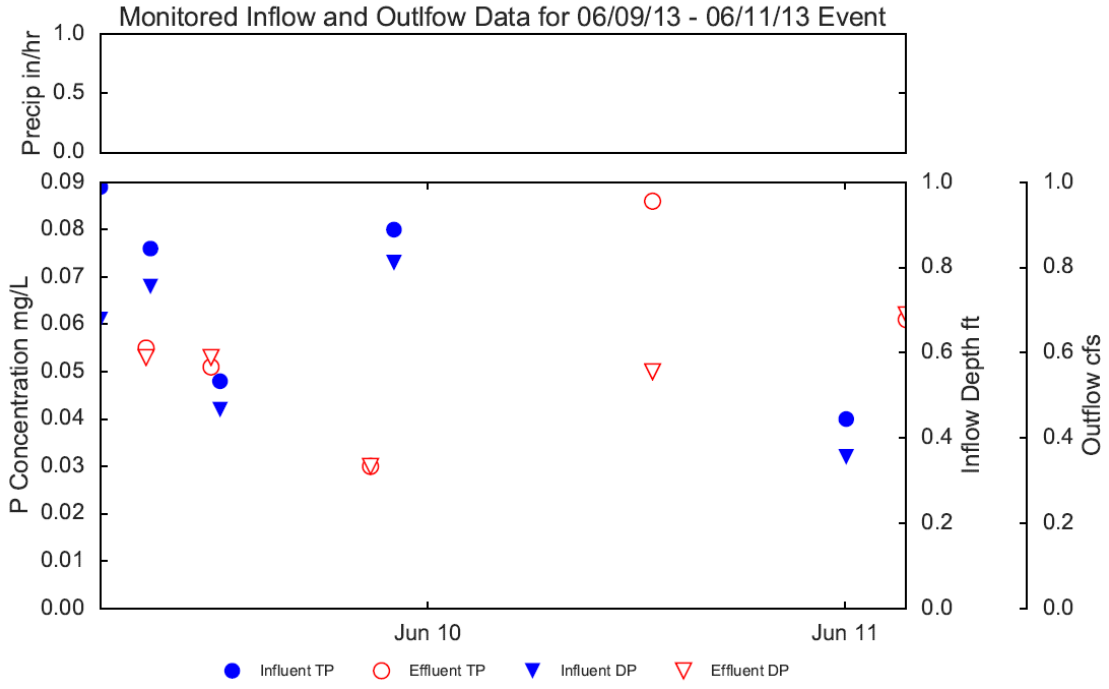

Figure A. 16 Measured influent and effluent TP and DP concentrations for the June 9 through June 11, 2013 monitoring event.

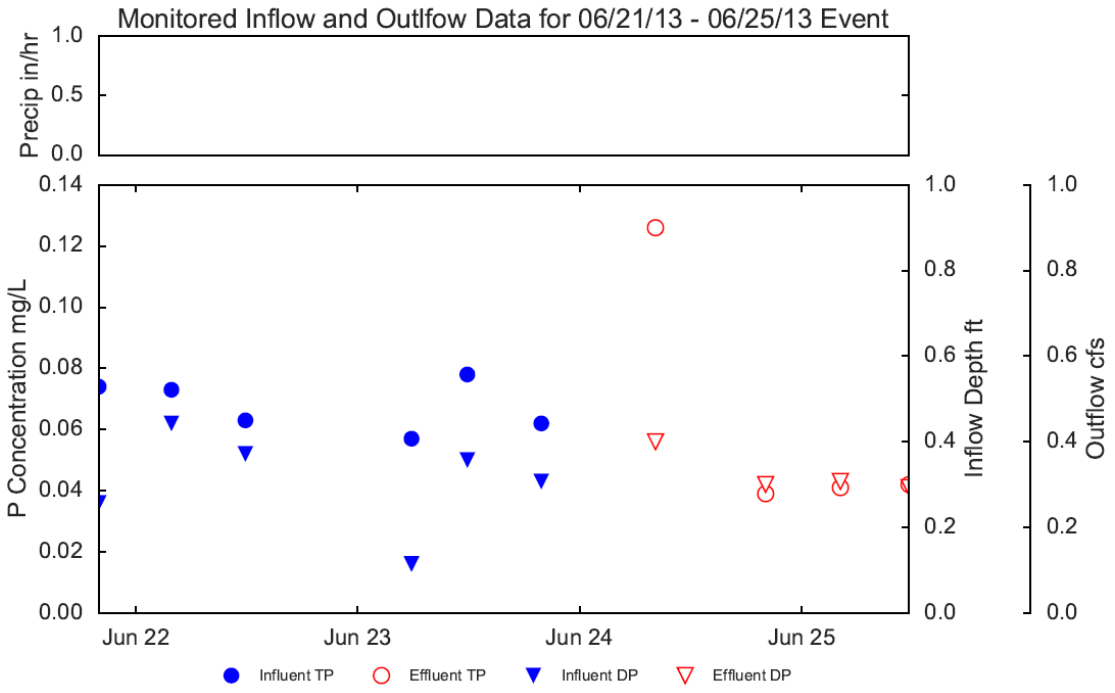

Figure A. 17 Measured influent and effluent TP and DP concentrations for the June 21 through June 25, 2013 monitoring event.

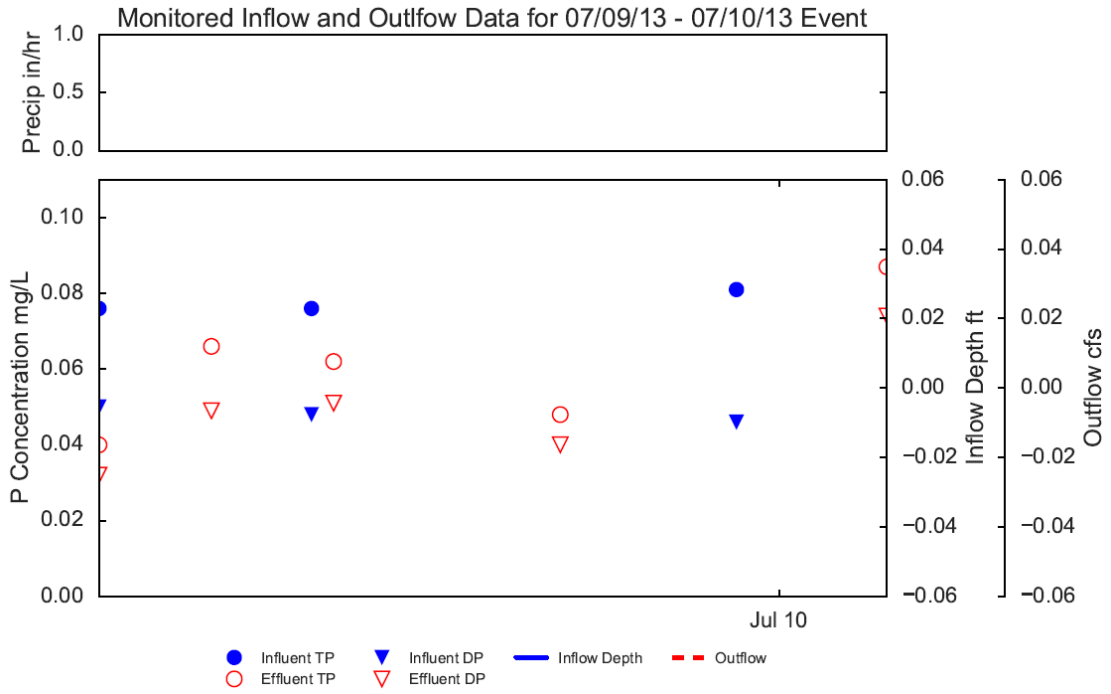

Figure A. 18 Measured influent and effluent TP and DP concentrations for the July 9 through July 10, 2013 monitoring event.

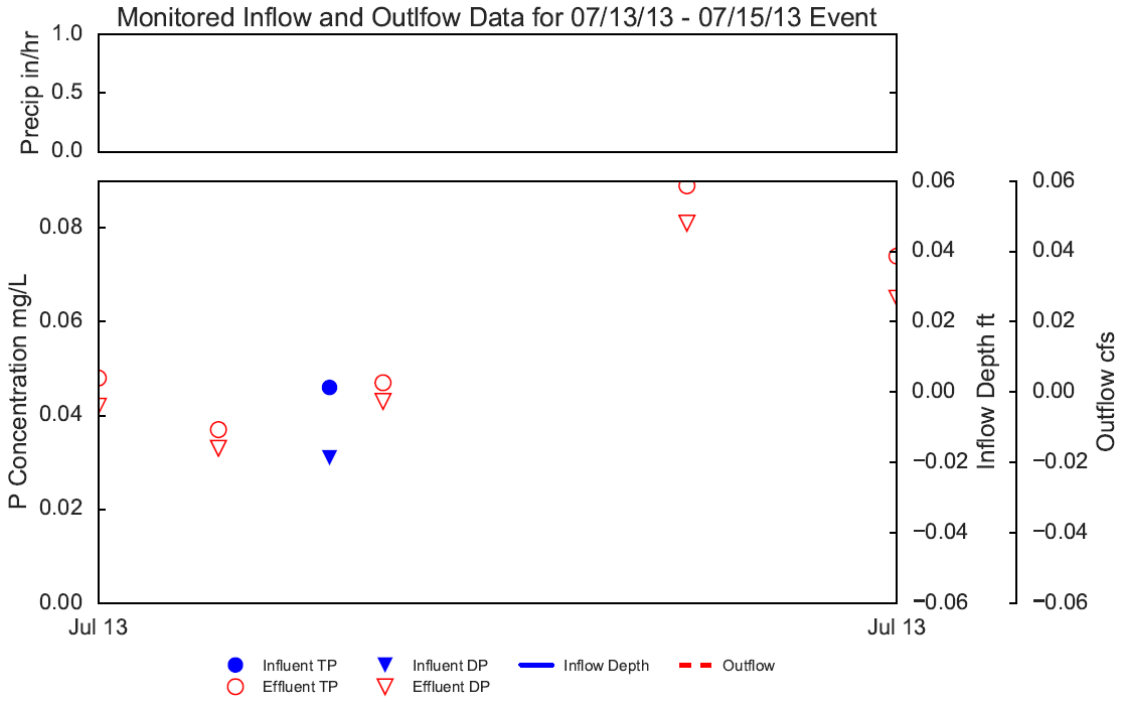

Figure A. 19 Measured influent and effluent TP and DP concentrations for the July 13 through July 15, 2013 monitoring event.

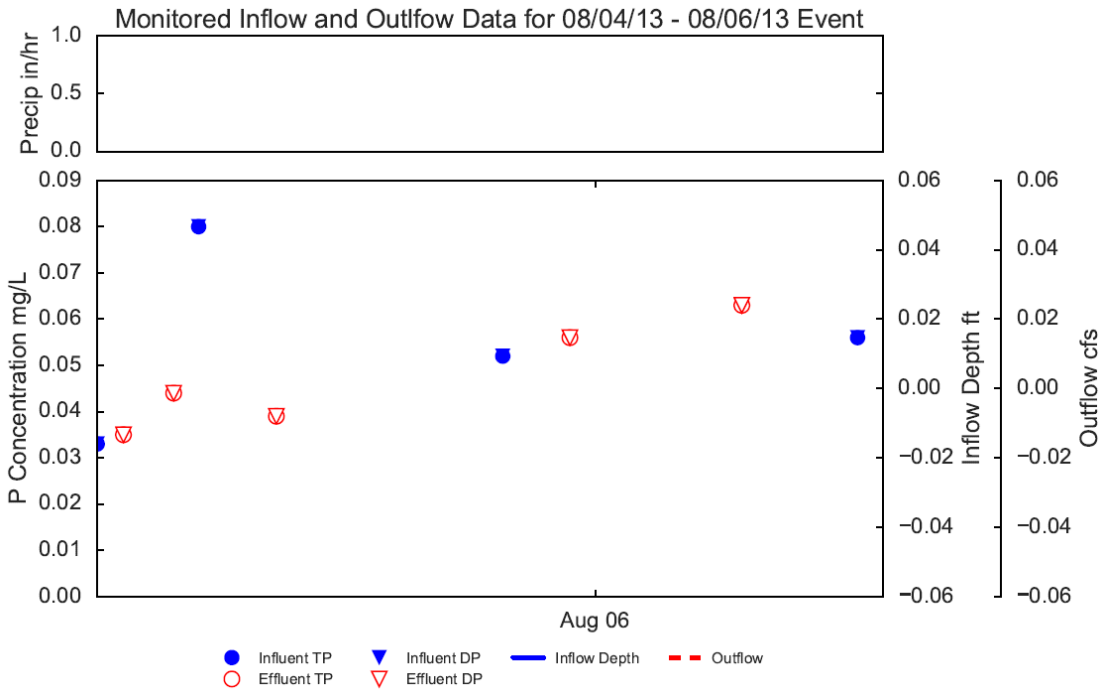

Figure A. 20 Measured influent and effluent TP and DP concentrations for the August 4 through August 6, 2013 monitoring event.

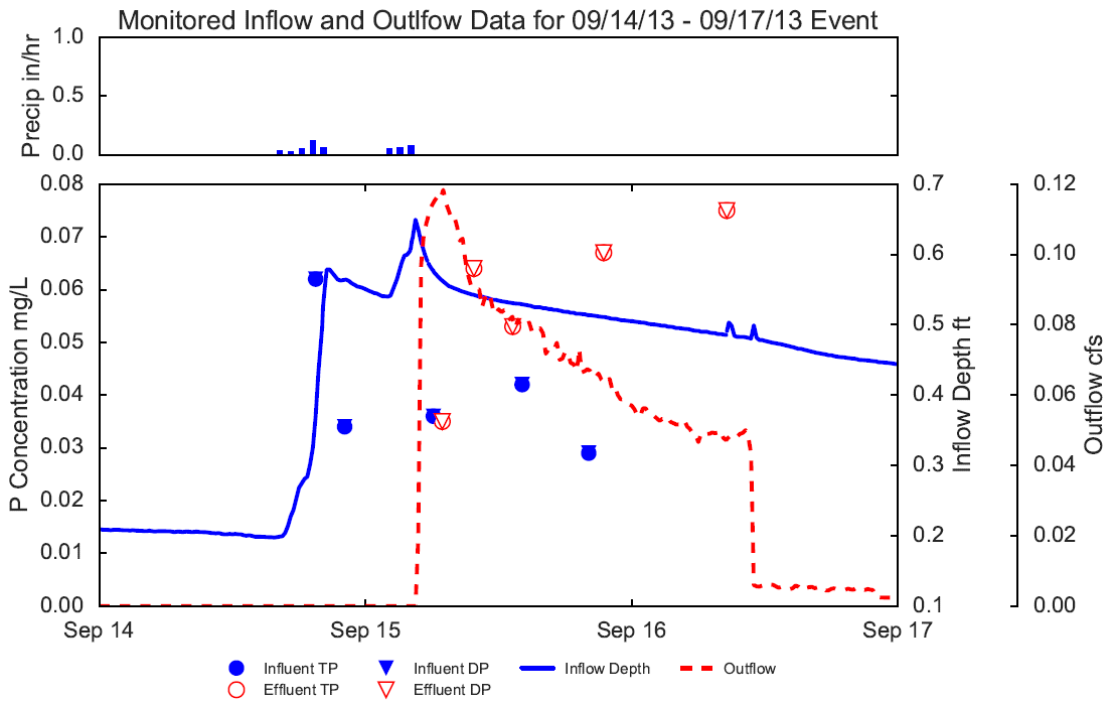

Figure A. 21 Measured influent and effluent TP and DP concentrations, inflow depth, outflow, and precipitation for the September 14 through September 17, 2013 monitoring event.

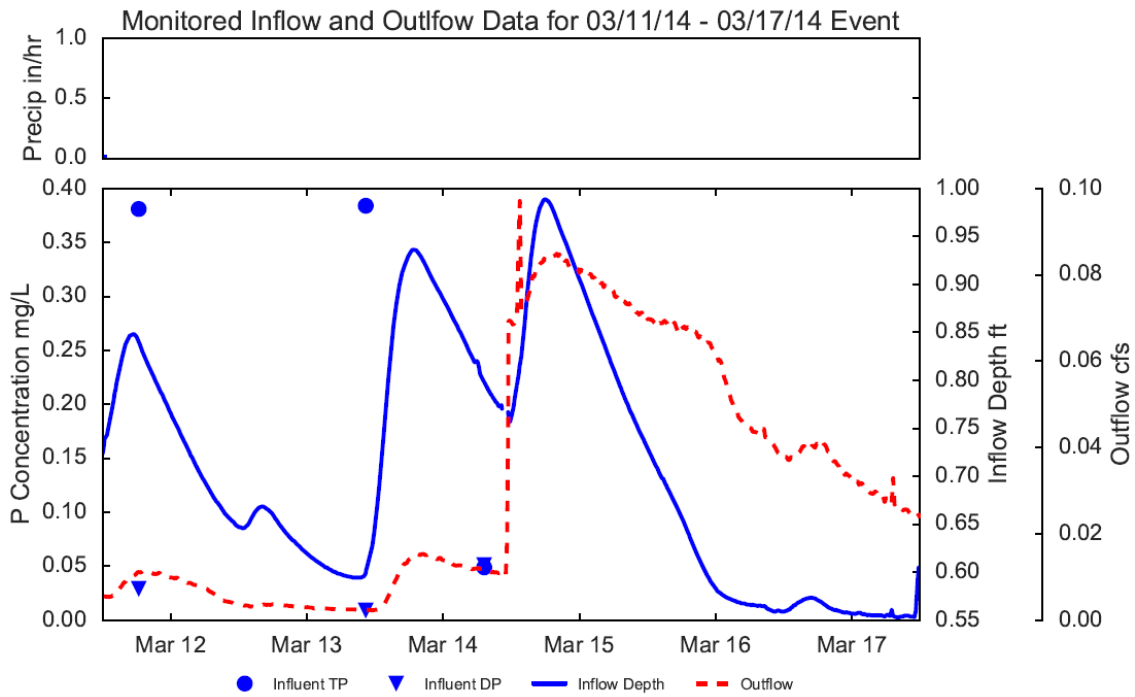

Figure A. 22 Measured influent TP and DP concentrations, inflow depth, and outflow for the March 11 through March 17, 2014 monitoring event

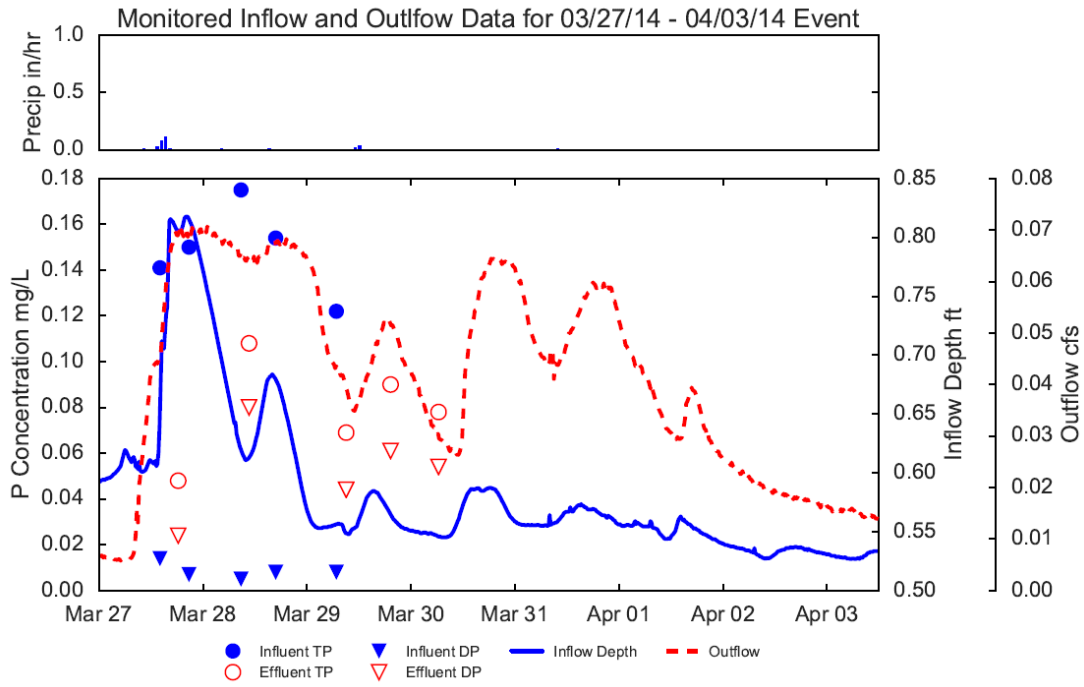

Figure A. 23 Measured influent and effluent TP and DP concentrations, inflow depth, outflow, and precipitation for the March 27 through April 3, 2014 monitoring event

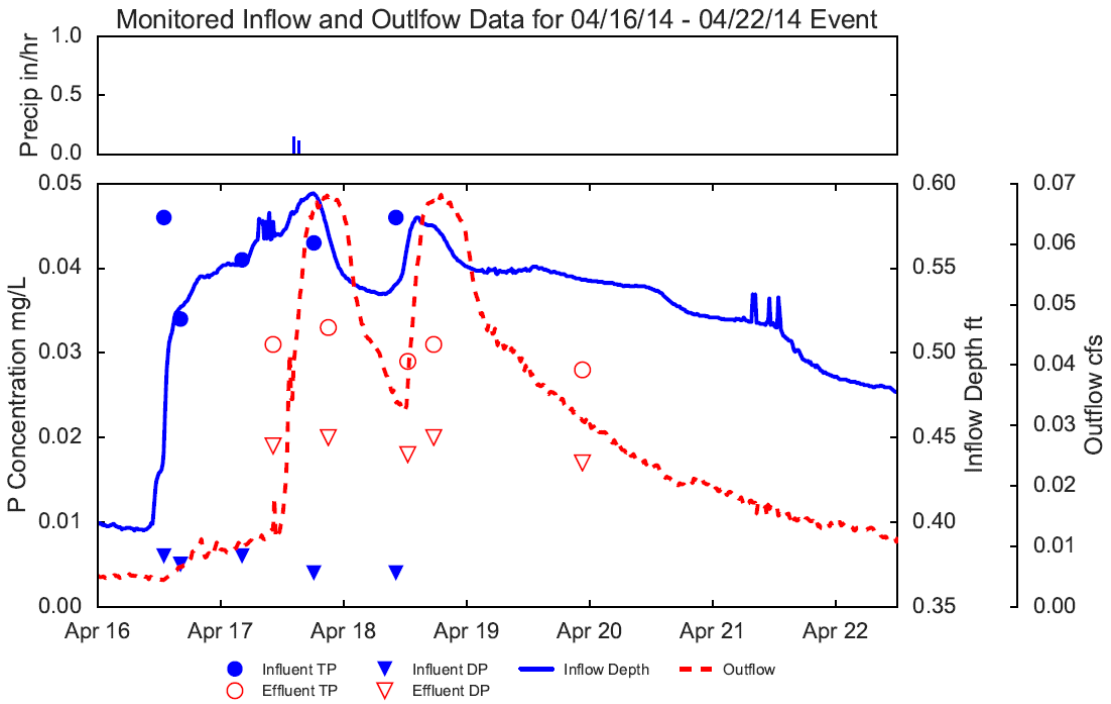

Figure A. 24 Measured influent and effluent TP and DP concentrations, inflow depth, outflow, and precipitation for the April 16 through April 22, 2014 monitoring event

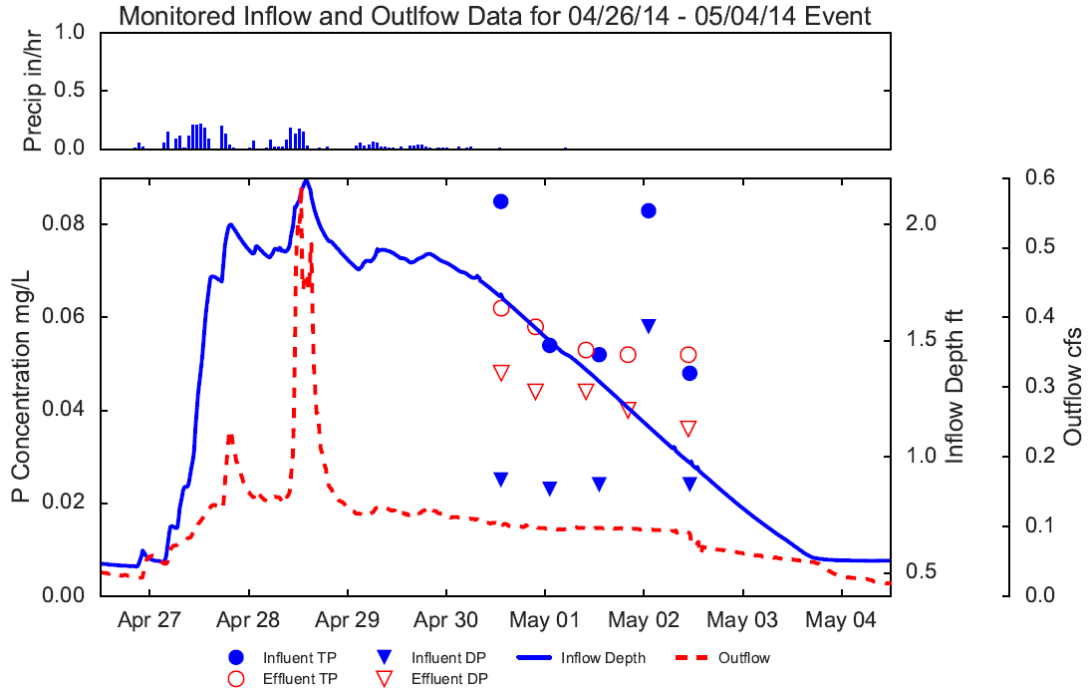

Figure A. 25 Measured influent and effluent TP and DP concentrations, inflow depth, outflow, and precipitation for the April 26 through May 4, 2014 monitoring event

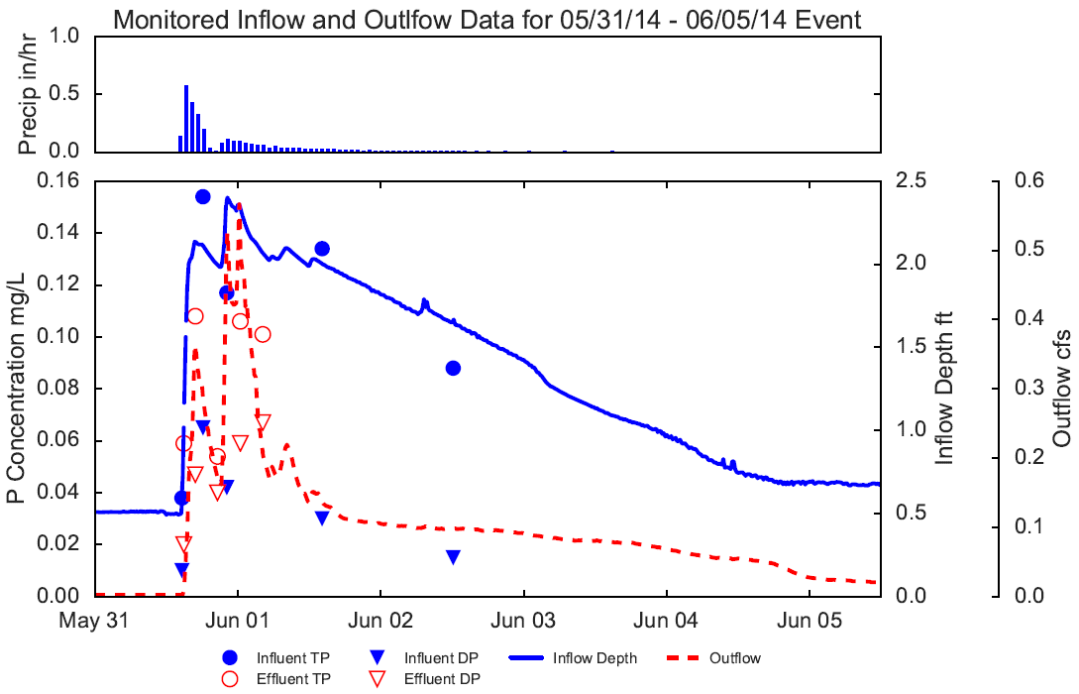

Figure A. 26 Measured influent and effluent TP and DP concentrations, inflow depth, outflow, and precipitation for the May 31 through June 5, 2014 monitoring event

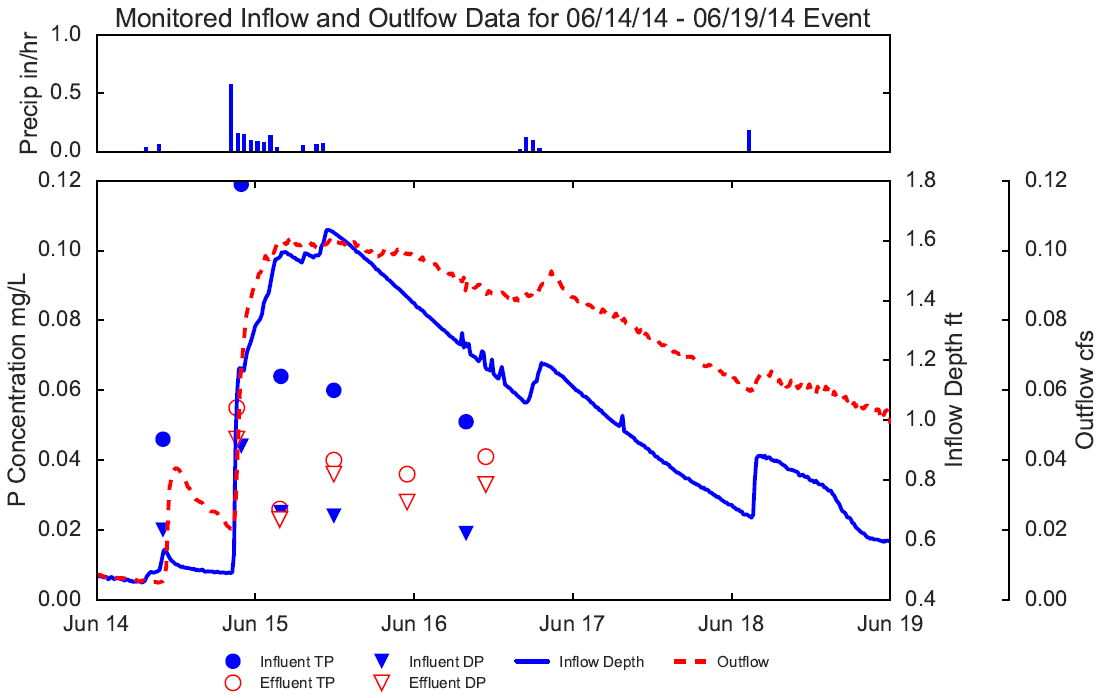

Figure A. 27 Measured influent and effluent TP and DP concentrations, inflow depth, outflow, and precipitation for the June 14 through June 19, 2014 monitoring event

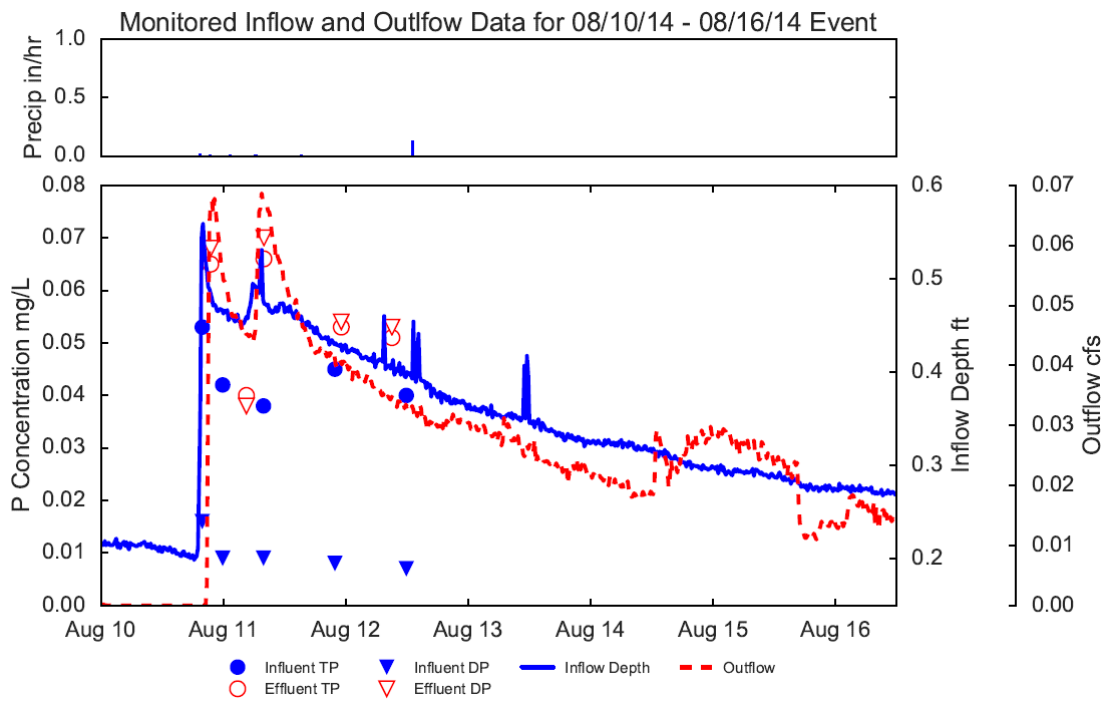

Figure A. 28 Measured influent and effluent TP and DP concentrations, inflow depth, outflow, and precipitation for the August 10 through August 16, 2014 monitoring event

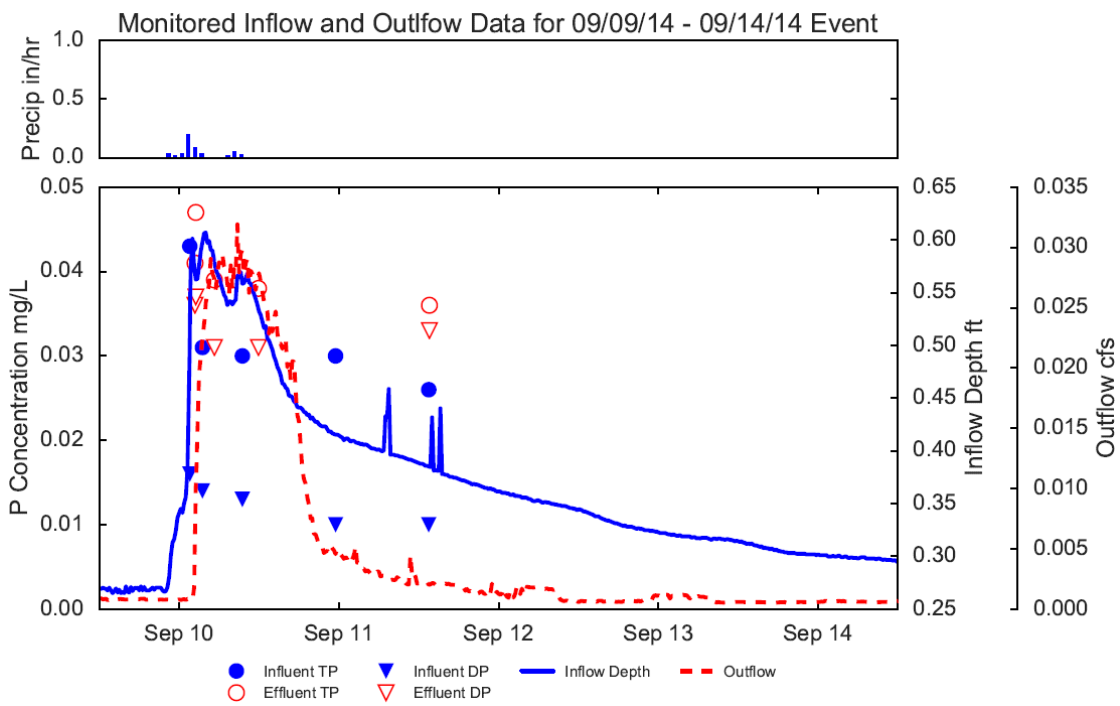

Figure A. 29 Measured influent and effluent TP and DP concentrations, inflow depth, outflow, and precipitation for the September 9 through September 14, 2014 monitoring event

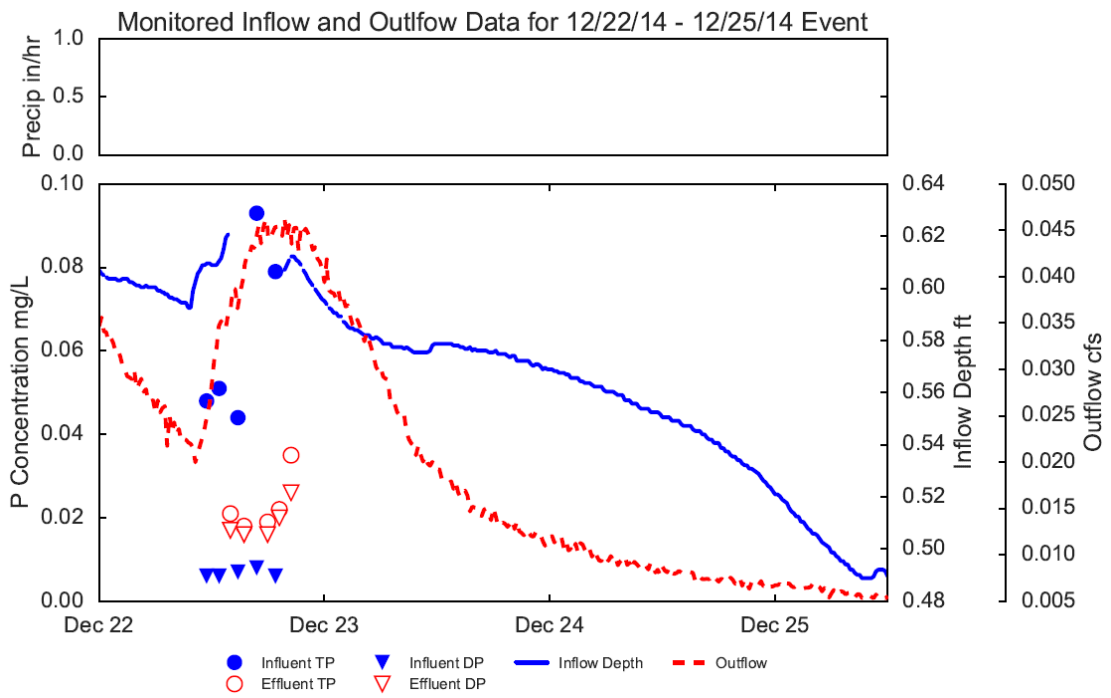

Figure A. 30 Measured influent and effluent TP and DP concentrations, inflow depth, and outflow for the December 22 through December 25, 2014 monitoring event

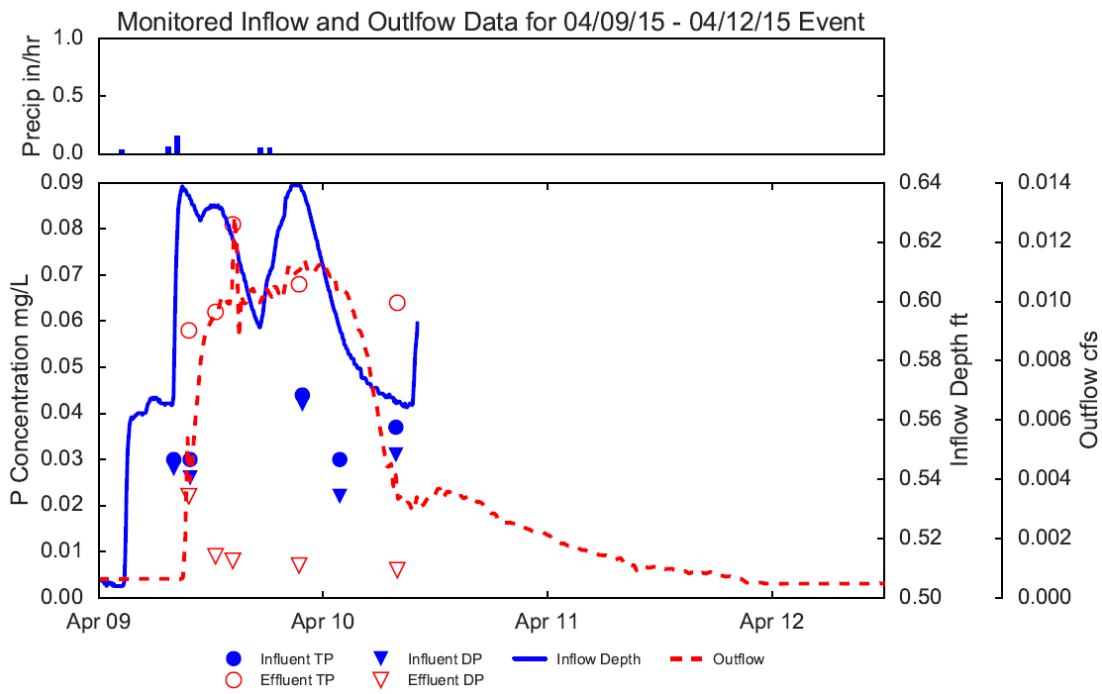

Figure A. 31 Measured influent and effluent TP and DP concentrations, inflow depth, outflow, and precipitation for the April 9 through April 12, 2015 monitoring event

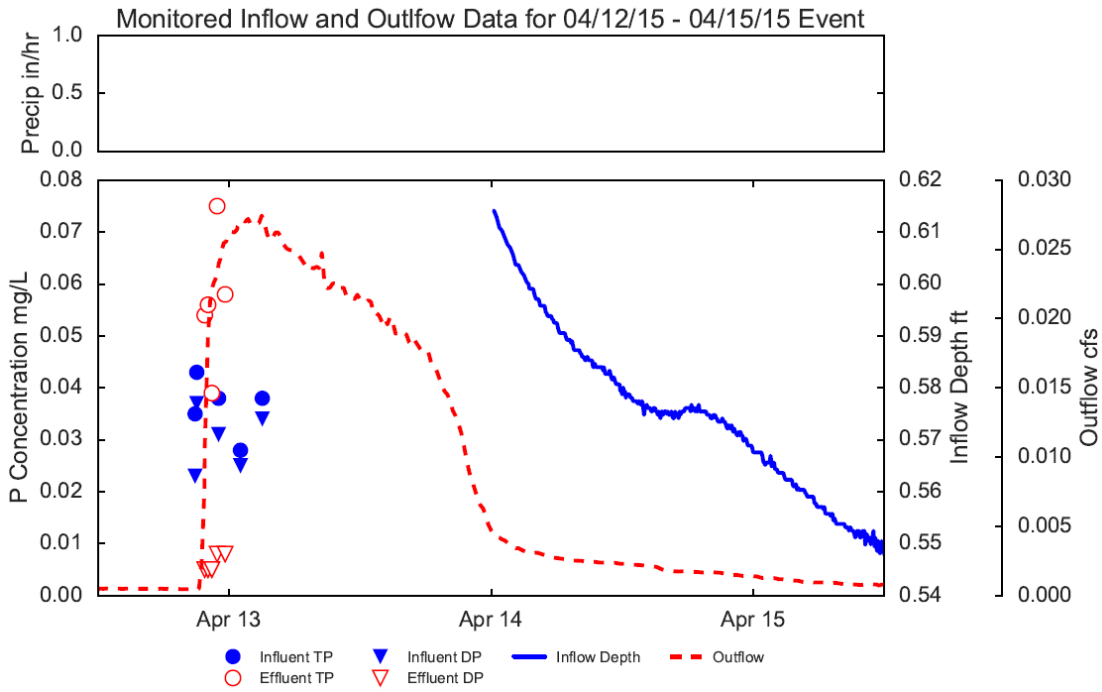

Figure A. 32 Measured influent and effluent TP and DP concentrations, inflow depth, and outflow for the April 12 through April 15, 2015 monitoring event

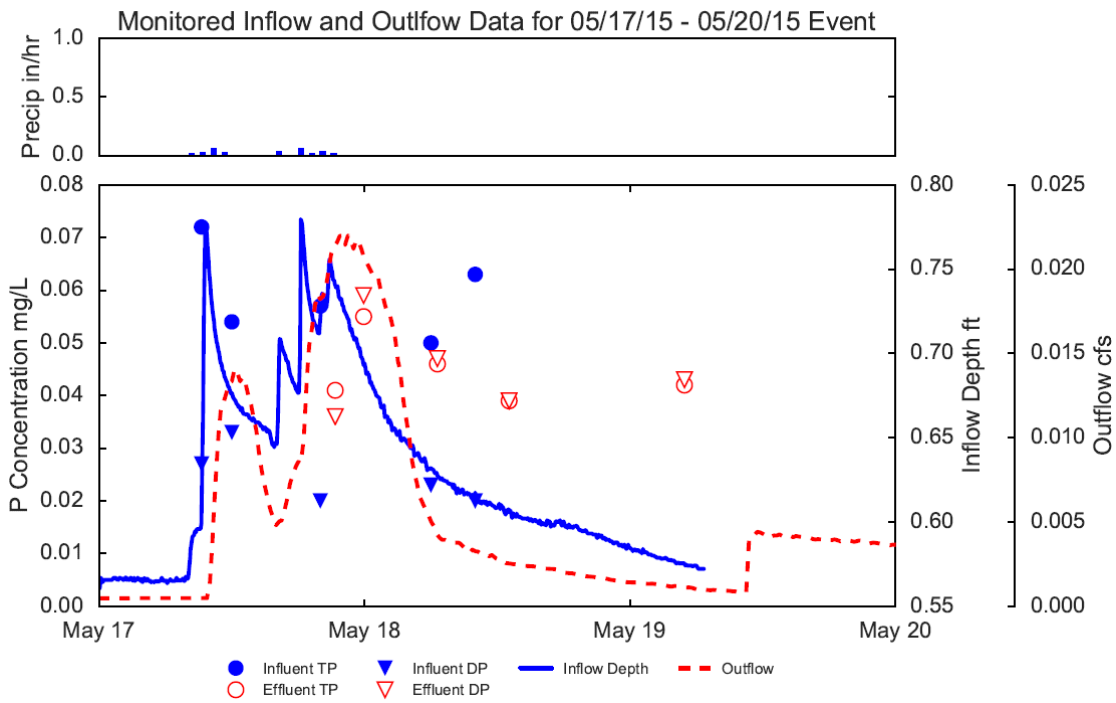

Figure A. 33 Measured influent and effluent TP and DP concentrations, inflow depth, outflow, and precipitation for the May 17 through May 20, 2015 monitoring event

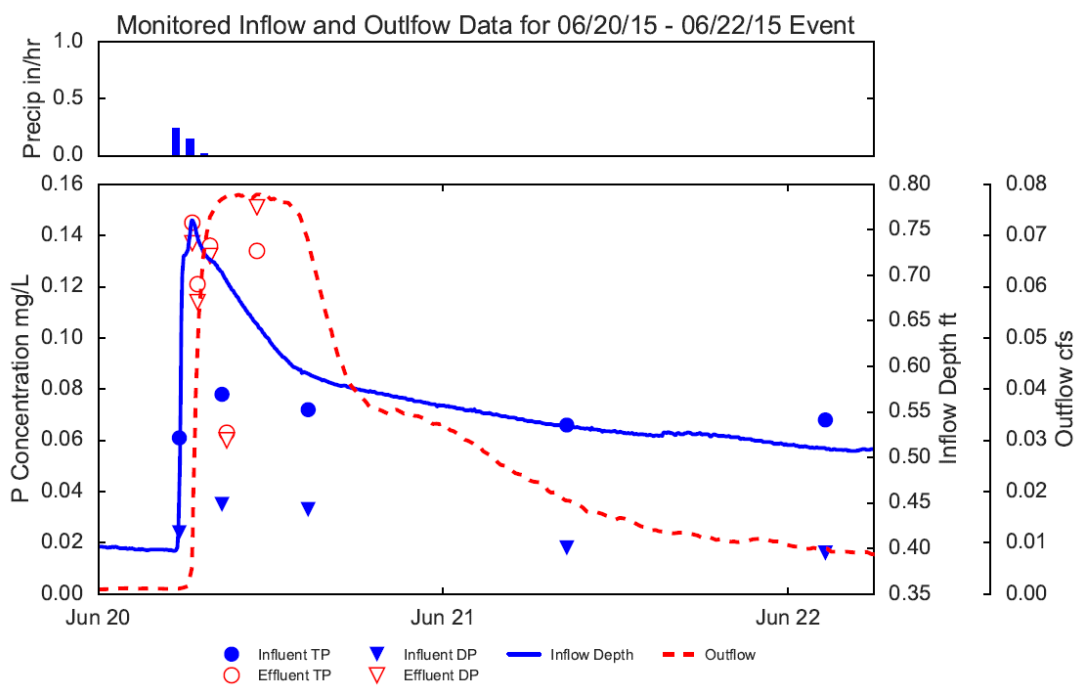

Figure A. 34 Measured influent and effluent TP and DP concentrations, inflow depth, outflow, and precipitation for the June 20 through June 22, 2015 monitoring event

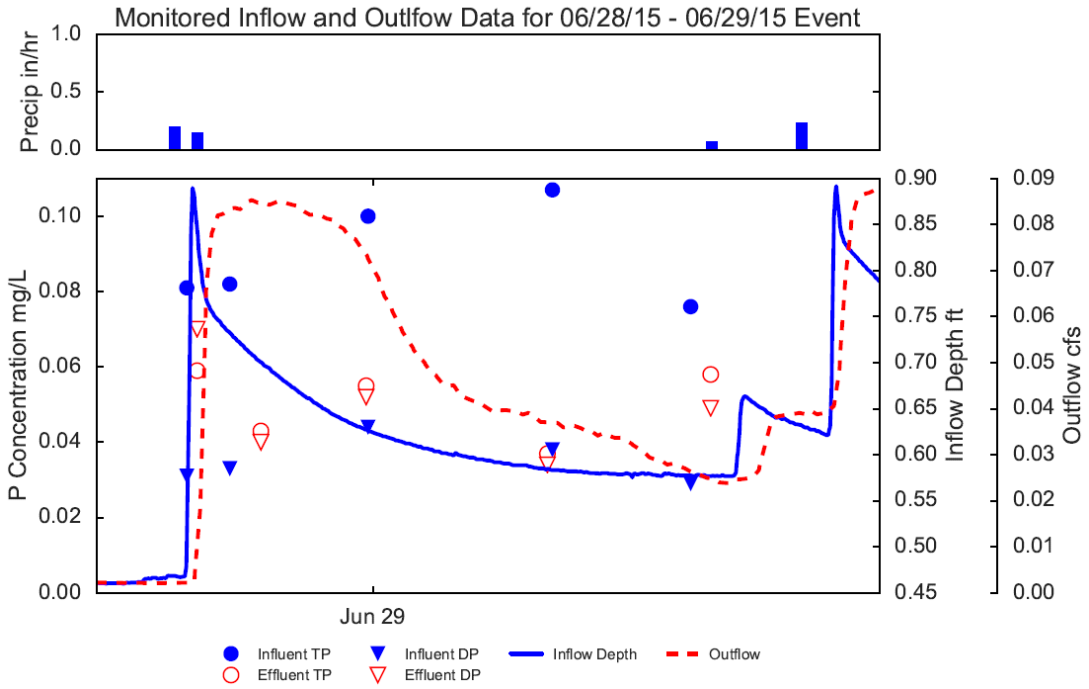

Figure A. 35 Measured influent and effluent TP and DP concentrations, inflow depth, outflow, and precipitation for the June 28 through June 29, 2015 monitoring event

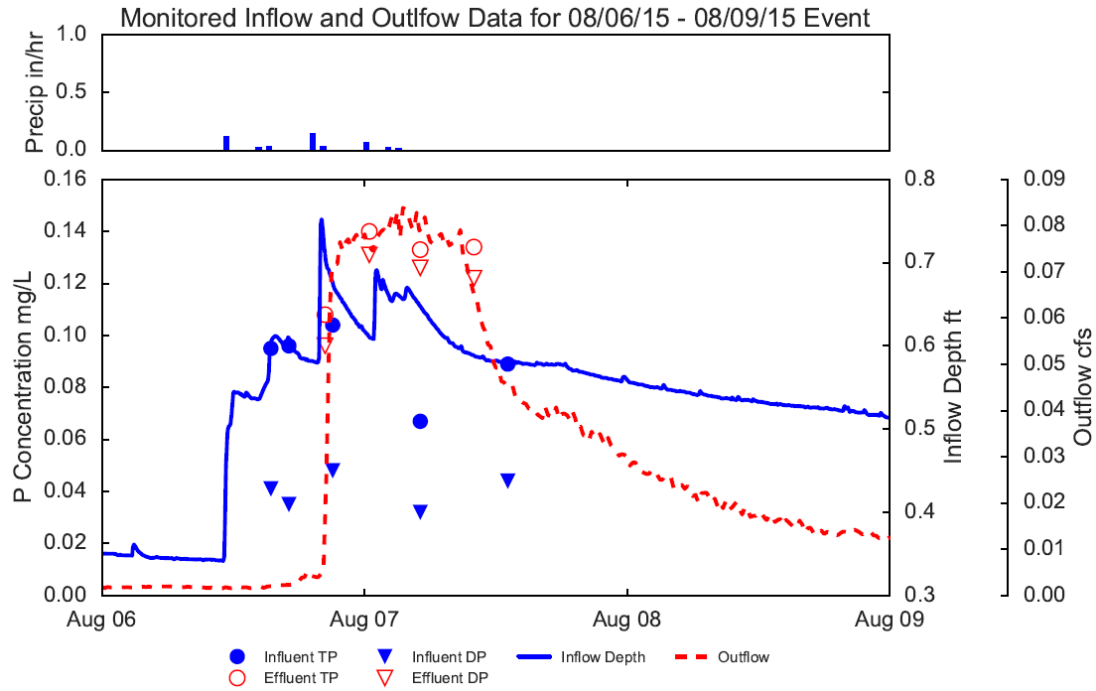

Figure A. 36 Measured influent and effluent TP and DP concentrations, inflow depth, outflow, and precipitation for the August 6 through August 9, 2015 monitoring event

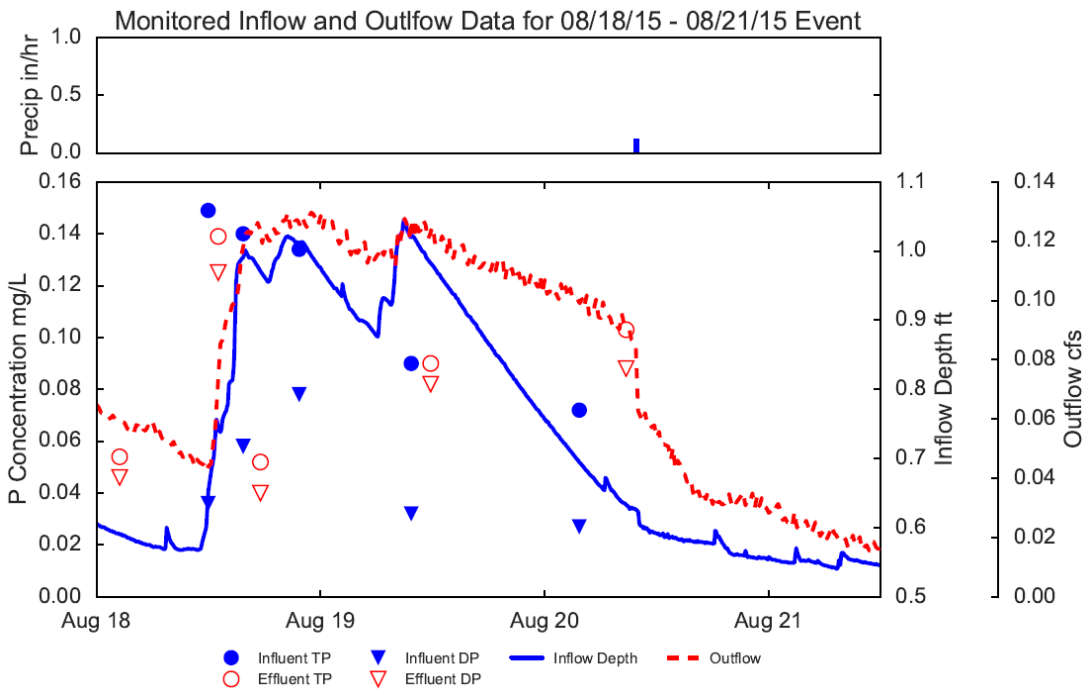

Figure A. 37 Measured influent and effluent TP and DP concentrations, inflow depth, outflow, and precipitation for the August 18 through August 21, 2015 monitoring event

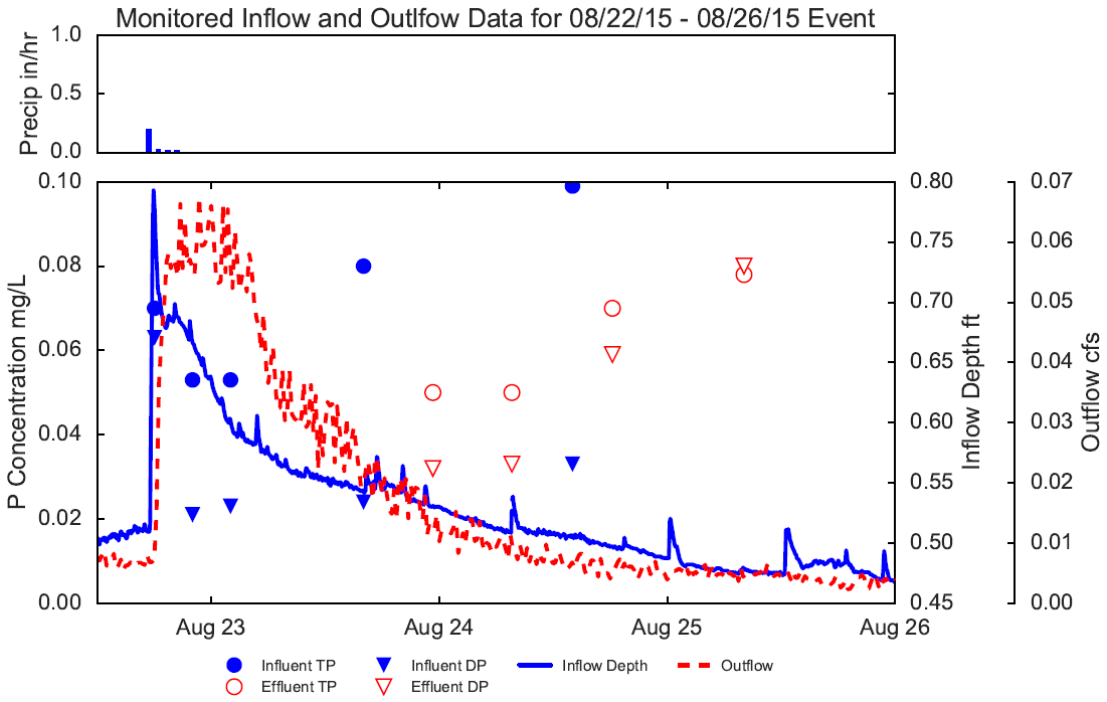

Figure A. 38 Measured influent and effluent TP and DP concentrations, inflow depth, outflow, and precipitation for the August 22 through August 26, 2015 monitoring event

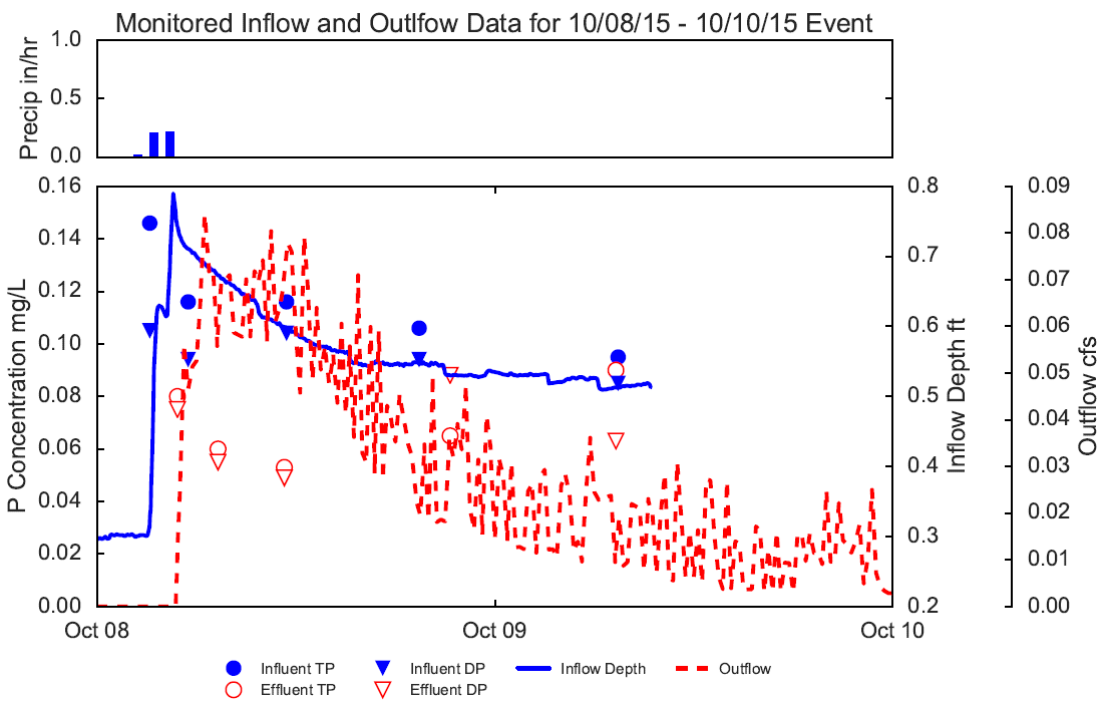

Figure A. 39 Measured influent and effluent TP and DP concentrations, inflow depth, outflow, and precipitation for the October 8 through October 10, 2015 monitoring event

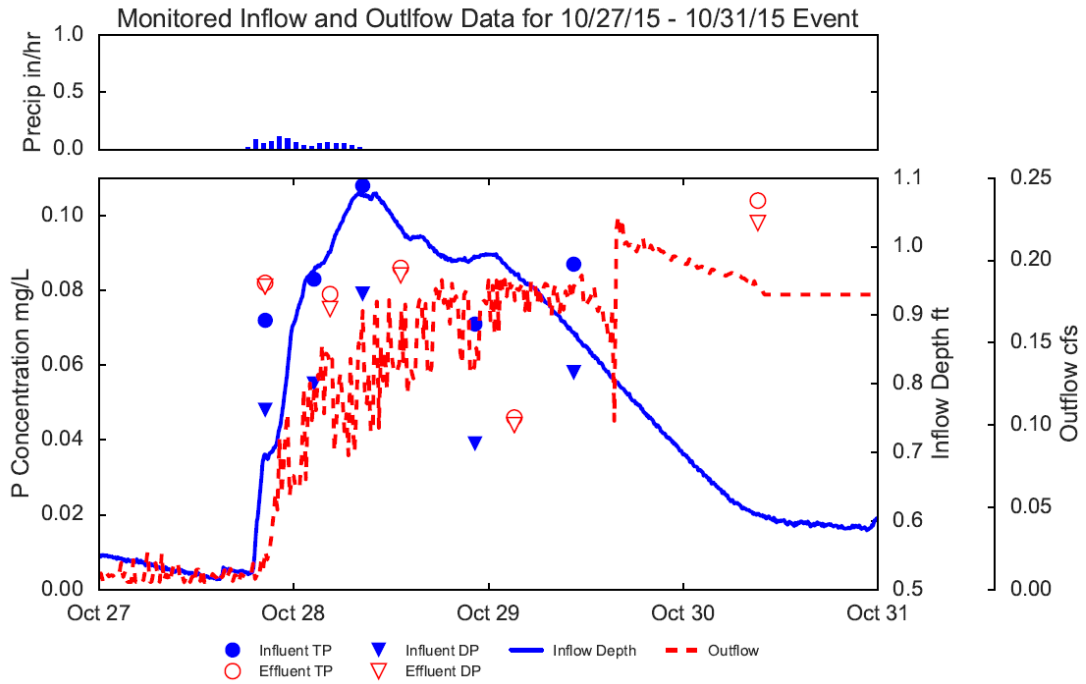

Figure A. 40 Measured influent and effluent TP and DP concentrations, inflow depth, outflow, and precipitation for the October 27 through October 31, 2015 monitoring event

APPENDIX B
2016 THROUGH 2018 POLLUTOGRAPHS

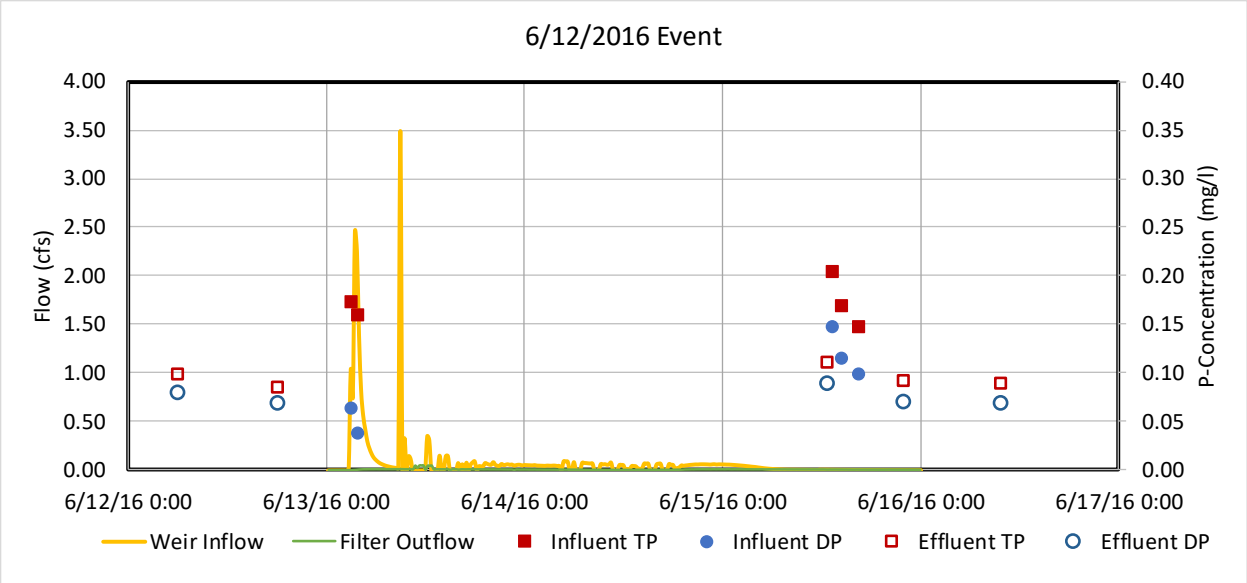

Figure B. 1 Measured influent and effluent TP and DP concentrations, weir inflow and outflow for the June 12 through June 17, 2016 monitoring event.

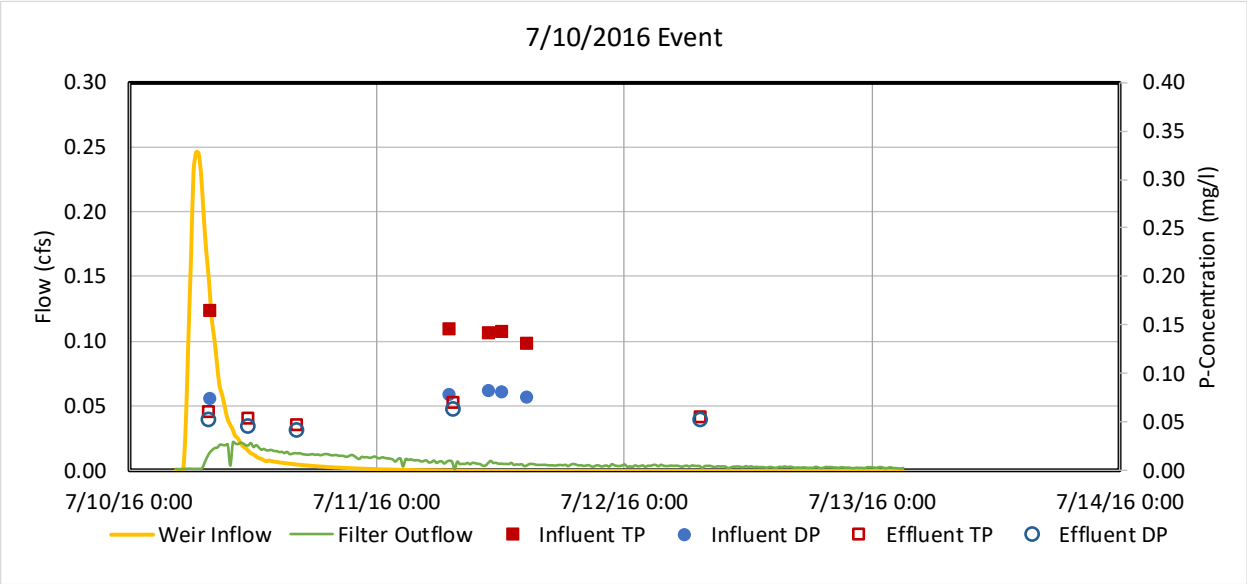

Figure B. 2 Measured influent and effluent TP and DP concentrations, weir inflow and outflow for the July 10 through July 14, 2016 monitoring event.

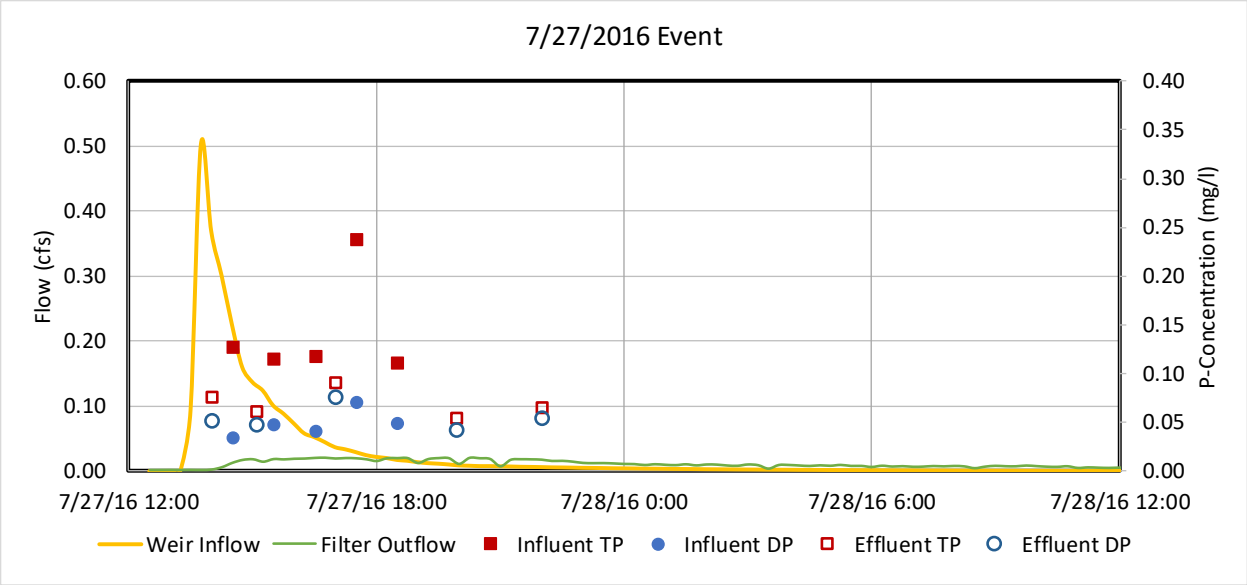

Figure B. 3 Measured influent and effluent TP and DP concentrations, weir inflow and outflow for the July 27, 2016 monitoring event.

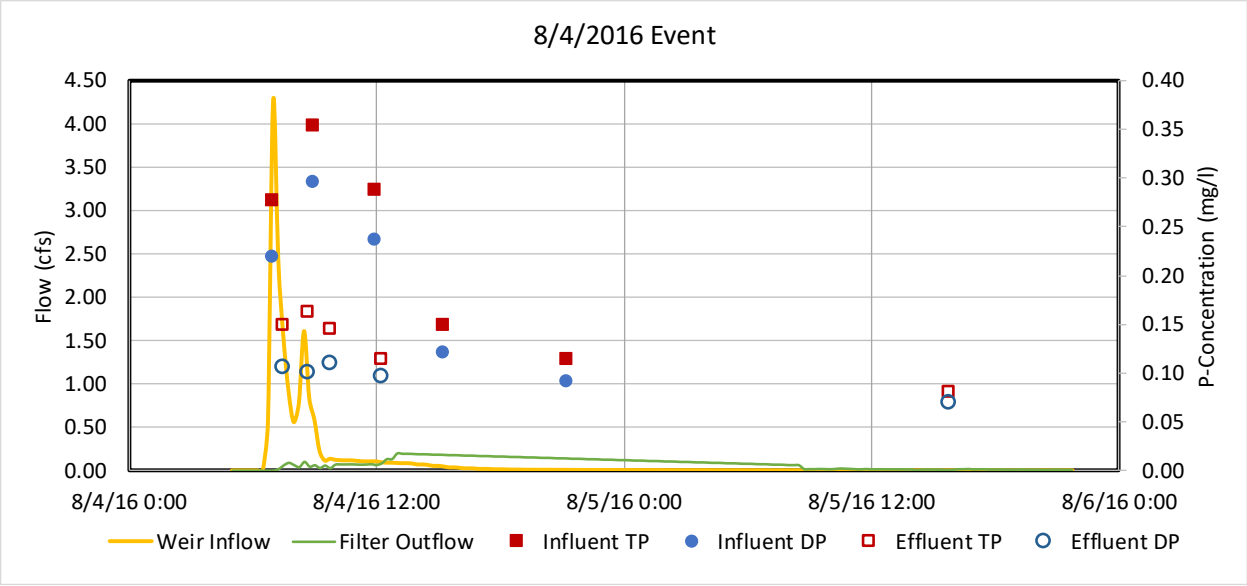

Figure B. 4 Measured influent and effluent TP and DP concentrations, weir inflow and outflow for the August 4 through August 5, 2016 monitoring event.

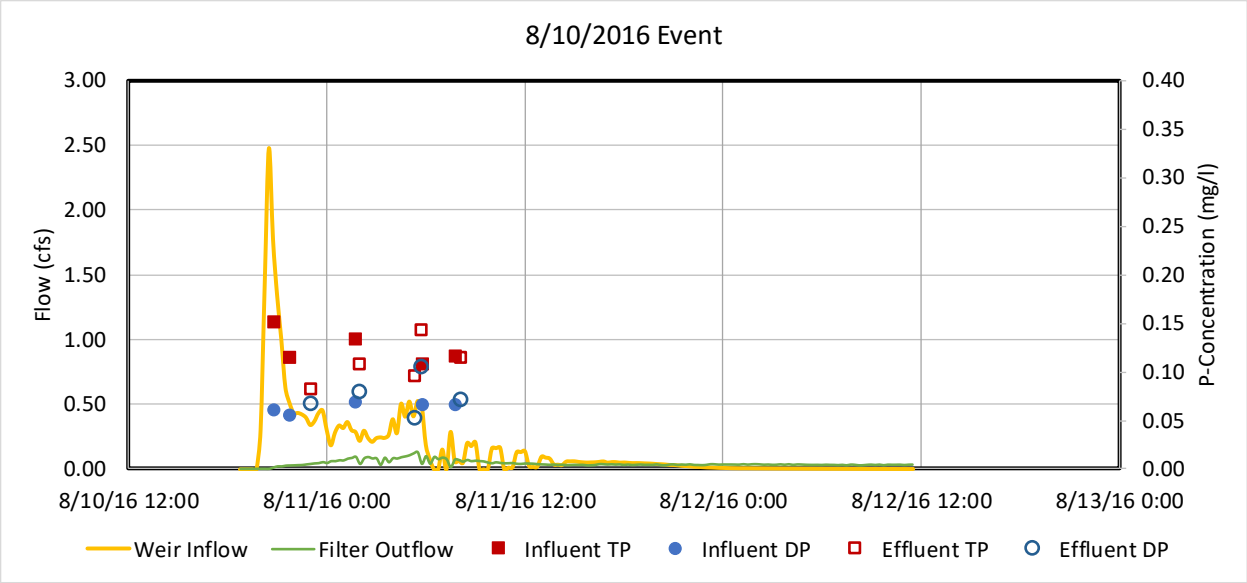

Figure B. 5 Measured influent and effluent TP and DP concentrations, weir inflow and outflow for the August 10 through August 11, 2016 monitoring event.

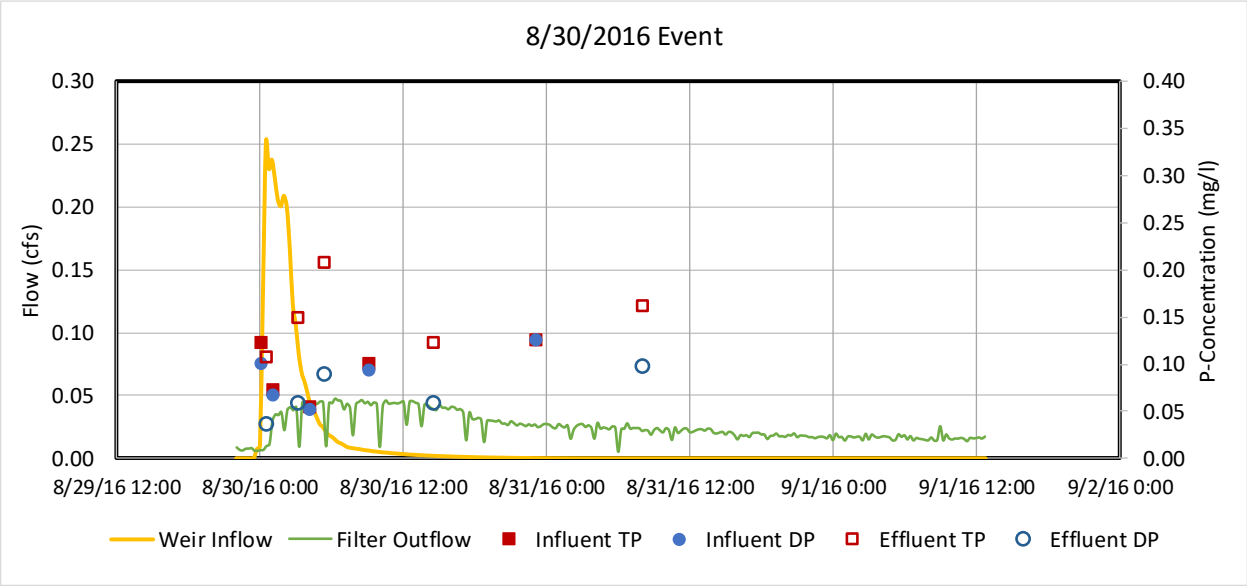

Figure B. 6 Measured influent and effluent TP and DP concentrations, weir inflow and outflow for the August 29 through August 31, 2016 monitoring event.

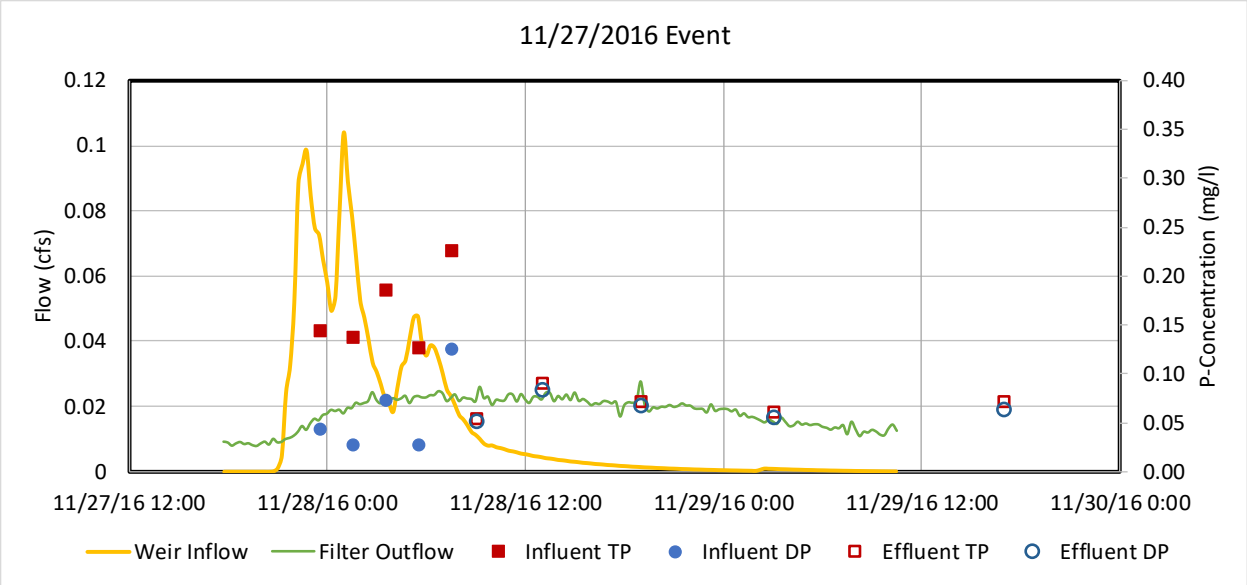

Figure B. 7 Measured influent and effluent TP and DP concentrations, weir inflow and outflow for the November 27 through November 29, 2016 monitoring event.

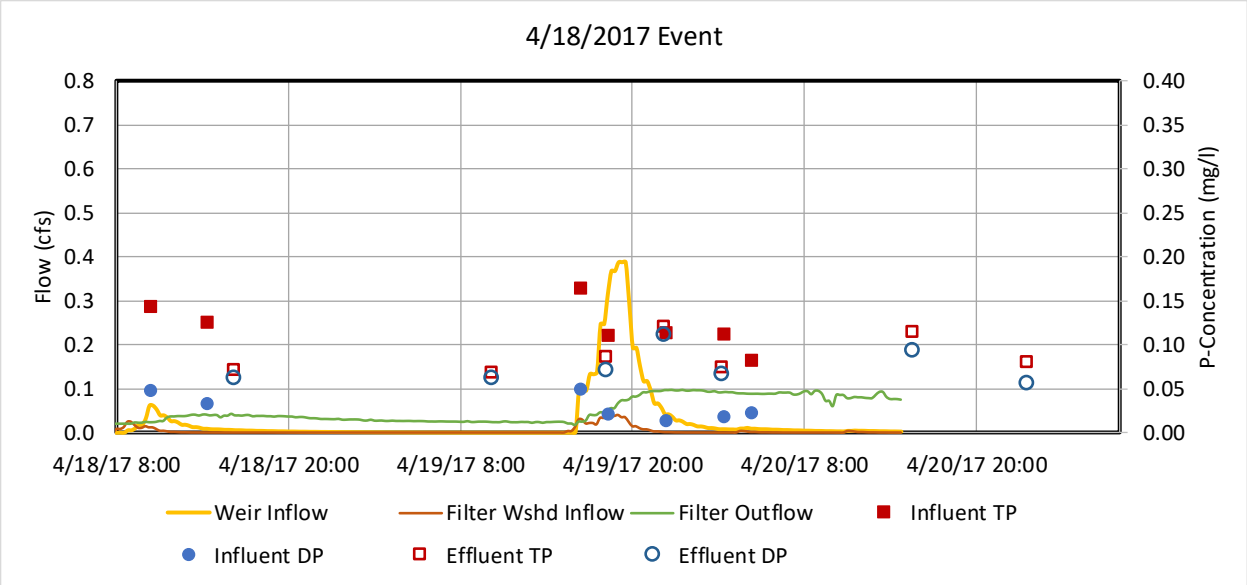

Figure B. 8 Measured influent and effluent TP and DP concentrations, measured weir inflow and outflow, and estimated filter watershed inflow for the April 18 through April 20, 2017 monitoring event.

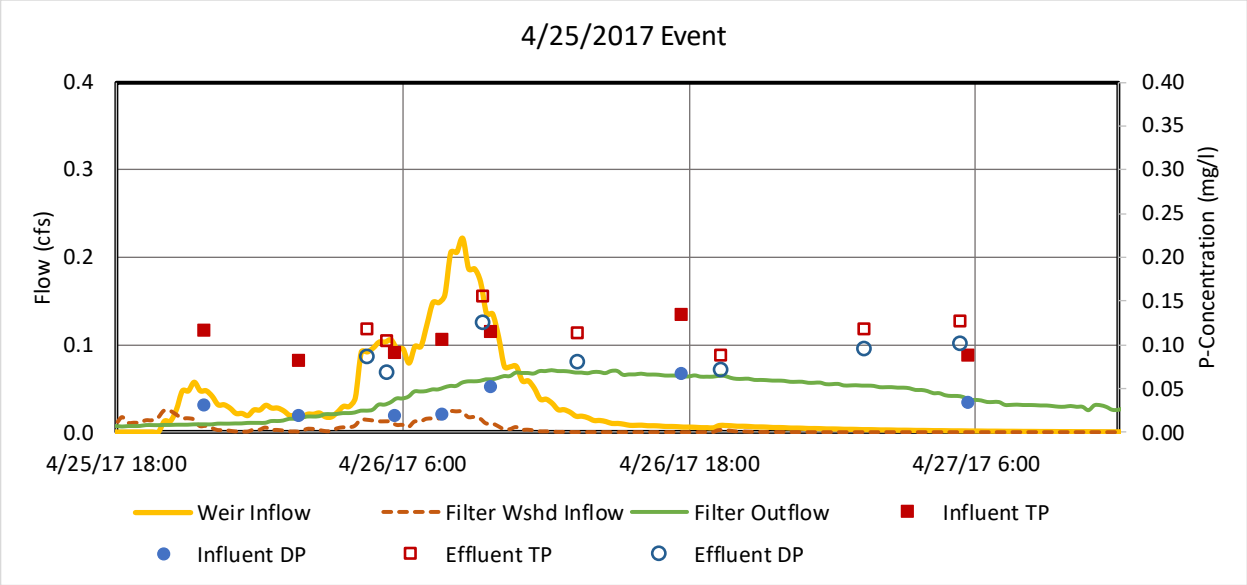

Figure B. 9 Measured influent and effluent TP and DP concentrations, measured weir inflow and outflow, and estimated filter watershed inflow for the April 25 through April 27, 2017 monitoring event.

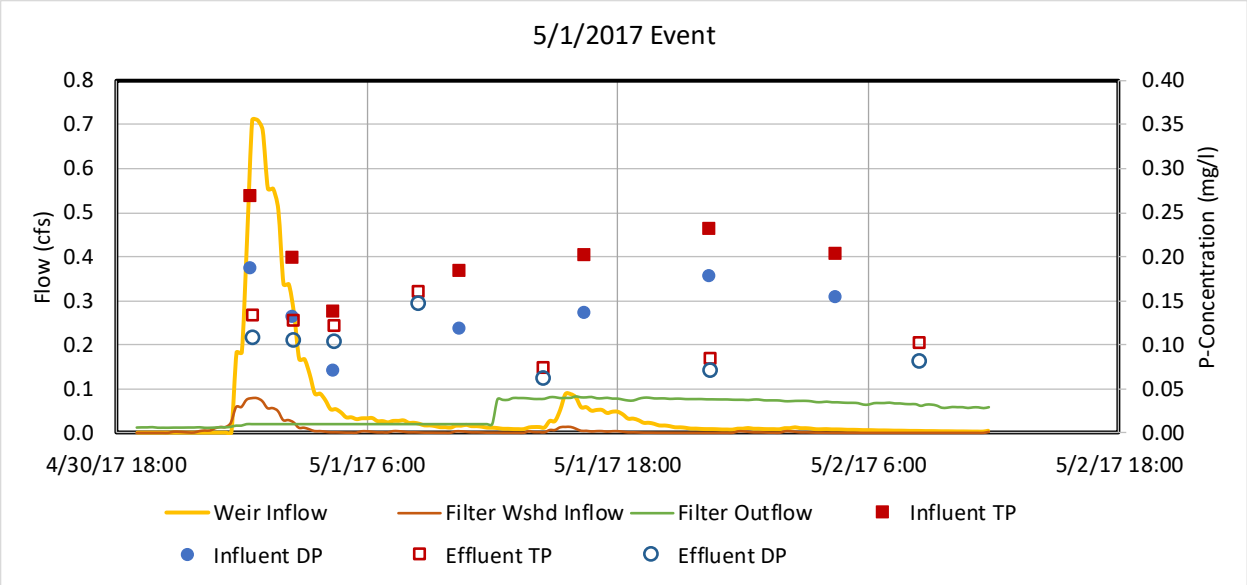

Figure B. 10 Measured influent and effluent TP and DP concentrations, measured weir inflow and outflow, and estimated filter watershed inflow for the May 1 through May 2, 2017 monitoring event.

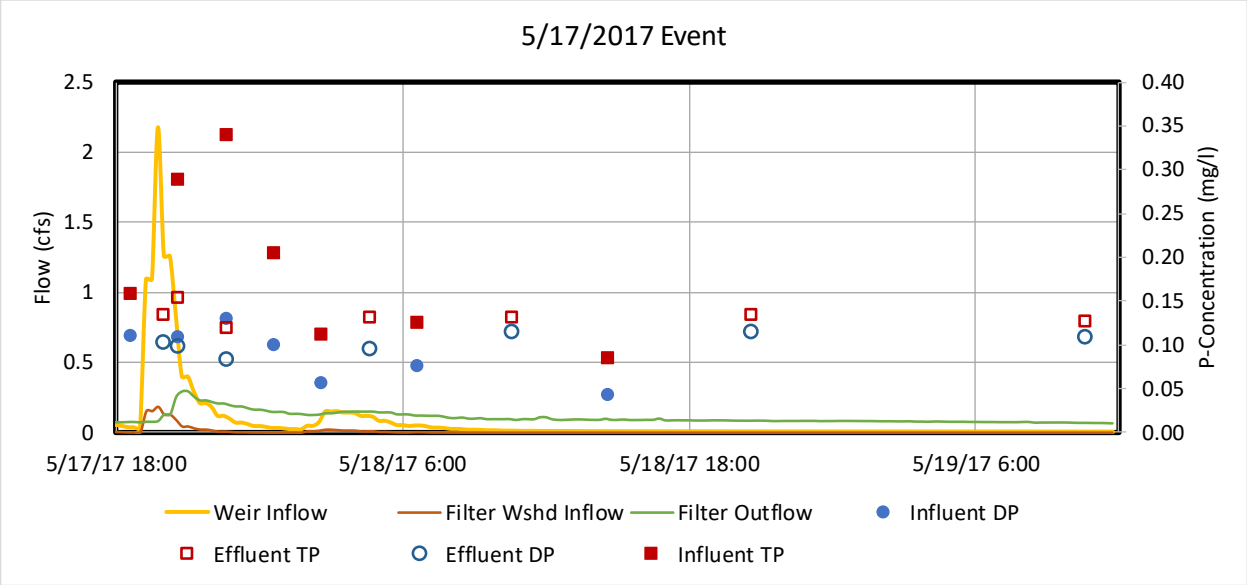

Figure B. 11 Measured influent and effluent TP and DP concentrations, measured weir inflow and outflow, and estimated filter watershed inflow for the May 17 through May 19, 2017 monitoring event.

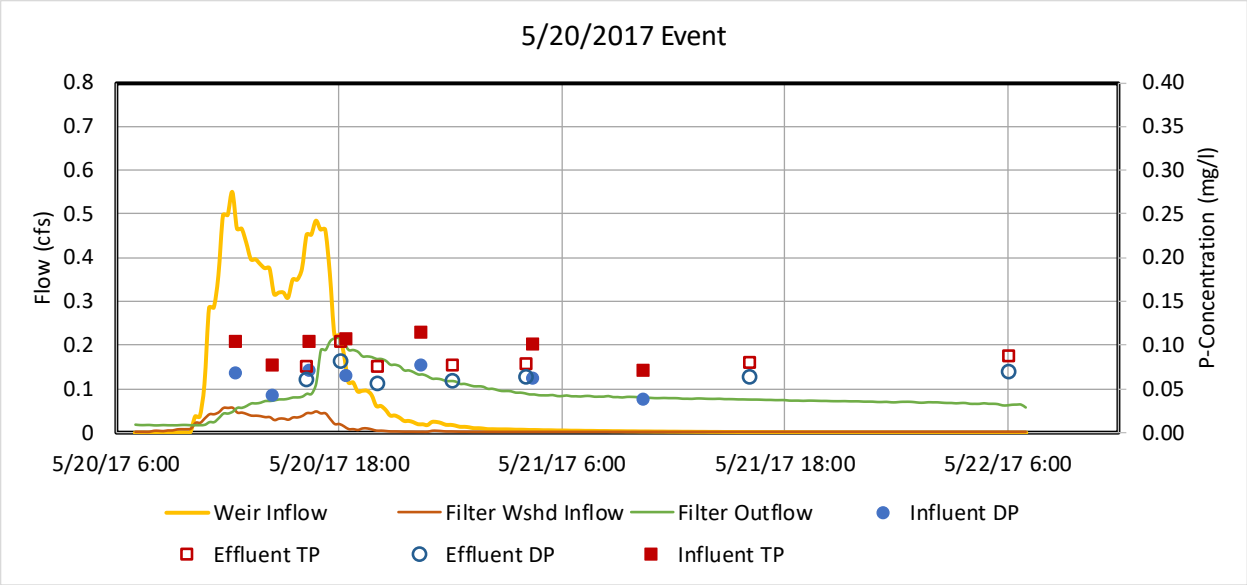

Figure B. 12 Measured influent and effluent TP and DP concentrations, measured weir inflow and outflow, and estimated filter watershed inflow for the May 20 through May 22, 2017 monitoring event.

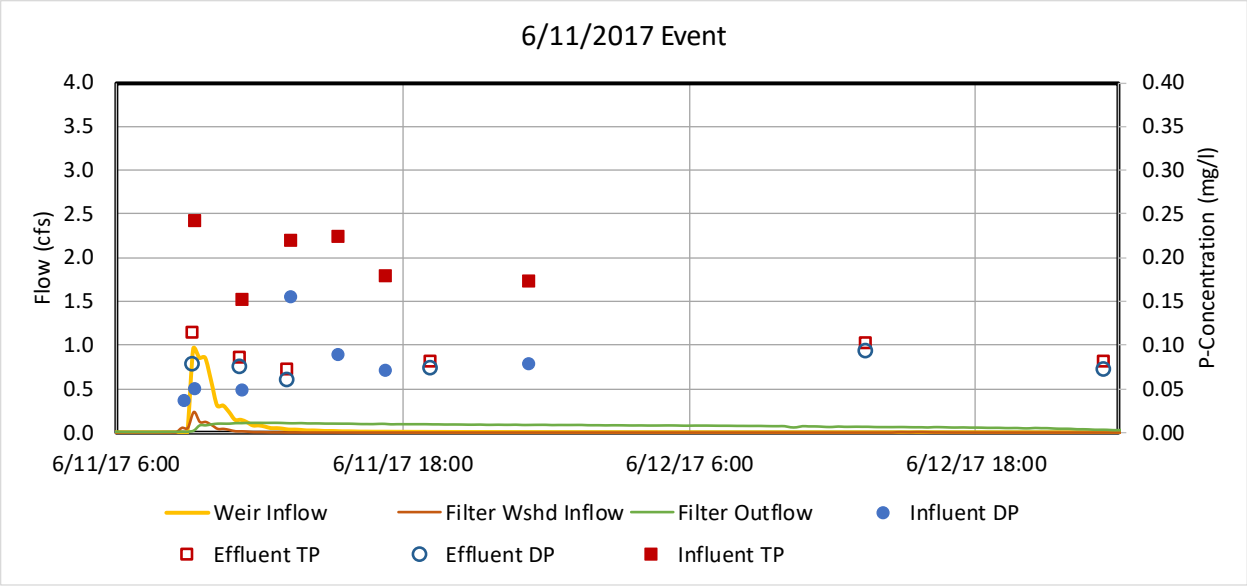

Figure B. 13 Measured influent and effluent TP and DP concentrations, measured weir inflow and outflow, and estimated filter watershed inflow for the June 11 through June 12, 2017 monitoring event.

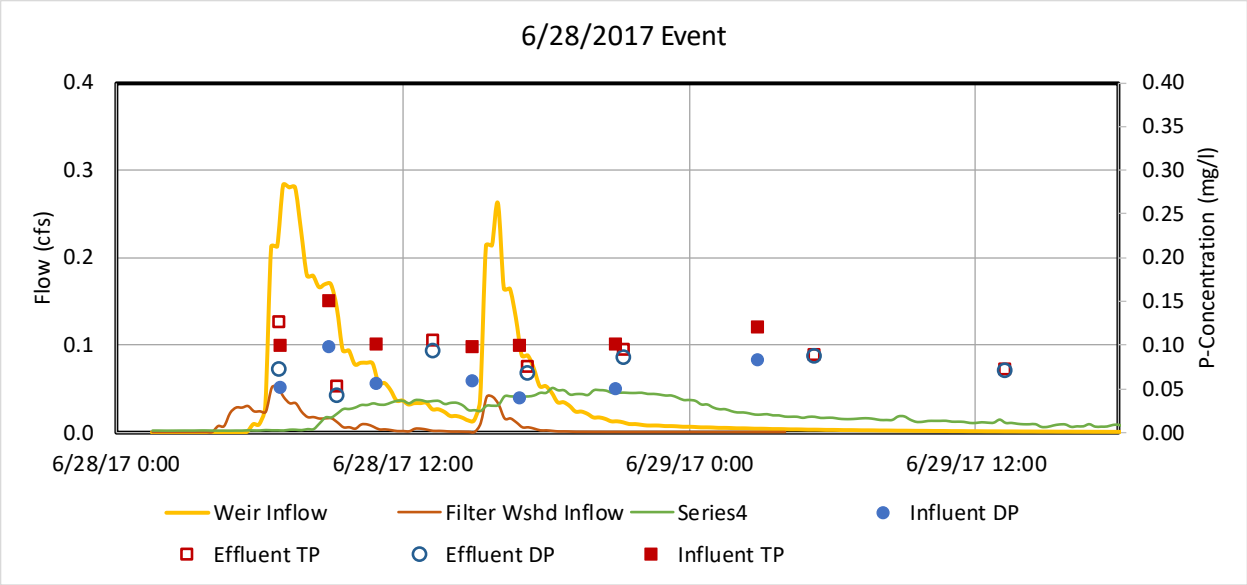

Figure B. 14 Measured influent and effluent TP and DP concentrations, measured weir inflow and outflow, and estimated filter watershed inflow for the June 28 through June 29, 2017 monitoring event.

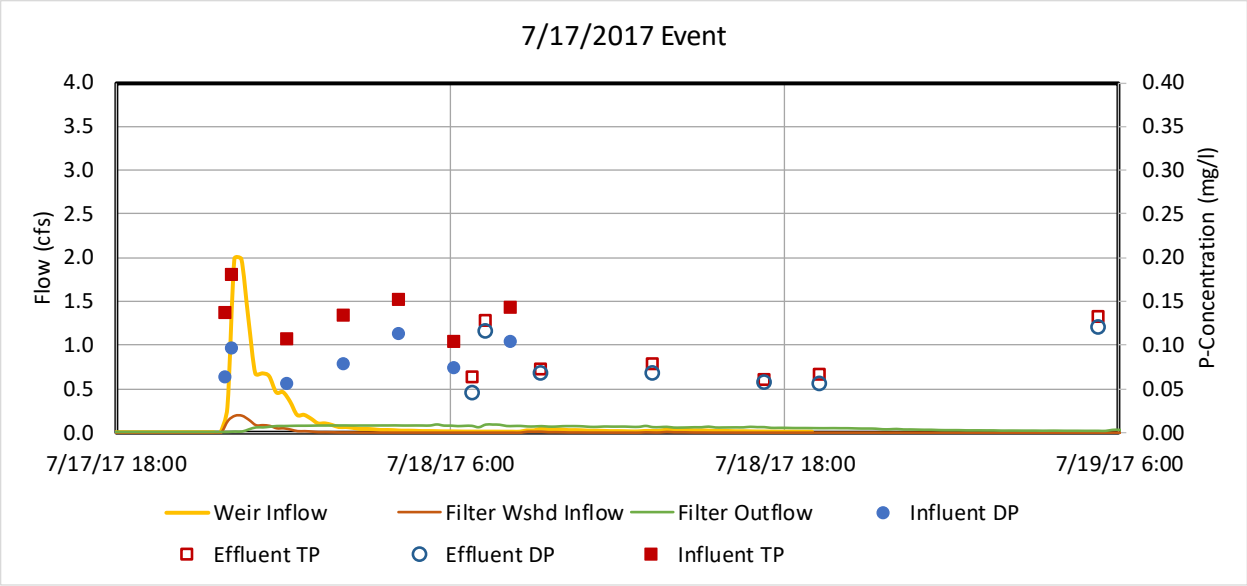

Figure B. 15 Measured influent and effluent TP and DP concentrations, measured weir inflow and outflow, and estimated filter watershed inflow for the July 17 through July 19, 2017 monitoring event.

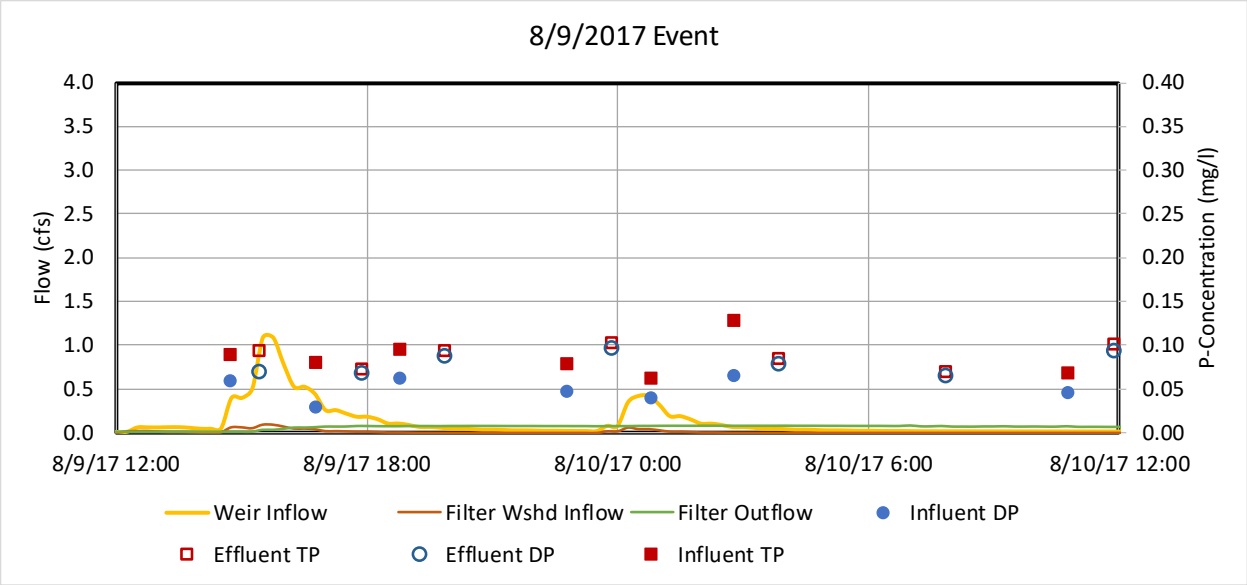

Figure B. 16 Measured influent and effluent TP and DP concentrations, measured weir inflow and outflow, and estimated filter watershed inflow for the August 9 through August 10, 2017 monitoring event.

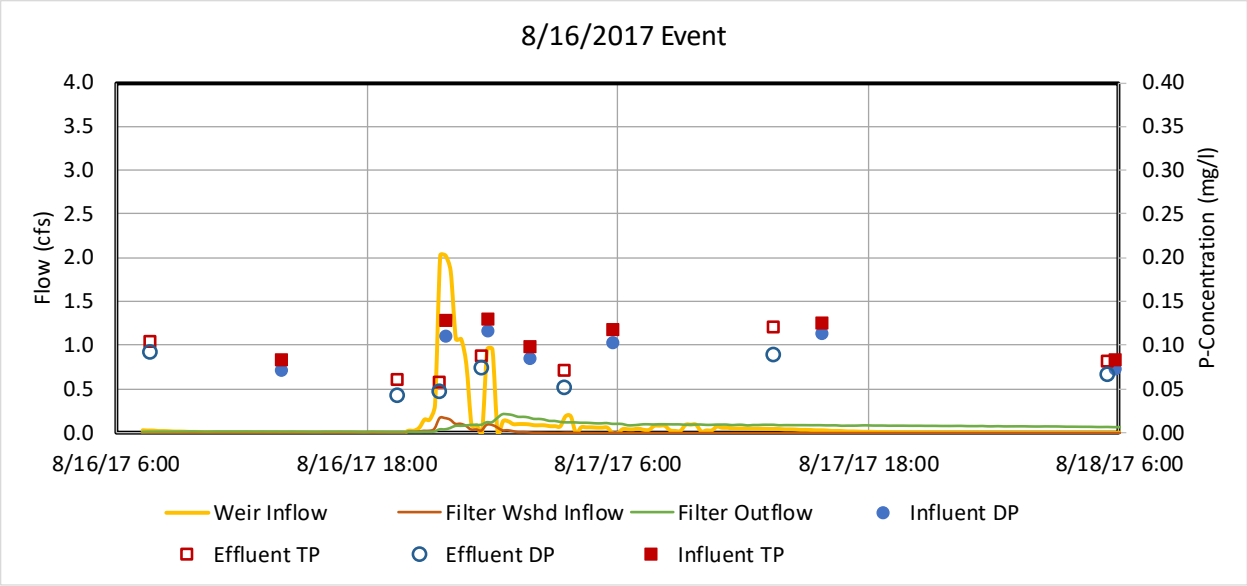

Figure B. 17 Measured influent and effluent TP and DP concentrations, measured weir inflow and outflow, and estimated filter watershed inflow for the August 16 through August 18, 2017 monitoring event.

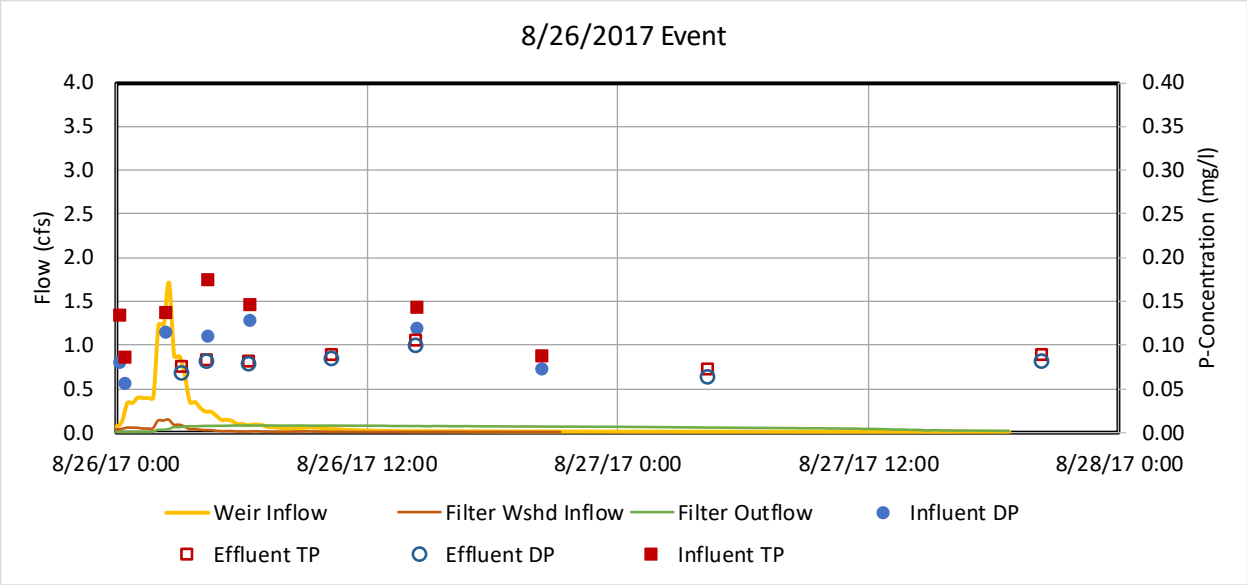

Figure B. 18 Measured influent and effluent TP and DP concentrations, measured weir inflow and outflow, and estimated filter watershed inflow for the August 26 through August 27, 2017 monitoring event.

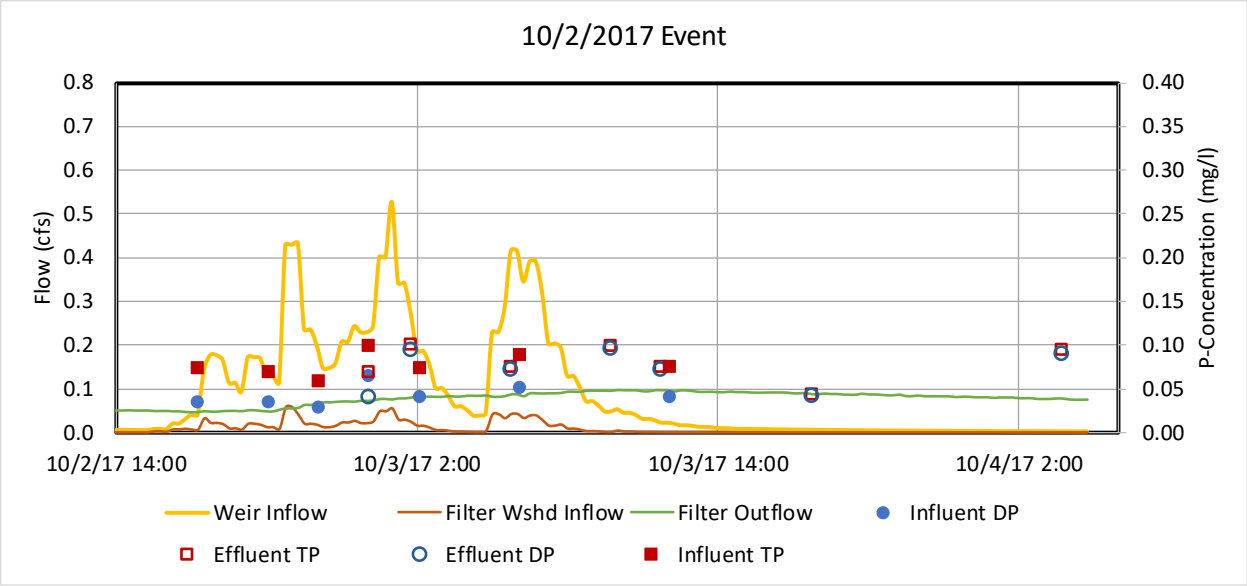

Figure B. 19 Measured influent and effluent TP and DP concentrations, measured weir inflow and outflow, and estimated filter watershed inflow for the October 2 through October 4, 2017 monitoring event.

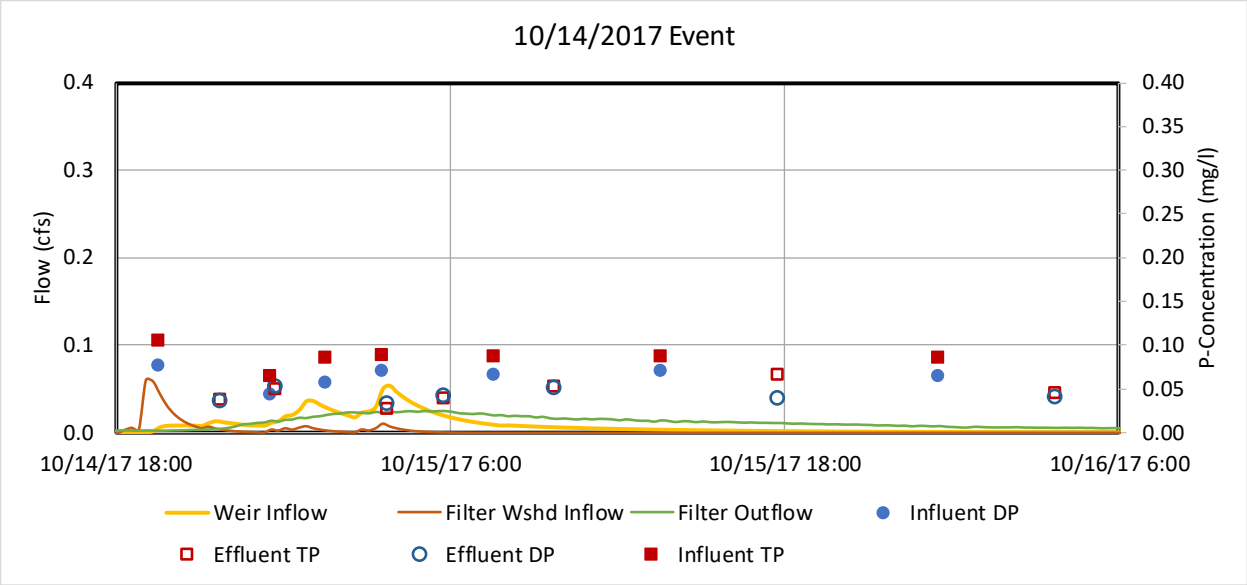

Figure B. 20 Measured influent and effluent TP and DP concentrations, measured weir inflow and outflow, and estimated filter watershed inflow for the October 14 through October 16, 2017 monitoring event.

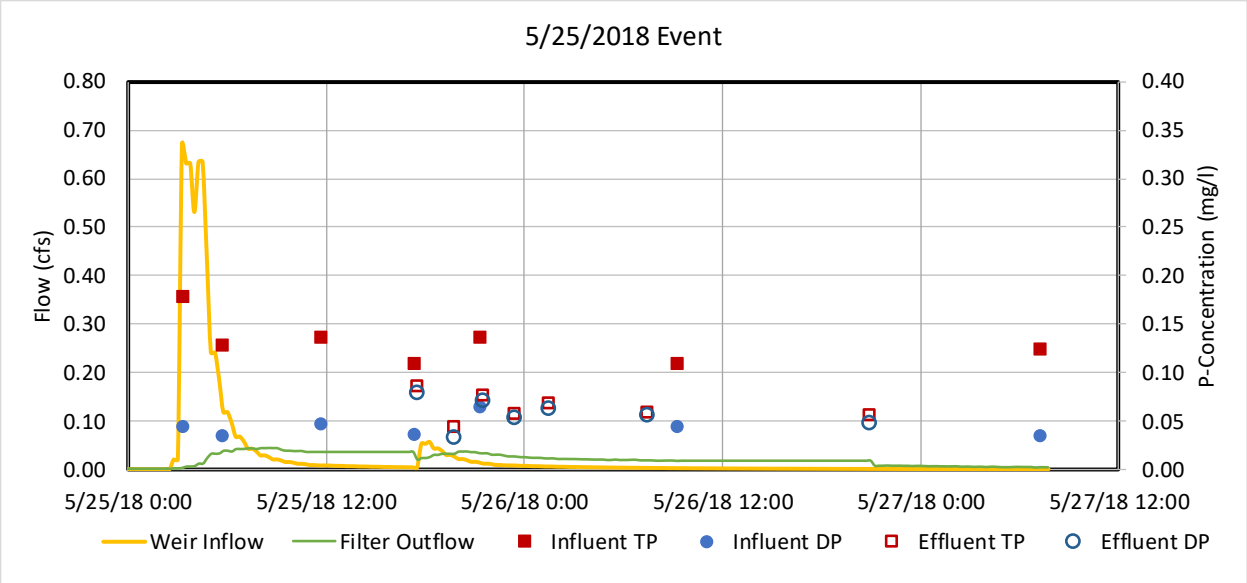

Figure B. 21 Measured influent and effluent TP and DP concentrations, measured weir inflow and outflow for the May 25 through May 27, 2018 monitoring event.

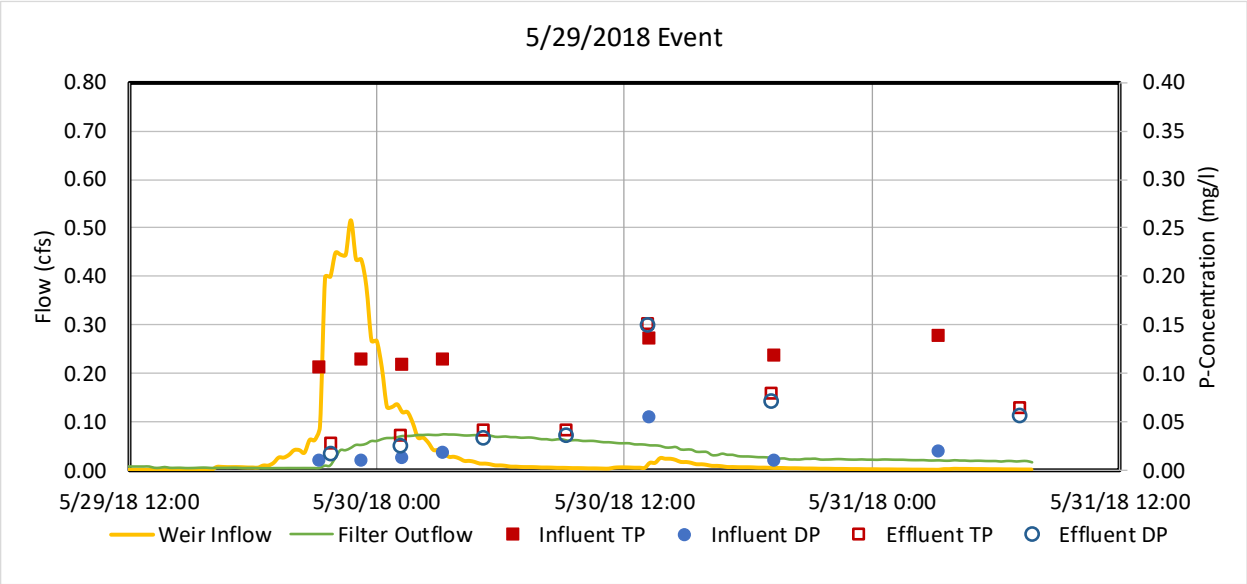

Figure B. 22 Measured influent and effluent TP and DP concentrations, measured weir inflow and outflow for the May 29 through May 31, 2018 monitoring event.

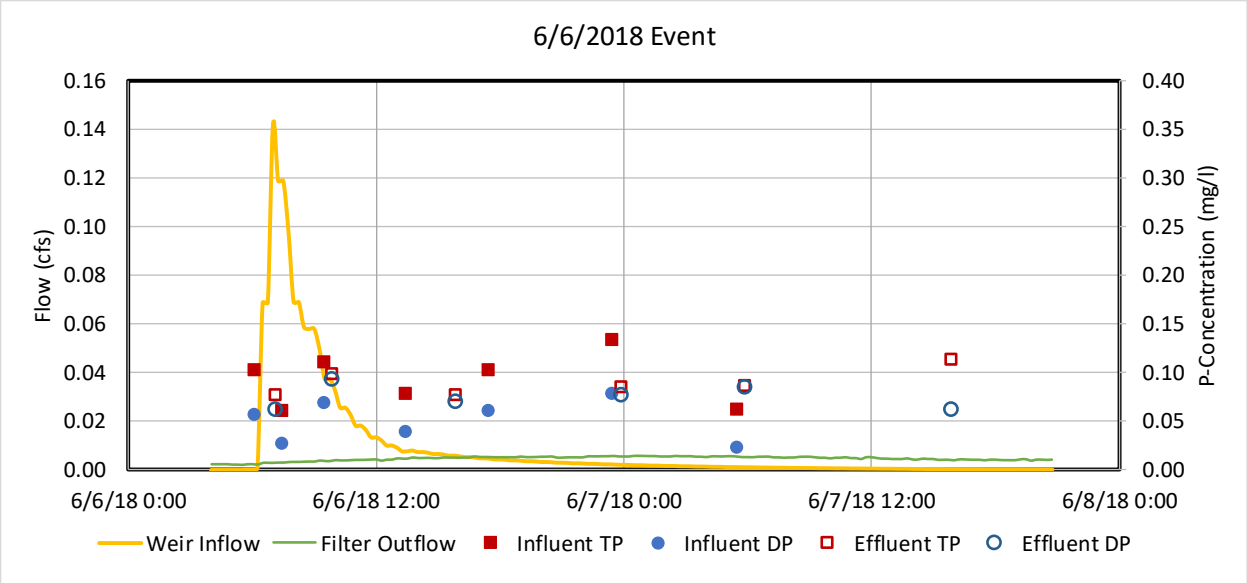

Figure B. 23 Measured influent and effluent TP and DP concentrations, measured weir inflow and outflow for the June 6 through June 7, 2018 monitoring event.

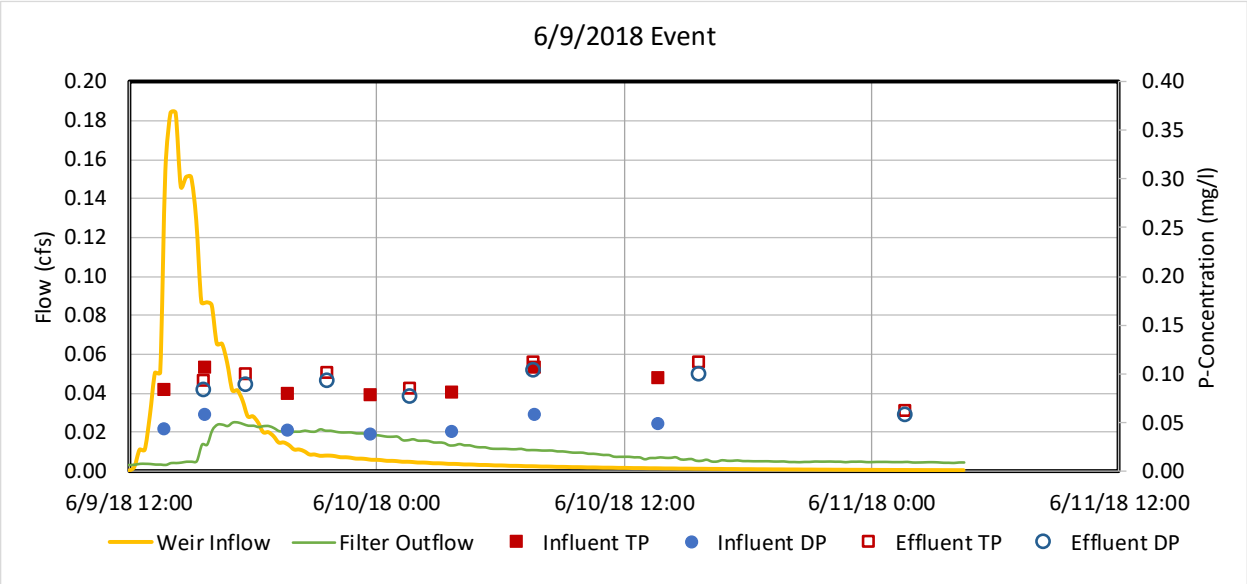

Figure B. 24 Measured influent and effluent TP and DP concentrations, measured weir inflow and outflow for the June 9 through June 11, 2018 monitoring event.

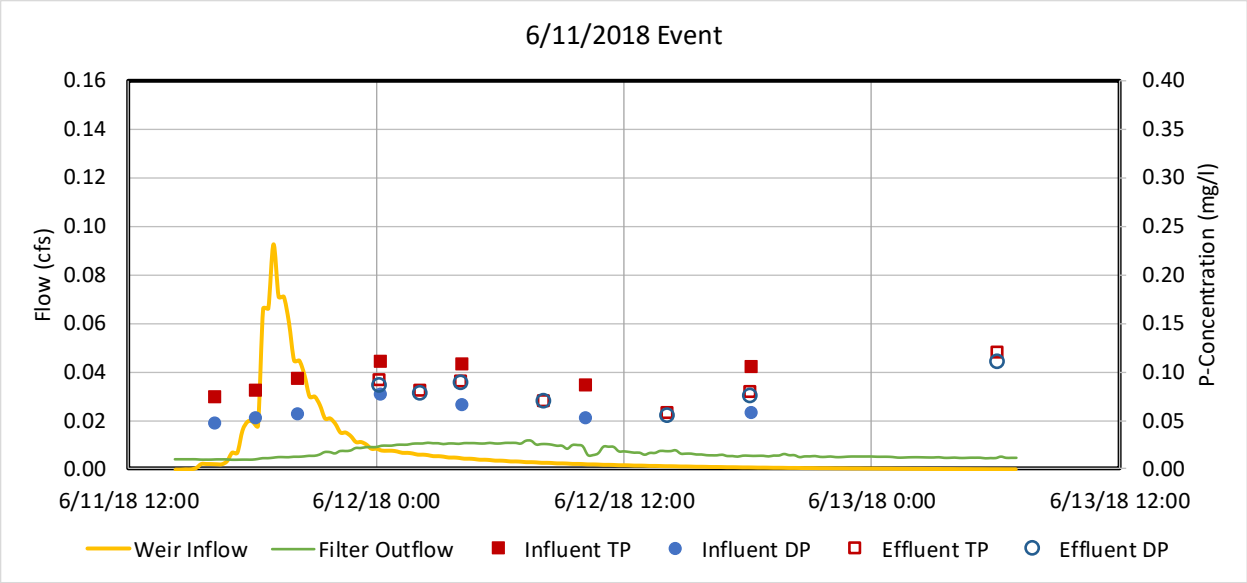

Figure B. 25 Measured influent and effluent TP and DP concentrations, measured weir inflow and outflow for the June 11 through June 13, 2018 monitoring event.

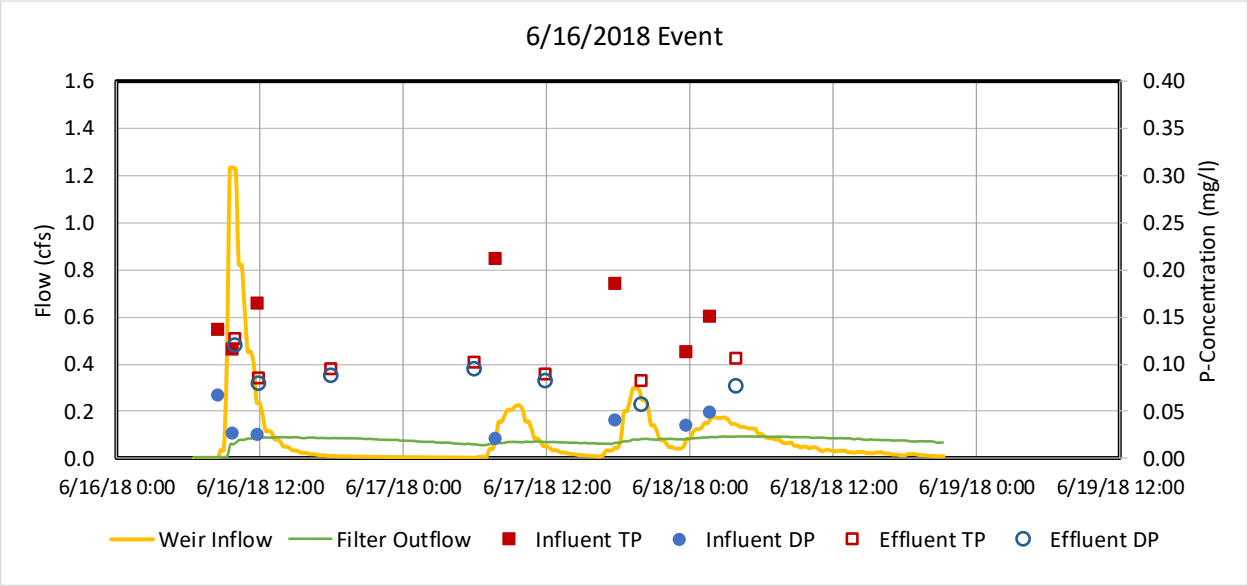

Figure B. 26 Measured influent and effluent TP and DP concentrations, measured weir inflow and outflow for the June 16 through June 18, 2018 monitoring event.

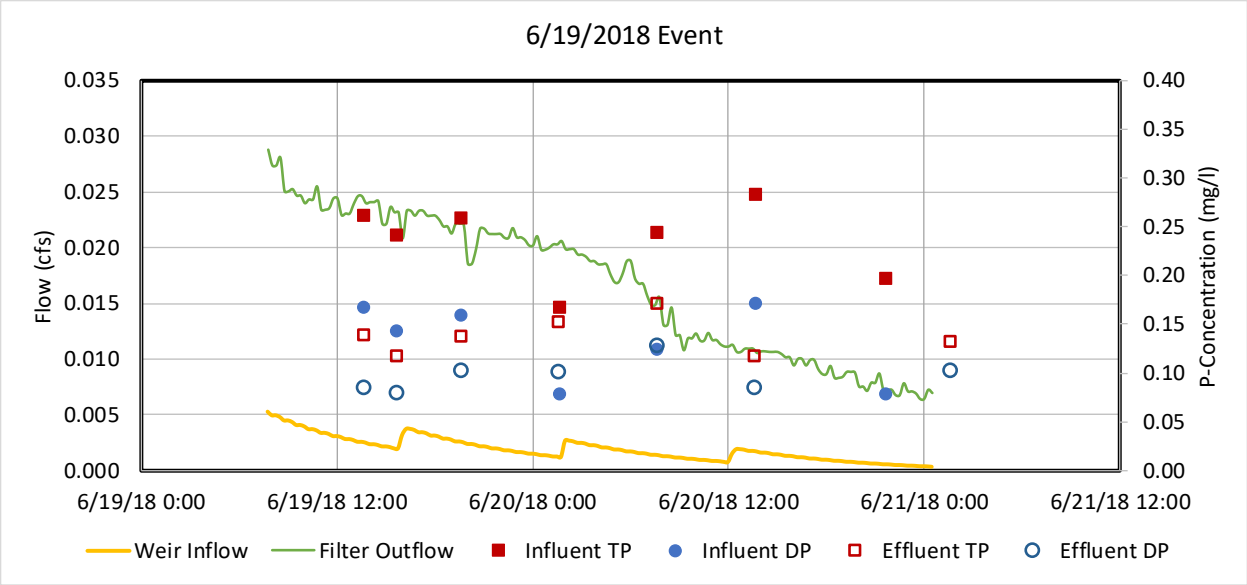

Figure B. 27 Measured influent and effluent TP and DP concentrations, measured weir inflow and outflow for the June 19 through June 21, 2018 monitoring event.

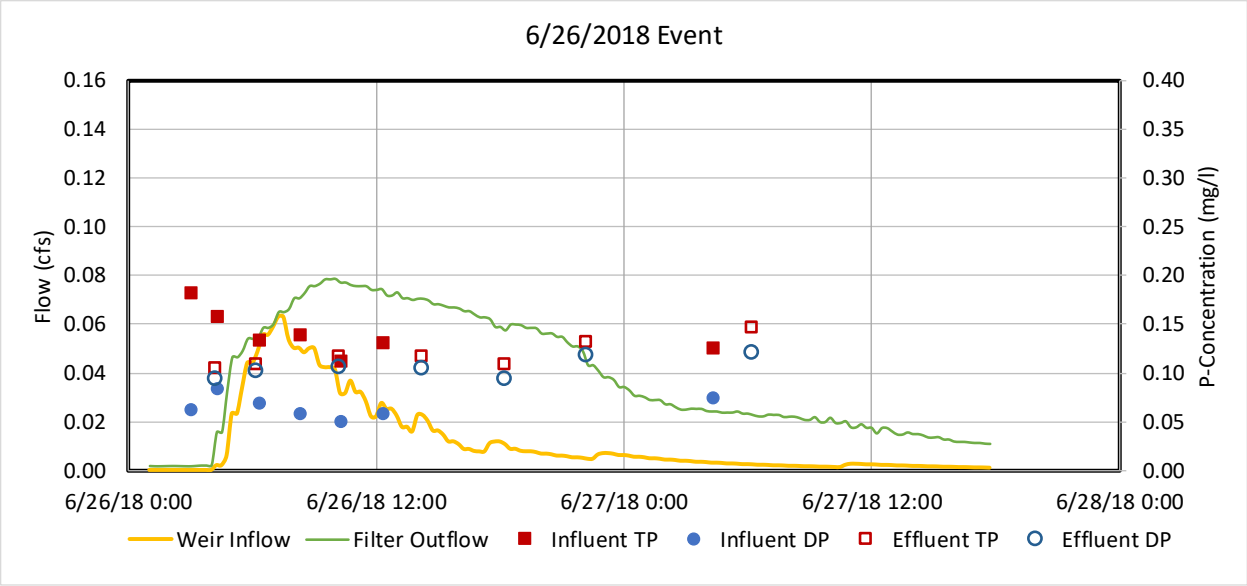

Figure B. 28 Measured influent and effluent TP and DP concentrations, measured weir inflow and outflow for the June 26 through June 27, 2018 monitoring event.

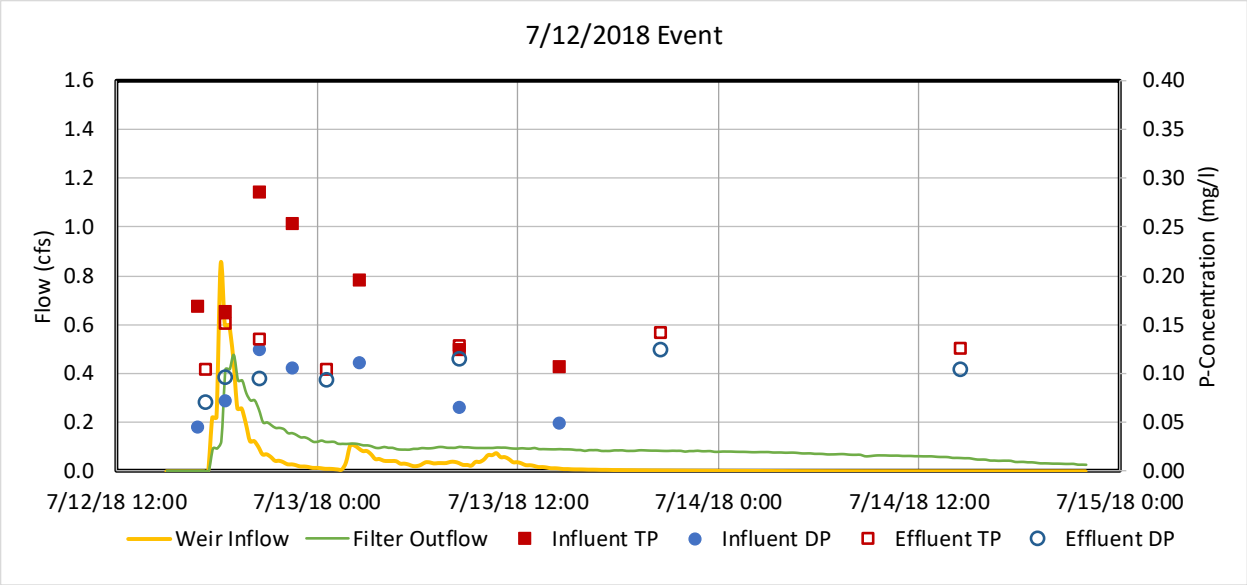

Figure B. 29 Measured influent and effluent TP and DP concentrations, measured weir inflow and outflow for the July 12 through July 14, 2018 monitoring event.

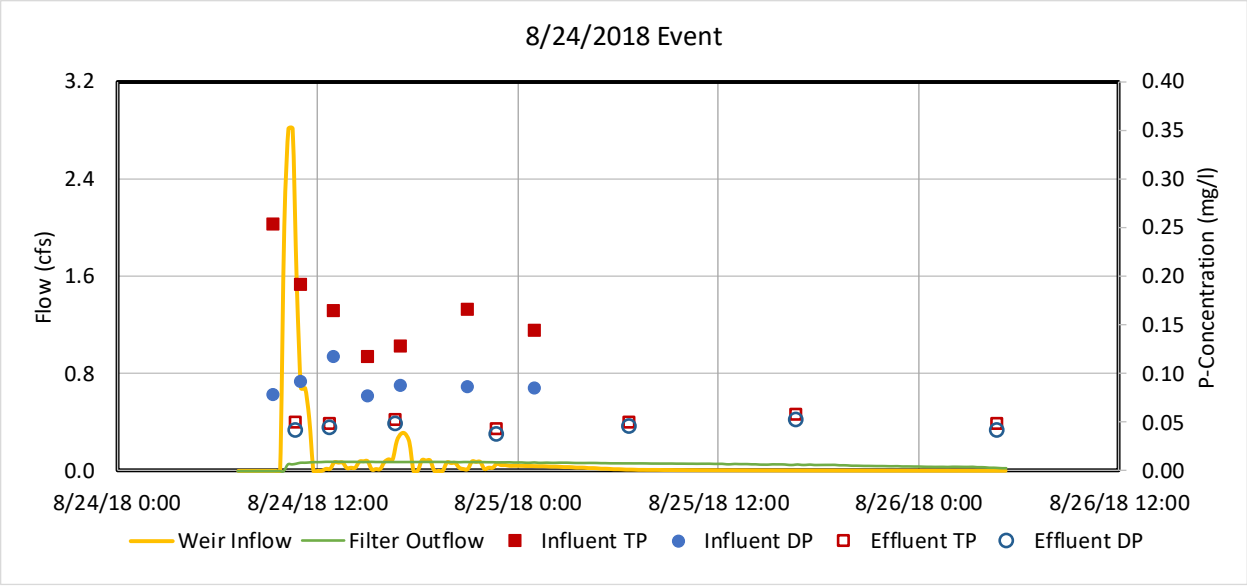

Figure B. 30 Measured influent and effluent TP and DP concentrations, measured weir inflow and outflow for the August 24 through August 26, 2018 monitoring event.

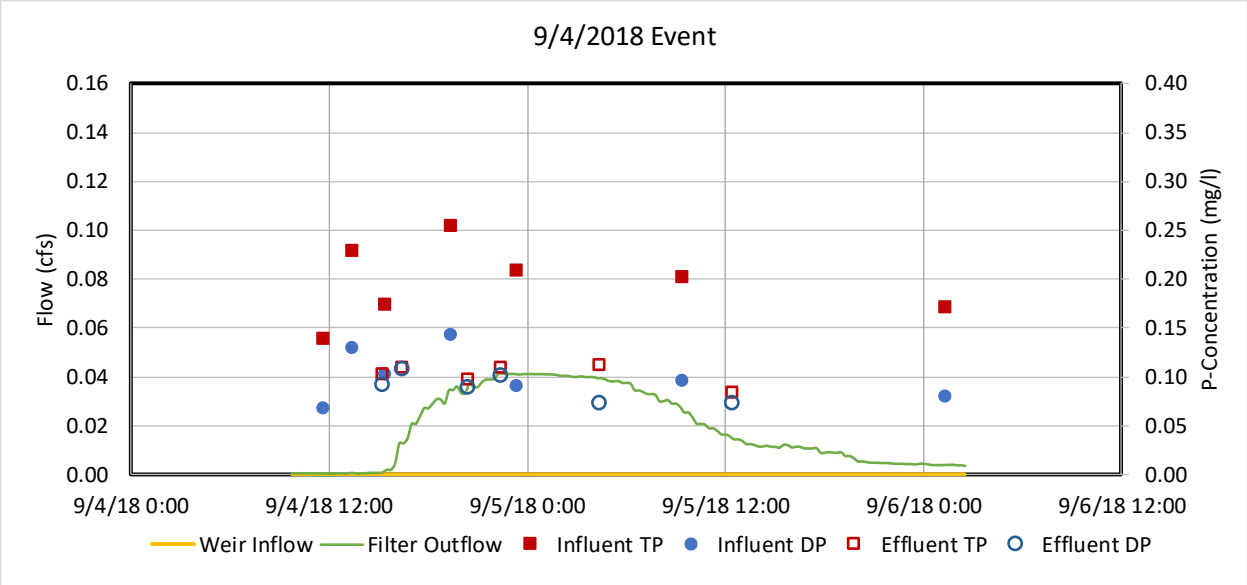

Figure B. 31 Measured influent and effluent TP and DP concentrations, measured weir inflow and outflow for the September 4 through September 6, 2018 monitoring event.

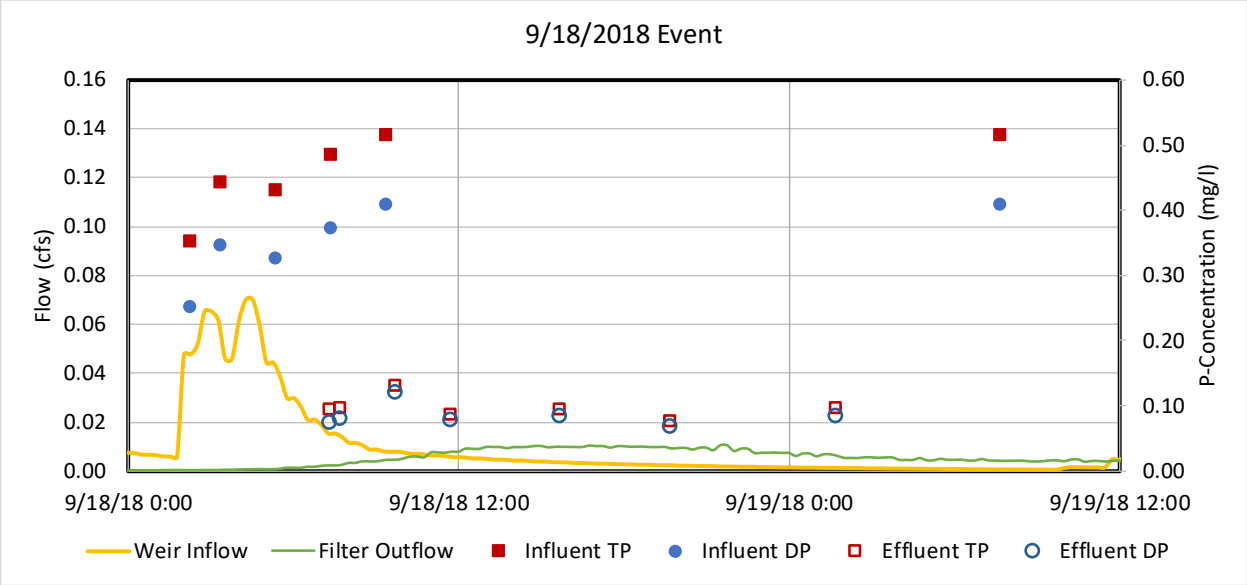

Figure B. 32 Measured influent and effluent TP and DP concentrations, measured weir inflow and outflow for the September 18 through September 19, 2018 monitoring event.

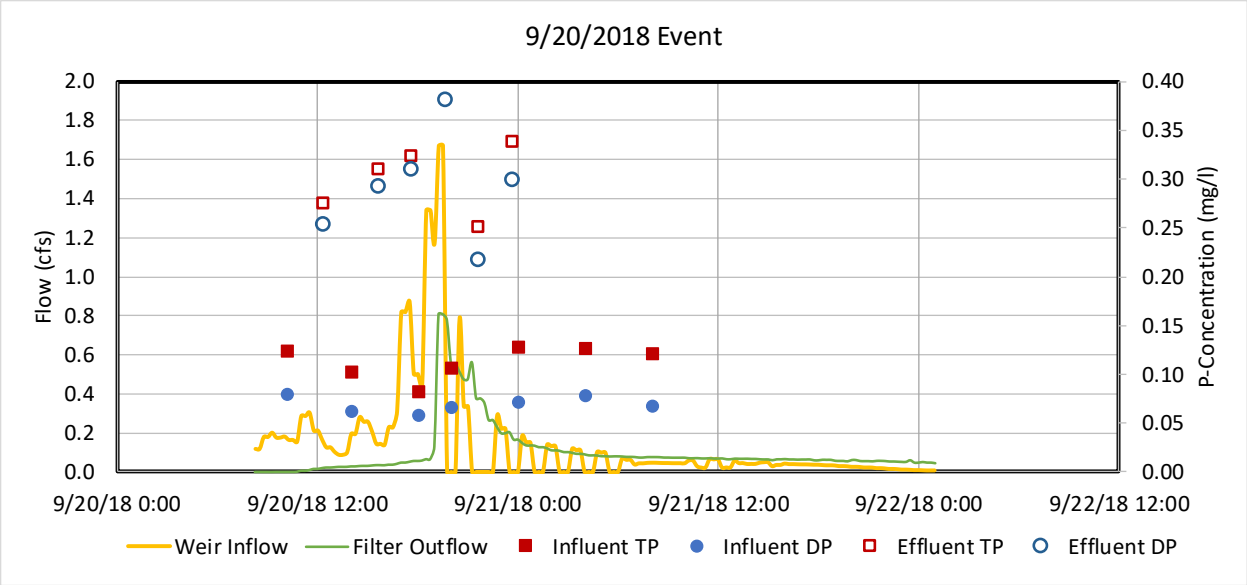

Figure B. 33 Measured influent and effluent TP and DP concentrations, measured weir inflow and outflow for the September 20 through September 21, 2018 monitoring event.

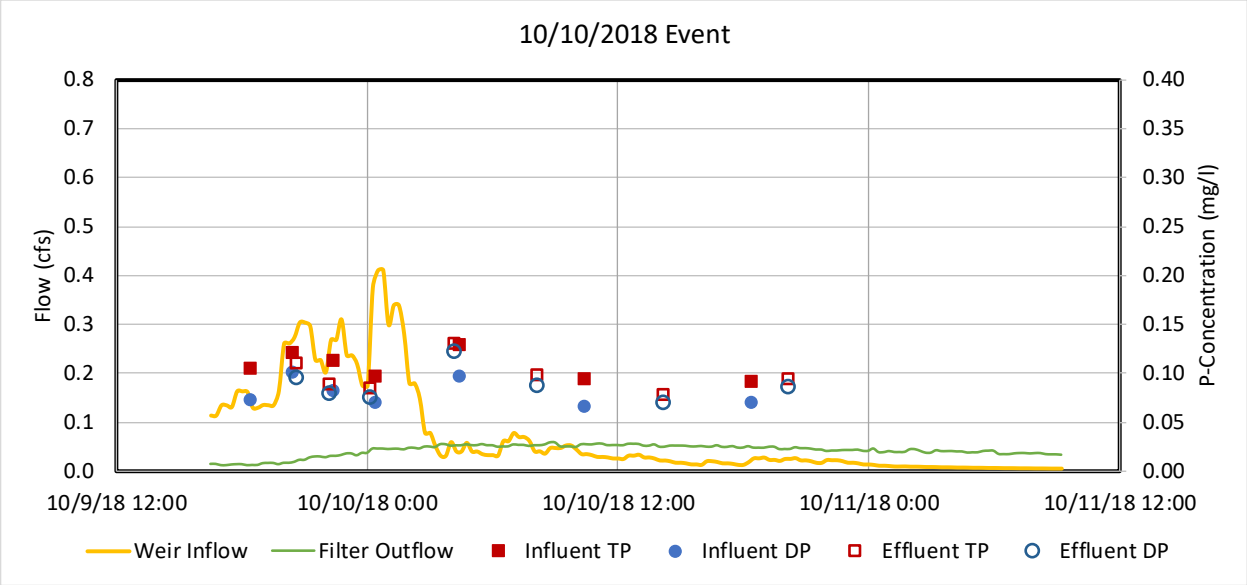

Figure B. 34 Measured influent and effluent TP and DP concentrations, measured weir inflow and outflow for the October 9 through October 10, 2018 monitoring event.